



# Bergvesenet

Postboks 3021, N-7441 Trondheim

## Rapportarkivet

Bergvesenet rapport nr <b>5256</b>	Intern Journal nr <input type="text"/>	Internt arkiv nr <input type="text"/>	Rapport lokalisering <input type="text"/>	Gradering <input type="text"/>
Kommer fra arkiv Grong Gruber AS	Ekstern rapport nr NGU 1228 A	Oversendt fra Grong Gruber a.s.	Fortrolig pga <input type="text"/>	Fortrolig fra dato: <input type="text"/>

### Titel

Geokjemiske undersøkelser av kaledonske vulkanitter og intrusiver i Midt- og Syd - Norge  
Del I - Tolkning av analysedata, september 1971 - mars 1974

### Forfatter

George H. Gale

### Dato

16.12 1974

### År

### Bedrift (oppdragsgiver og/eller oppdragstaker)

### Kommune

### Fylke

### Bergdistrikt

### 1: 50 000 kartblad

### 1: 250 000 kartblad

### Fagområde

Geokjemi

### Dokument type

### Forekomster (forekomst, gruvefelt, undersøkelsesfelt)

### Råstoffgruppe

### Råstofftype

### Sammenheng, innholdsfortegnelse eller innholdsbeskrivelse

#### Innholdsfortegnelse i rapport:

Introduction  
Acknowledgements  
Analytical data  
The Grong area  
The Løkken area  
The Stavenes area  
The Bømlo - Stord area  
Conclusions  
References

NGU rapport nr. 1228 A

Geokjemiske undersøkelser  
av kaledonske vulkanitter og intrusiver  
i Midt- og Syd-Norge

Del I - Tolkning av analysedata

september 1971 - mars 1974

**NORGES GEOLOGISKE UNDERSØKELSE**

NGU-rapport nr. 1228 A

GEOKJEMISKE UNDERSØKELSER AV KALEDONSKE VULKANITTER  
OG INTRUSIVER I MIDT- OG SYD-NORGE.

Del I - Tolkning av analysedata

September 1971 Mars 1974

Saksbehandler: George H. Gale, geolog

Norges geologiske undersøkelse

Leiv Eirikssons vei 39

Postboks 3006, 7001 Trondheim

Tlf. (075) 20166

CONTENTS	Page
1. INTRODUCTION	7
2. ACKNOWLEDGEMENTS	8
3. ANALYTICAL DATA	8
3.1 TiO <sub>2</sub> Check Analyses	8
3.2 Inter Laboratory Check on Trace Element Analyses	9
4. THE GRONG AREA	11
4.1 Analytical data	11
4.2 The Sanddøla Area	11
4.3 The Joma Area Lavas	12
4.4 The Skorovatn Andesite	16
4.5 The Bjørkvatn - Gjersvik Profile	16
4.6 Other Analyses from the Grong Area	17
4.7 Variation Diagrams	17
4.8 Summary	20
5. THE LØKKEN AREA	31
5.1 General geology	31
5.2 Analytical data	31
5.3 Geochemistry	32
5.4 Summary	36
6. THE STØREN AREA	46
6.1 Introduction	46
6.2 Analytical data	46
6.3 Geochemistry of the Støren area basalts	47
6.4 Geochemistry of the Hølonda porphyry	49
6.5 Summary	49
7. THE STAVENES AREA	58
7.1 Introduction	58
7.2 Analytical data	59
7.3 Geochemistry	59
7.4 Summary	62
8. THE BØMLO - STORD AREA	68
8.1 Introduction	68
8.2 Analytical data	68
8.3 Geochemistry of the basic rocks	68
8.4 Geochemistry of the acidic volcanics	76

	Page
8.5 The Stord Analyses	80
8.6 Summary	81
9. CONCLUSIONS	91
10. REFERENCES	94

## LIST OF TABLES

Page

3.1	Comparison of $\text{TiO}_2$ determinations by quantometric and wet chemical methods.	9
3.2	Comparison of trace element analyses between the East Anglia and the NGU Laboratories.	9
3.3	Comparison of Sr and Rb determinations between the Mineralogisk - Geologisk Museum and the NGU Laboratories.	10
3.4	Comparison of trace element data obtained by XRF techniques at Durham University and the NGU Laboratories.	10
4.1	Additional analyses for rocks of the Grong Area.	13
4.2	Major and trace elements data for 7 greenstones from the Grong Area collected by S.Kollung in 1973.	14
5.1	Additional data for the upper greenstone member, Løkken.	33
5.2	Summary data for Løkken basaltic lavas.	34
5.3	Summary data for 8 Løkken intrusive rocks	34
6.1	Mean and standard deviations of Støren basalts and the Hølonda porphyry.	48
7.1	Additional trace element data for rocks of the Stavenes Area	60
7.2	Summary data for 12 ocean floor type basalts from the Stavenes Area.	61
8.1	Summary data for East Block basic lavas.	70
8.2	Summary data for the Central Block basaltic to andesitic and rhyolitic lavas.	71
8.3	Summary data for the Finaasviki Block basaltic to andesitic lavas.	72
8.4	Analyses of acidic rocks from the East and West Blocks.	77
8.5	Analyses of acidic rocks from the Central and Finaasviki Blocks with comparisons.	78
8.6	Comparison of selected analyses from Bømlo with island arc, ocean island and "Andean type" continental volcanics.	79

## ILLUSTRATIONS

## Page

Figure 4.1	Alkali-silica variation diagram for Grong analyses	23
4.2	AFM variation diagram	24
4.3	SiO <sub>2</sub> -FeO/MgO and FeO-FeO/MgO variation diagrams	25
4.4	TiO <sub>2</sub> -FeO/MgO variation diagrams	26
4.5	Ti-Zr-Y discriminant diagram for basic lavas of the Grong area.	27
4.6	Ti-Zr discriminant diagram.	28
4.7	Ti-Zr-Sr discriminant diagram.	29
4.8	Ti-Cr discriminant diagram.	30
5.1	Alkali-silica variation diagram for rocks of the Løkken Area.	38
5.2	AFM variation diagram.	39
5.3	SiO <sub>2</sub> -FeO/MgO and FeO-FeO/MgO variation diagram	40
5.4	TiO <sub>2</sub> -FeO/MgO variation diagrams from the Løkken area (a) and the Støren area (b).	41
5.5	Ti-Zr-Y discriminant diagram.	42
5.6	Ti-Zr discriminant diagram.	43
5.7	Ti-Zr-Sr discriminant diagram.	44
5.8	Ti-Cr discriminant diagram	45
6.1	Alkali-silica variation diagram for rocks of the Støren area.	51
6.2	AFM variation diagram.	52
6.3	SiO <sub>2</sub> -FeO/MgO and FeO/MgO variation diagram.	53
6.4	Ti-Zr-Y discriminant diagram.	54
6.5	Ti-Zr discriminant diagram.	55
6.6	Ti-Zr-Sr discriminant diagram.	56
6.7	Ti-Cr discriminant diagram.	57
7.1	Geological map of the Stavenes area (after Skjerlie, 1974).	64
7.2	(a) AFM variation diagram for rocks of the Stavenes area. (b) Alkali-silica variation diagram.	65
7.3	TiO <sub>2</sub> -FeO/MgO, SiO <sub>2</sub> -FeO/MgO and FeO-FeO/MgO variation diagrams.	66
7.4	Ti-Zr-Y discriminant diagram.	67
7.5	Ti-Zr discriminant diagram.	67
7.6	Ti-Zr-Sr discriminant diagram.	67
7.7	Ti-Cr discriminant diagram.	67

## Illustrations (Con't)

## Page

Figure 8.1	General geology of Bømlo	83
8.2	Alkali-silica variation diagram for rocks from Bømlo and Stord.	84
8.3	AFM variation diagram.	85
8.4	FeO-FeO/MgO and SiO <sub>2</sub> -FeO/MgO variation diagrams.	86
8.5	TiO <sub>2</sub> -FeO/MgO variation diagram.	87
8.6	Ti-Zr-Y discriminant diagram.	88
8.7	Ti-Zr discriminant diagram.	89
8.8	Ti-Cr discriminant diagram	90



## 1. INTRODUCTION

During the winter of 1972 the writer compiled information on volcanic rocks in the south Norwegian Caledonides in an attempt to establish if any regional zonation patterns existed which might give clues to understanding the tectonic environments of formation of the Cambro-Ordovician volcanic piles. Information on the conditions of magma generation was considered necessary to provide an understanding of the tectonic evolution of the Scandinavian Caledonides and to establish a model which could then be tested by further studies. As a result of this literature compilation about 50 whole rock analyses were obtained from published articles and from the unpublished data of colleagues at NGU. Although a preliminary interpretation was made utilizing the data obtained (Gale & Roberts, 1972) it was readily apparent that much more data would have to be collected in order to establish even the regional characteristics of magmatism in the southern Norwegian Caledonides.

A proposal for further sampling of volcanic terrains in southern Norway was submitted to Director P. Padget in May 1972. The broad objectives of the sampling program were to provide a reconnaissance sampling of selected volcanic terrains in southern Norway in order to:

- 1) establish if regional variations existed within and between different volcanic terrains;
- 2) establish if there were any correlations between magma compositions (and tectonic environment) and the important sulfide mineralisations;
- 3) test the validity of the initial plate tectonic model.

This proposal was accepted in the summer of 1972. In view of limited resources it was necessary that the sampling be restricted to profiles across volcanic terrains in several areas within central and southern Norway. Samples were collected from the Grong area in the course of reconnaissance geological mapping in the summer of 1972, and from the Stavenes area, the islands of Bømlo and Stord, and the Støren and Løkken areas in the autumn of 1972 and the spring of 1973. A suite of 13 specimens from drill cores through the upper part of the Støren group at Løkken was supplied by G. Grammeltvedt.

The major and trace element analyses performed in the NGU laboratories during 1972 and 1973 are presented in NGU report 1228 B. Additional analyses carried out in 1974 are included in this report.

In this report the data are presented statistically and in variation diagrams.

## 2. ACKNOWLEDGEMENTS

The writer is indebted to Director P. Padget for his assistance in initiating the project and to Dr. D. Roberts who has cooperated in sampling the Støren and Løkken areas and provided many hours of stimulating discussions on the geological implications of the data obtained. The writer has benefited greatly from discussions with Professor F. M. Vokes on the mineralizations in the Caledonides. Harald Elstad assisted in preparation of the diagrams. J. R. Cann and Brenda Jensen have kindly provided check analyses for some of the data. The analyses were carried out by G. Faye, P. R. Graff and M. Ødegård. Lars Holiløkk and his staff are thanked for photographic assistance and tender care in assembling the report.

## 3. ANALYTICAL DATA

The bulk of the data on which this report is based is presented in report 1228 B. Since preparation of that report additional data (+ check analyses) have become available on some of the previously analysed specimens and a number of additional specimens have been analysed. The check analyses are presented below along with the earlier data for comparison. The new data on the additional samples are presented in the section of the report dealing with the particular area from which the samples were collected.

### 3.1 $\text{TiO}_2$ Check Analyses

It was apparent from the earlier data that the  $\text{TiO}_2$  values obtained from the Quantometer were slightly higher than those obtained by rapid wet chemical methods (cf Table 2, page 5 of report 1228 B). There appeared to be a difference of approximately 0,2%  $\text{TiO}_2$ . Accordingly a number of samples which plotted close to the dividing line between ocean floor basalts (OFB) and the field occupied by both OFB and low potassium tholeiites (LKT) of island arcs on the Ti-Zr diagrams were re-analysed for  $\text{TiO}_2$  by wet chemical methods. The quantometric and wet chemical data are presented in Table 3.1. It can be seen from this table that the difference between the two analytical methods is about 0,2%  $\text{TiO}_2$ . This means that on the

Ti-Zr diagrams used later in this report the samples plotting close to the OFB and OFB+LKT boundary line probably belong to the field of OFB+LKT rather than the OFB field. However, since only a small number of samples plot in this region the inclusion of analyses with slightly high (by approximately 0.2%)  $\text{TiO}_2$  does not affect the conclusions drawn from the diagrams. In the triangular diagrams employing Ti the error introduced is negligible and can thus be ignored.

Table 3.1 Comparison of %  $\text{TiO}_2$  determinations by quantometric and wet chemical methods.

Sample	Quanto	wet chem	Sample	Quanto	wet chem.
132	1.38	0.51	269	0.99	0.75
138	1.42	1.24	277	1.01	0.78
141	1.33	1.18	279	2.02	1.77
143	1.37	1.16	282	2.02	1.78
378	1.26	0.99	295	1.38	1.29
389	1.16	0.97	302	1.50	1.38
390	1.18	0.93	327	1.90	1.71
391	1.17	1.11	359	1.06	0.89
392	1.28	1.08	379	1.52	1.37
265	0.38	0.15	173	1.72	1.52

### 3.2 Laboratory Check on Trace Element Analyses.

Five partial trace element analyses were performed by Dr. J.R.Cann at the University of East Anglia, England, by the XRF method in use there. These are presented along with the NGU analyses in Table 3.2.

Table 3.2 Comparison of trace element data between the East Anglia and the NGU laboratories. NGU analyses in parenthesis.

Sample	Rb	Sr	Y	Zr	Nb
153	1(0)	52 (50)	10 (13)	18 (33)	2 (-)
281	19 (18)	332 (398)	23 (25)	164 (220)	17 (-)
291	49 (47)	275 (322)	25 (28)	175 (212)	16 (-)
314	33 (33)	297 (353)	23 (26)	146 (175)	12 (-)
325	0.5 (0)	132 (166)	42 (48)	147 (194)	4 (-)

Five samples were analysed for Sr and Rb by Brenda Jensen XRF in the Mineralogisk-Geologisk Museum in Oslo. Her results, which are the average of 3 determinations except for sample 320 which was run five times, are presented in Table 3.3.

Table 3.3 Comparison of Sr and Rb determinations between the Mineralogisk - Geologisk Museum and the NGU laboratories. NGU values are given in parenthesis.

Sample	Sr	Rb
259	70 (69)	230 (228)
280	249 (279)	53 ( 53)
320	147 (164)	0.5 (0)
378	161 (186)	16 (13)
383	128 (139)	17 (18)

Table 3.4 is a comparison of NGU data obtained on a basalt specimen from Newfoundland with that determined by the author in the Departement of Geology at the University of Durham, England. This sample was included as an unknown in a suite of samples from Norway.

Table 3.4 Comparison of trace element data obtained by XRF techniques at Durham University and the NGU laboratories. NGU data in parenthesis.

Zr	Y	Sr	Rb	Zn	Cu	Ni	Ba
131 (150)	25 (23)	329 (331)	17 (12)	88 (79)	57 (55)	97 (92)	86 (46)

It can readily be seen from Tables 3.2 to 3.4 that the data obtained between the different laboratories is reassuringly comparable. The Zr values obtained in the NGU laboratories appear to be slightly higher than those obtained at East Anglia and Durham University. Although we cannot be certain which set of data is closer to the absolute value in the rocks, a slightly high Zr value from the NGU laboratories would readily explain why a few of the samples from the areas of dominantly ocean floor basalts plot just inside the field of withinplate basalts on Ti-Zr-Y plots since they would be biased toward the Zr corner of the diagram.

## 4. THE GRONG AREA

### 4.1 Analytical data

Thirty-five complete major and trace element analyses and 8 major element analyses are presented in report 1228 B. Additional data are presented in Tables 4.1 and 4.2. The major element data for three of the samples in Table 4.1 (71-65B, 71-65B and 71-6) are also presented in report 1228B. Data are presented on a total of 51 samples which are distributed as follows:

- a) the Sanddøla area - 5 basic lavas and pillow lavas
  - 1 fine-grained gabbro
  - 1 medium-grained trondhjemite
  - 1 keratophyre tuff
- b) the Joma area - 2 basic lavas overlying the ore-body
  - 3 pillow lavas from road side near Solberg farm
  - 1 pillow lava from Orklumpen
- c) Skorovatn - 1 andesite lava from the Skorovass mine
- d) the Bjørkvatn - Gjersvik profile
  - 16 basic lavas and pillow lavas
  - 1 acidic pyroclastic lava
  - 3 fine-grained trondhjemitic dikes
- e) other areas - 16 samples of basic and acidic rocks scattered over the Grong area between Gjersvik, Skorovatn and the western limits of the Grong concession area.

### 4.2 The Sanddøla Area.

The 5 basic lavas of the Sanddøla area (analyses 1189/35, 130, 132, 133 and 134) have  $\text{SiO}_2$  values in the range 46.60 to 51.20 %,  $\text{K}_2\text{O}$  values in the range 0.23 to 0.26 % and  $\text{Na}_2\text{O}$  from 2.76 to 5.89 %. These basic lavas are basalts which on the basis of their greenschist facies mineral assemblages and  $\text{Na}_2\text{O}$  contents can be classified as spilites (see Fiala, 1974). However, since I do not intend to discuss the spilite problem here such rocks will be referred to throughout this report as basalts. The major element analyses of these rocks are comparable, with the greatest variations in chemistry occurring in  $\text{MgO}$  (4.27 to 10.70 %) and  $\text{CaO}$  (6.45 to 10.40 %). The only marked difference in the trace element contents is that shown by Cr which is 19 and 27 ppm for analyses 1189/35 and 130, resp. and 381, 374 and 303 ppm for analyses 132, 133 and 134, resp. Ni and Sr are also signifi-

cantly higher in the latter three analyses than in the former two. The significantly higher Cr, Ni and Sr values in analyses 132, 133 and 134 also correlates with higher CaO and MgO than in analyses 1189/35 and 130. The small sample population here makes it difficult to draw a firm conclusion as to whether or not this represents different magma types.

The fine-grained gabbro, analysis 131 is chemically similar to the basic lavas with the exception of  $\text{Al}_2\text{O}_3$ , Zr, Sr and Ba which are markedly higher than in any of basic lavas from this area.

The medium-grained thordhemite, analysis 272, has only 64.70 %  $\text{SiO}_2$  in contrast to 71.90 %  $\text{SiO}_2$  for trondhemite from the type locality (see analysis 249 from the Støren area). The high  $\text{Na}_2\text{O}$  (6.64 %) and low  $\text{K}_2\text{O}$  (1.54 %) contents in comparison with other acidic plutonic rocks indicate that this intrusive does belong to the trondhemite class of igneous rocks.

The keratophyric tuff, analysis 271, is most similar to the trondhemite in its  $\text{Na}_2\text{O}$  content (6.22 %) and the minor element oxides MnO and  $\text{P}_2\text{O}_5$ . The  $\text{K}_2\text{O}$  content (0.16 %) as well as the other element concentrations, are comparable to those of other keratophyres in the Grong area (cf. analyses 252, 253 and 254).

#### 4.3 The Joma Area Lavas.

The six analyses of rocks from this area; No 3, a sample of pillow lava from Orklumpen, NE of the Joma mine; Nos. 149 and 150, samples from a drill hole in the hanging wall lavas at the Joma mine; and Nos 333, 334 and 335, samples of pillow lavas in road-cuts near Solberg farm. Analysis No. 3 contains only major element data.

With the exception of Loss On Ignition there does not appear, from a visual inspection of the data, to be any obvious difference in the chemistry of the five samples and all appear to represent the same magma type. The slightly lower  $\text{K}_2\text{O}$  and Rb in the two analyses from the hanging wall of the Joma ore body may, according to theories put forward by B. Bølviken (pers. comm.), reflect depletion of these elements by electrochemical leaching due to the presence of the ore deposit itself.

An outstanding feature of the Joma analyses is the higher mean  $\text{K}_2\text{O}$  and lower mean  $\text{Na}_2\text{O}$  than the other groups of basalts in the Grong region. It will be shown later by means of variation diagrams that the basalts of the Joma area are distinctly different from those found elsewhere in the Grong area.

**Table 4.1** Additional analyses of rocks from the Grong area. Major element data for 71-GJB, 71 GJC and 71-6 are also given in Rapport 1228 B.

	1189/35 <sup>x</sup>	71-GJB	71-GJC	71-6
SiO <sub>2</sub>	50.80	41.57	43.89	65.70
TiO <sub>2</sub>	2.20	0.74	1.21	0.82
M <sub>2</sub> O <sub>3</sub>	16.17	16.04	17.59	12.34
Fe <sub>2</sub> O <sub>3</sub>	3.89	3.48	2.78	2.46
FeO	8.90	6.23	10.16	4.59
MnO	0.23	0.18	0.27	0.20
MgO	4.27	8.21	7.54	1.71
CaO	6.45	11.06	5.83	3.01
Na <sub>2</sub> O	5.89	2.48	3.14	5.98
K <sub>2</sub> O	0.26	0.34	1.32	0.14
H <sub>2</sub> O <sup>-</sup>	0.05	0.04	0.02	0.01
H <sub>2</sub> O <sup>+</sup>	1.25	3.19	4.94	1.77
CO <sub>2</sub>	0.03	0.72	0.96	1.80
P <sub>2</sub> O <sub>5</sub>	<u>0.12</u>	<u>0.06</u>	<u>0.14</u>	<u>0.15</u>
Total	100.51	100.34	99.79	100.68
Zr	132	41	55	118
Y	43	12	25	42
Sr	67	402	275	72
Rb	0	0	12	0
Zn	121	70	185	161
Cu	0	32	2	0
Ni	0	56	15	0
Cr	19	267	50	1
Ba	138	32	319	31

<sup>x</sup> Grong (1:50 000) 1823 IV; UTM 71516 03856.

Table 4.2. Major and trace element analyses of 7 greenstone samples from the Grong area collected by S. Kollung in 1973. Sample 2444 is described as an epidote banded greenstone, the other samples are described as greenstone.

	2444	2560	2741	2742	2743	2746	2776
SiO <sub>2</sub>	48,36	48,29	49,46	49,81	47,29	51,05	49,33
TiO <sub>2</sub>	0,82	0,87	0,64	1,16	0,95	1,40	0,81
Al <sub>2</sub> O <sub>3</sub>	16,48	16,41	16,74	16,72	15,82	15,28	14,85
Fe <sub>2</sub> O <sub>3</sub>	3,71	2,81	2,92	5,79	3,85	6,28	2,01
FeO	4,72	4,60	5,97	6,56	6,23	6,54	7,71
MnO	0,17	0,29	0,17	0,24	0,18	0,24	0,18
MgO	7,63	6,92	7,90	4,17	8,00	5,41	5,15
CaO	12,40	10,68	7,43	7,59	12,84	4,47	9,41
Na <sub>2</sub> O	3,57	4,36	4,67	4,82	2,68	5,19	4,86
K <sub>2</sub> O	0,54	0,34	0,30	0,06	0,14	0,49	0,12
H <sub>2</sub> O <sup>-</sup>	ikke påv.	ikke påv.	ikke påv.	ikke påv.	0,02	0,49	0,02
H <sub>2</sub> O <sup>+</sup>	1,86	2,78	3,16	2,08	2,42	3,37	2,70
CO <sub>2</sub>	0,04	1,79	0,68	0,64	0,02	0,09	3,17
P <sub>2</sub> O <sub>5</sub>	0,04	0,08	0,06	0,09	0,06	0,09	0,08
	100,34	100,22	100,10	99,73	100,50	100,33	100,40
Zr	45	54	19	63	50	32	32
Y	21	20	14	30	26	23	14
Sr	279	164	192	103	168	126	151
Rb	3	4	1	0	0	5	0
Zn	80	69	82	111	77	98	82
Cu	8	44	44	53	6	5	0
Ni	146	113	63	7	130	0	3
Cr	492	351	291	17	354	11	15
Ba	195	105	50	146	105	86	8



TABLE 4.2 (continued).

<u>Prøve</u>	<u>Type</u>	<u>Lok. nr.</u>	<u>Lokalitet</u>	<u>Kartblad</u>	<u>Koordinater.</u>
2444	Epidotfoliert grønnstein	293	Vegskjæring i Grøndalen 1200m SV Kvernå.	Namsskogan	N 3012 Ø 3046
2741	Lys, grovere grønnstein (Kirmatype).	592	1000m NV Gjersvik gård.	Røyrvik	N 5353 Ø 4970
2742	Mørk grønnstein (Gjersviktype).	593	Ø Bjørkvann	Røyrvik	N 4970 Ø 4770
2743	Foliet grønnstein	594	1000m NV Bjørkvann	Røyrvik	N 5288 Ø 4478
2746	Stilpnomelangrønnstein	607	500m S Gjersviktjern	Røyrvik	N 4870 Ø 5067
2776	Grønnstein i Stekenjokknivå		Vegskjæring 400m SV Kjernes gård. Huddingsdalen.	Huddingsvann	N 5682 Ø 6900
2560	Porfyrisk grønnstein (Nounatype)		500m NV Ingulsvann gård	Tunnsjøen	N 3326 Ø 5570

Koordinater: reference to 1:20 000 airphoto mosaics

Major elements by P.R. Graff

Trace element by G. Faye and M. Ødegaard.

#### 4.4 The Skorovatn Andesite.

This lava/dike from the Skorovass mine is of andesitic composition with 65.70%  $\text{SiO}_2$  (Analysis 71-6, Table 4.1). The  $\text{K}_2\text{O}$  (0.14%) content is low for rocks with this amount of  $\text{SiO}_2$  but andesites with low  $\text{K}_2\text{O}$  are found in early island arc terrains (cf Jake's and White, 1972). It will be shown later that this rock has trace element characteristics of calc-alkaline rocks.

#### 4.5 The Bjørkvatn - Gjersvik Profile.

The analyses of basic lavas and pillow lavas sampled along the section from Bjørkvatn to the Gjersvik mine are presented in report 1228 B - analyses 4, 5, 7, 8, and 135-146. The trace element data are missing for analyses 4 and 5 but are presented in Table 4.1 for analyses 7 and 8.

The majority of these basic volcanics can be classified as basalts since they have  $\text{SiO}_2$  contents less than 51 %. Three of the analyses 140, 144 and 145 have 55.80, 55.20 and 58.40 %  $\text{SiO}_2$  resp., and could be classified as basaltic andesites. Analysis 140 is from a fragment of a coarse pyroclastic near Bjørkvatn while analyses 145 and 146 are of basic lavas from immediately west of the Gjersvik mine.

The acidic pyroclastic lava, analysis 284, was collected from a massive non-fragmental silicic rock which overlies an agglomerate on the south shore of Bjørkvatn. This analysis is distinctive from that of the other keratophyres in that it has 2.64 %  $\text{Na}_2\text{O}$  and 1.19 %  $\text{K}_2\text{O}$  whereas the keratophyres generally have 4-7 %  $\text{Na}_2\text{O}$  and less than 0.5 %  $\text{K}_2\text{O}$ . An analysis, 273, of a fine-grained acidic intrusive with 2.00 %  $\text{Na}_2\text{O}$  and 3.70 %  $\text{K}_2\text{O}$  resembles analysis 284 in that their alkali contents are different from those of two other acidic intrusives Nos 270 and 6, which are relatively high in  $\text{Na}_2\text{O}$  and low in  $\text{K}_2\text{O}$  and are thus similar to the keratophyres found elsewhere in the Grong area. More detailed sampling and mapping by Ole Lutro, University of Bergen, may provide information on the differing geochemistries of those acidic rocks since it is not possible to determine from such a small sample population whether the data is significant with regard to the origin of the acidic rocks.

#### 4.6 Other Analyses from the Grong Area.

The 16 "other" analyses of rocks from the Grong area included an andesitic lava (analysis No 2) associated with agglomerates southeast of Rorvatn, basaltic lava (analysis no 148) northeast of Skorovatn, 7 basaltic lavas collected by S. Kollung (Table 4.2) and 7 acidic volcanics mapped as keratophyre and finegrained trondhjemite (analyses 147, 252, 253, 274, 285 and 332).

The andesitic lava (analysis no 2) which has 68,47 %  $\text{SiO}_2$  is comparable to the andesite from Skorovatn in its major element constituents. The  $\text{K}_2\text{O}$  content 0,87 % is considerably higher than the 0,14 % obtained on the Skorovatn sample even though the  $\text{Na}_2\text{O}$  contents are quite similar. Trace element data are not available for this sample. Analyses 148 and the analyses in Table 4.2 are similar to the analyses of basaltic lavas from the Bjørkvatn - Gjersvik profile. The 7 acidic volcanics are characterized by high  $\text{Na}_2\text{O}$  and low  $\text{K}_2\text{O}$  and there does not appear to be any obvious geochemical discriminant between the lavas and the intrusives.

#### 4.7 Variation Diagrams.

Variation diagrams for distinguishing theoleiitic, calc-alkaline magmas have been devised by various authors. These are based on element ratios or on normative mineralogy.

In Fig. 4.1 the majority of the basic volcanics of the Grong area can be seen to plot within the field of alkaline volcanics from Recent volcanoes and especially in the field of the alkaline suite defined by Irvine and Barager (1974). An inspection of the data, however, reveals that this is due to the high  $\text{Na}_2\text{O}$  contents of these rocks and with the exception of the Joma lavas, the basalts and andesites of the Grong area generally have less than 0,5 %  $\text{K}_2\text{O}$  - a  $\text{K}_2\text{O}$  content that is exceptionally low for rocks of alkaline affinities. It is well known that the alkali - silica variation diagram is of limited value in dealing with spilitized basalts. Fig. 4.1 does show, by the spreading of samples from the individual subareas over both the alkaline and sub alkaline fields, that there is no distinction between subareas on the basis of alkali and silica.

On a standard AFM diagram, Fig. 4.2, the Grong volcanic and plutonic rocks exhibit a definite iron enrichment when all the analyses are considered

together. This tendency towards iron enrichment is typical of tholeiitic magmas rather than calcalkaline magmas which tend to plot towards the center of AFM diagrams. The tholeiitic trend of the Grong magmas is further accentuated by the tendency for most of the basalts to plot above the boundary that Irvine and Barager (1971) defined to separate tholeiitic (above) and calcalkaline (below) magmas. The various subareas, with the exception of the Joma basalts, also exhibit a definite iron enrichment. The tholeiitic nature of the Grong volcanics is further accentuated by Fig. 4.3 (% FeO vs FeO/MgO and % SiO<sub>2</sub> vs FeO/MgO) and Fig. 4.4 (% TiO<sub>2</sub> vs FeO/MgO) which show that the analyses plot predominantly within the field of the island arc tholeiitic series as defined by Miyashiro (1974).

A particularly interesting feature of Fig. 4.4 is the tendency for the Joma lavas and most of those of the Sanddøla subarea to plot well outside the general trend for the Grong area as a whole and away from the trend of the tholeiitic series (Miyashiro 1974). In the case of the Joma subgroup the higher TiO<sub>2</sub> contents are consistent with the more alkaline nature of the magma in contrast to the tholeiitic nature of magmas found elsewhere in the Grong area.

Although various authors have noted the mobility of FeO and MgO during spilitization (eg. Cann, 1969), it can be concluded from the AFM diagram and the variation diagrams of Miyashiro that the rocks of the Grong area are predominantly of tholeiitic affinity.

Pearce and Cann (1973) have shown that some of the trace elements which are unaffected by greenschist grade metamorphism (Cann 1969-1970) can be used to determine the tectonic environments of magma generation. In Fig. 4.5 it can be seen that the Joma lavas plot within the field for "withinplate" basalts (WPB). With the exception of the andesite from the Skorovass mine which plots within the calc-alkaline basalt field (CAB), the remainder of the Grong volcanics plot mainly within the fields for low-potassium tholeiites of island arcs (LKT) and ocean floor basalts (OFB). The one analysis plotting just within the field of WPB is not considered to represent magma of the WPB type but a point displaced from the LKT and OFB fields by analytical errors.

Since low-potassium tholeiites of island arcs cannot be distinguished from those of ocean floor basalts on the basis of the Ti-Zr-Y discriminant, all non "within-plate basalts" are plotted on a Ti-Zr variation diagram (Fig. 4.6) which provides a better discrimination between OFB and LKT basalts. Fig. 4.6 indicates that rocks of both island arc and ocean floor

affinity occur in the Grong area. In field B of this diagram there is an overlap of OFB and LKT compositions.

In Fig. 4.6 the andesite from the Skorovas mine plots within the field for CAB (see also Fig. 4.5) and although the majority of the analyses plot within the fields of LKT and LKT+OFB a number of analyses do plot firmly in the fields for OFB alone. Those analyses plotting firmly within the OFB field include No. 148, from the Sanddøla area, as well as four (Nos. 139, 140, 313, 325) from the Bjørkvatn-Gjersvik profile; it should be noted that the three analyses connected by a dashed line could belong to field B since the symbol 'x' represents the position that these points would occupy if the  $\text{TiO}_2$  values obtained from the check wet chemical analyses were used in preference to those obtained by quantometric analysis.

A Ti-Zr-Sr discriminant can be used to separate OFB, CAB and LKT basalts as in Fig. 4.7. This diagram can, according to Pearce and Cann (1973), be misleading since Sr is a mobile element that can be removed during greenschist facies metamorphism and spilitisation. The depletion of Sr in some rocks and not in others in response to these two factors can account for the shift away from the Sr apex of a number of samples that should otherwise, on the basis of the Ti-Zr-diagram, have plotted in the LKT field.

It has been proposed (J. Pearce pers. comm. 1974) that a Ti-Cr discriminant can be used to distinguish OFB and LKT basalts. When the Grong analyses are plotted on such a diagram, Fig. 4.8, the majority of the analyses do plot within the field for LKT; however several analyses which should have plotted in the OFB field now plot in the LKT field i.e. they have Cr contents that are lower than those normally found in the ocean floor basalts. Three of the analyses (2444, 2560, 2743 in Table 4.2) which plot in the OFB field on the Ti-Cr diagram do, in fact, plot in the field of overlapping OFB and LKT compositions on the Ti-Zr diagram, i.e. field B of Fig. 4.6. However, the three samples from the Bjørkvatn-Gjersvik profile that plot firmly in the OFB field on the Ti-Zr diagram now plot in the LKT on Fig. 4.7, but only one of the Sanddøla OFB (No. 15) of Fig. 4.6 fails to plot in the OFB field of the Ti-Cr diagram. This apparent discrepancy in the Ti-Zr and Ti-Cr discriminants does not appear to be a result of analytical errors since the difference in Cr needed for the samples in question to plot in the OFB field is several hundred ppm Cr. It would then appear that some overlap in compositions of Cr contents can occur between ocean-floor and low potassium tholeiites of island arcs and the Ti-Cr discriminant is not totally effective in dis-

criminating these two rock-types: this is to be expected since the temperature-pressure conditions of magmas generated at ocean ridges and in the initial island arc phases can conceivably overlap especially if one is dealing with marginal basin spreading.

#### 4.8 Summary.

The greenstones of the Joma mine area are geochemically comparable to those near the Solberg farm which represent the southward continuation of the Joma greenstone unit (cf. Foslie's geological maps Namsvatn and Tunnsjøen). The Joma greenstone series is more alkaline than greenstones sampled elsewhere in the Grong area and exhibits trace element characteristics of "within plate" or "hot-spot" volcanics. The presence of abundant pillow lavas in the Joma greenstone series indicate a submarine environment of extrusion which together with the presence of abundant black shale and graphitic schists suggests that these within-plate basalts were probably formed in an oceanic island rather than a continental environment. However, we can not entirely rule out an environment of formation in which the magma was intruded through a thin continental crust with subsequent extrusion into a shallow marine basin.

The tholeiites basalts and basaltic andesites of the Bjørkvatn-Gjersvik profile appear to be dominantly of island arc affinity. Although several of the trace element discriminants suggest the presence of minor ocean floor material, the data are inconsistent and probably simply reflect local variations in the early island arc magma since there is no known consistent tectonic or stratigraphical restriction to the possible ocean floor material which is scattered throughout the Bjørkvatn-Gjersvik greenstone unit.

The samples of extrusive keratophyre have remarkably similar compositions, yet the Bjørkvatn acid pyroclastic unit does have significantly more  $K_2O$  and Rb than other acidic extrusives in the Grong area.

The analyses of greenstones from the "other" areas, i.e. the scattered individual samples, are tholeiitic and appear to contain both island arc and ocean-floor material. However, the sampling is too widely distributed to warrant the drawing of any firm conclusions on the nature of the magmatism but does serve as a basis for further studies. It is of interest that no compositions comparable to the Joma greenstone suite have been encountered elsewhere in the Grong area.

Five analyses from the Sanddøla area indicate that both island arc and ocean floor magmas exist in that area. Although the three analyses which consistently plot as ocean floor type basalts are restricted to the greenstone unit in the Hotjern area, Killingberget, this pillow lava sequence is only a few hundred meters thick and without other supporting geological evidence the writer considers it premature to assign a mid-ocean ridge environment for the generation of the basaltic magma in this area and an island arc environment for those of the Møklevann - Langtjern area, even though there are geological features to support the latter.

The Sanddøla trondhjemite was intruded into the greenstones of the Møklevann - Langtjern area and also those of the Nesaavann area prior to development of the regional tectonic fabric but near the end stages of the volcanic activity since trondhjemite dikes intrude conglomerates derived from the greenstone terrain. This indicates that the trondhjemite was intruded into the island arc sequence and is an island arc intrusion of a calc-alkaline magma (see analyses 272) with 1,5%  $K_2O$  and 65%  $SiO_2$ .

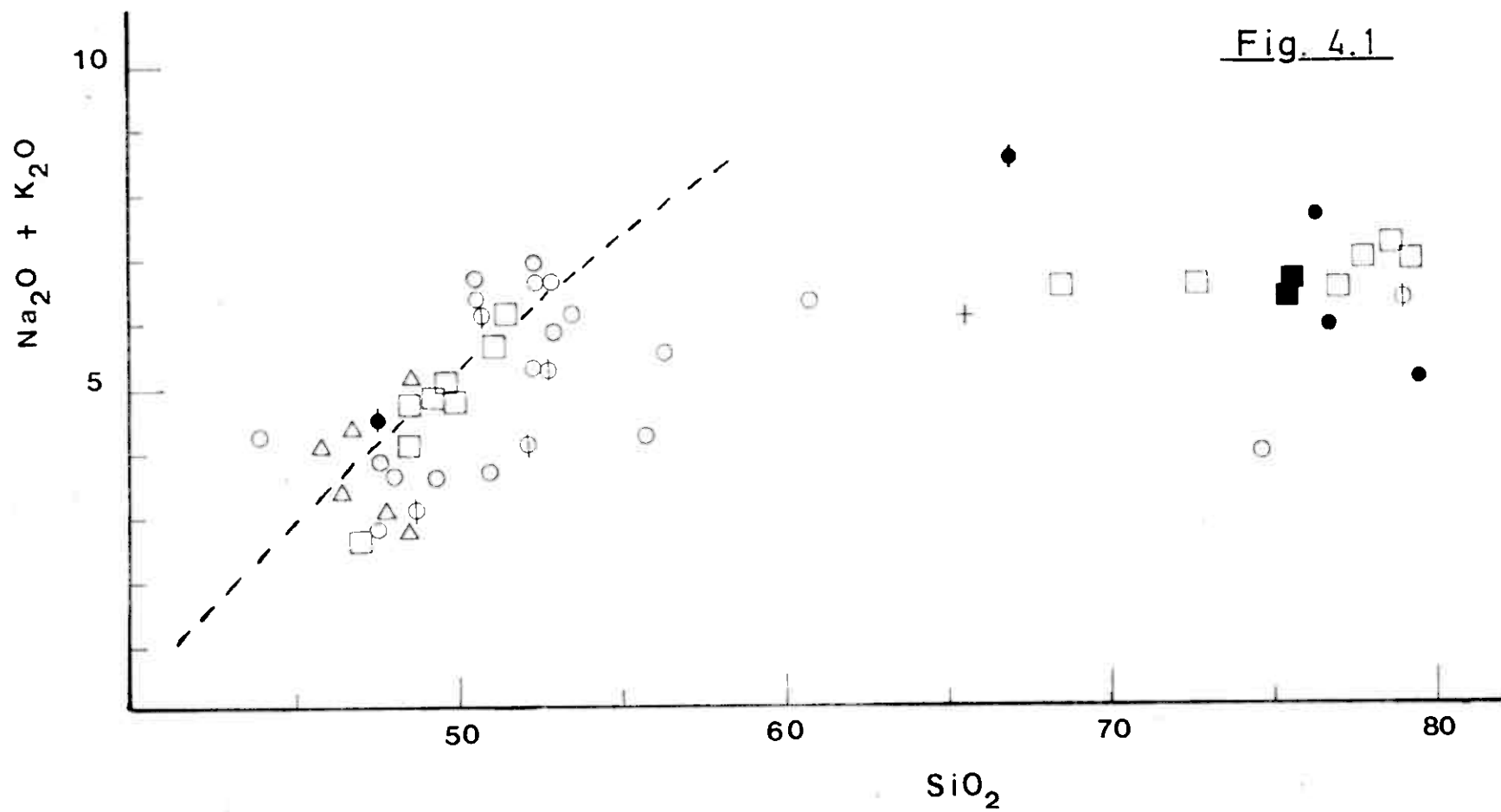
In addition to the calc-alkaline andesite reported here, other calc-alkaline extrusives as well as ocean-floor type basalts and early island arc tholeiites have been found in the general vicinity of the Skorovass mine by C. Halls and co-workers (Comm. read at the NATO symposium in Corner Brook, Newfoundland, May 1974). Thus it appears that the Grong area magmas represent a dominantly island arc series containing tholeiitic and calc-alkaline extrusives and that ocean-floor material is of limited areal extent and probably restricted to wedges that have been incorporated into the island arc material during obduction.

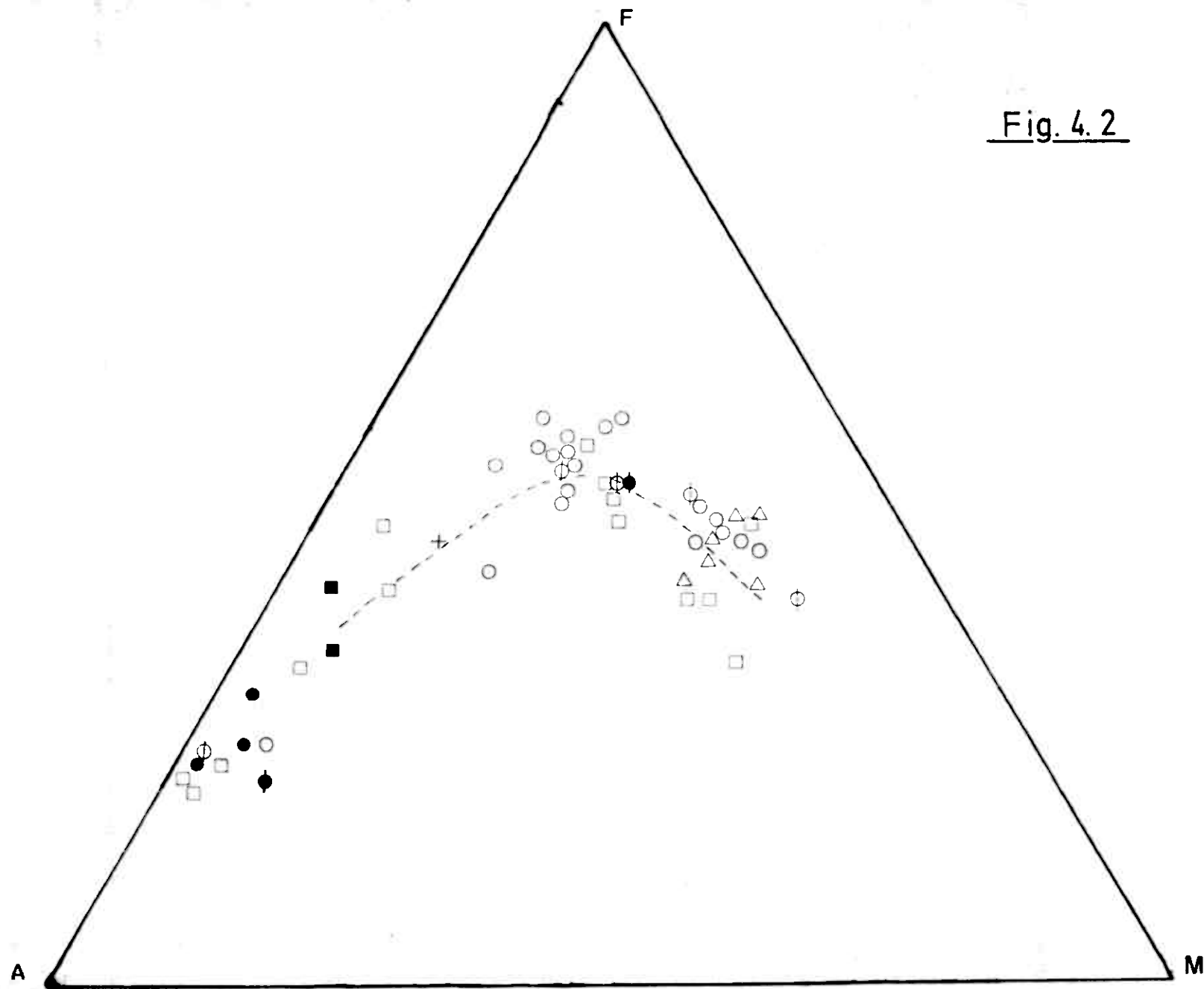
Captions for figures in section 4.

Figure 4.1 Alkali-Silica variation diagram for rocks of the Grong area. Oxides as wt.% (volatile free). The boundary line separating alkaline compositions (above) from subalkaline compositions (below) is after Irvine and Barager (1971). The symbols identifying rocks from the subareas are:  $\emptyset$  Sanddøla;  $\Delta$  Joma; + Skorovatn;  $\circ$  Bjørkvatn-Gjersvik;  $\square$  Other areas (samples scattered over other parts of the Grong Concession area). Solid symbols represent intrusive rocks.

- Figure 4.2  $A(\text{Na}_2\text{O} + \text{K}_2\text{O}) - F(\text{FeO, total Fe}) - M(\text{MgO})$  variation diagram. The boundary line separating tholeiitic compositions (above) from calc-alkaline compositions (below) is after Irvine and Barager (1971). Symbols as in Fig. 4.1.
- Figure 4.3  $\text{FeO} - \text{FeO}/\text{MgO}$  and  $\text{SiO} - \text{FeO}/\text{MgO}$  variation diagrams. Oxides as wt.% (volatile free); total iron as FeO. The field boundaries separating the tholeiitic (TH) and calc-alkaline (CA) series and the trend lines for abyssal tholeiites (A) and the Macauley Island tholeiites (M) are after Miyashiro (1974). Symbols as in Fig. 4.1.
- Figure 4.4  $\text{TiO}_2 - \text{FeO}/\text{MgO}$  variation diagram. The trend lines for abyssal tholeiites (A), the Macauley Island tholeiite series (M) and the Cyprus tholeiite series (CY) are after Miyashiro (1974). Symbols as in Fig. 4.1.
- Figure 4.5 Discriminant diagram using Ti, Zr, Y to distinguish "within plate" basalts (field D) from ocean floor type basalts (field B), calc-alkaline basalts (field C) and low potassium tholeiites of island arcs (fields A and B). Field boundaries after Pearce and Cann (1973). Symbols as in Fig. 4.1.
- Figure 4.6 Discriminant diagram using Ti and Zr for distinguishing ocean floor type basalts (fields B and D), calc-alkaline basalts (field C) and low-potassium tholeiites of island arcs (fields A and B). Field boundaries after Pearce and Cann (1973). Symbols as in Fig. 4.1.
- Figure 4.7 Discriminant diagram using Ti, Zr and Sr for distinguishing ocean floor type basalts (field C), low-potassium tholeiites (field A) and calc-alkaline basalts (field B). Field boundaries after Pearce and Cann (1973). Symbols as in Fig. 4.1.
- Figure 4.8 Discriminant diagram to distinguish ocean floor basalts (field A) from low-potassium tholeiites of island arcs (field B). The field boundary is after Pearce (Pers. comm. 1974). Symbols as in Fig. 4.1.







15 FeO

10

5

2

4

6

FeO/MgO

SiO<sub>2</sub>

70

60

50

2

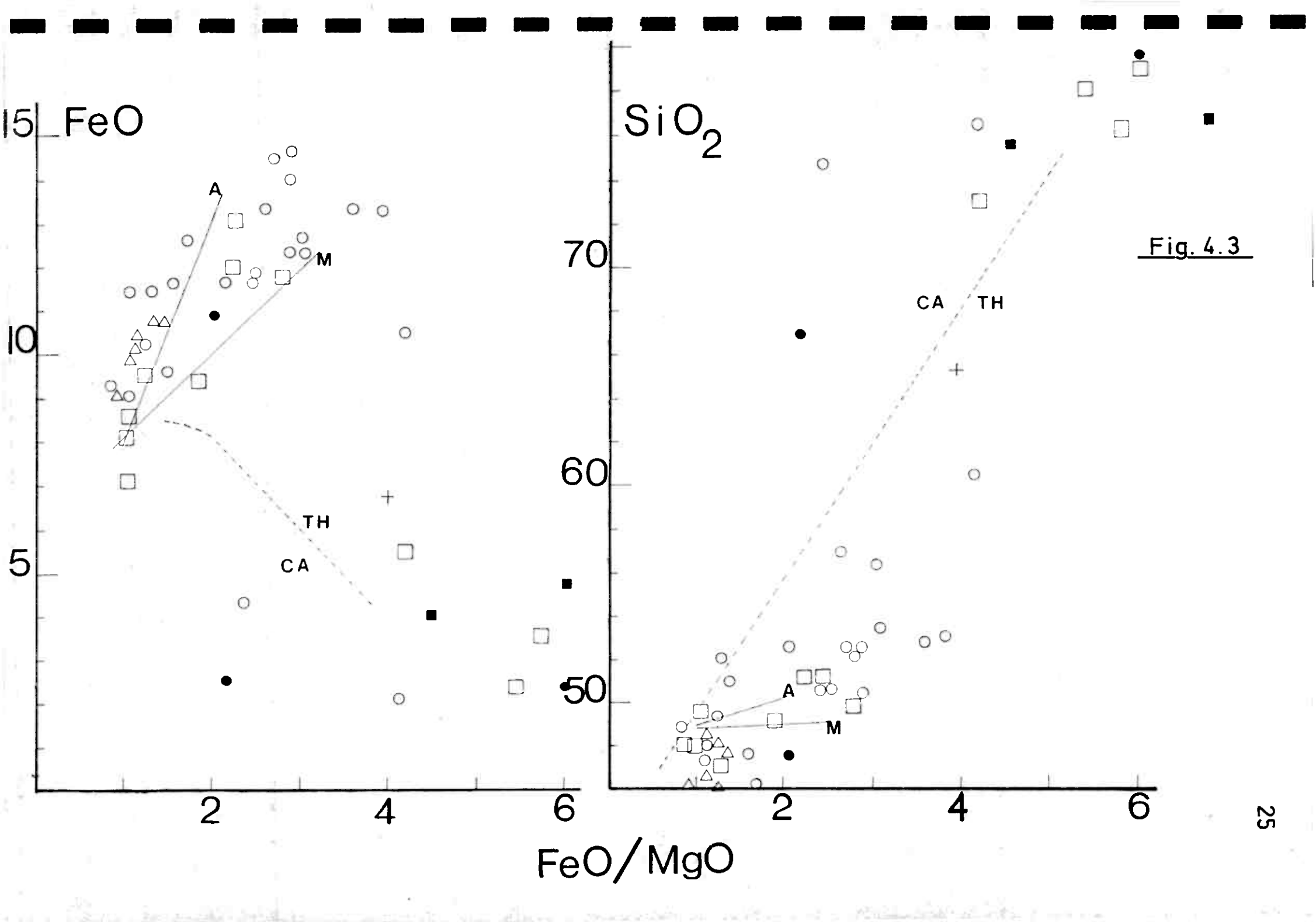
4

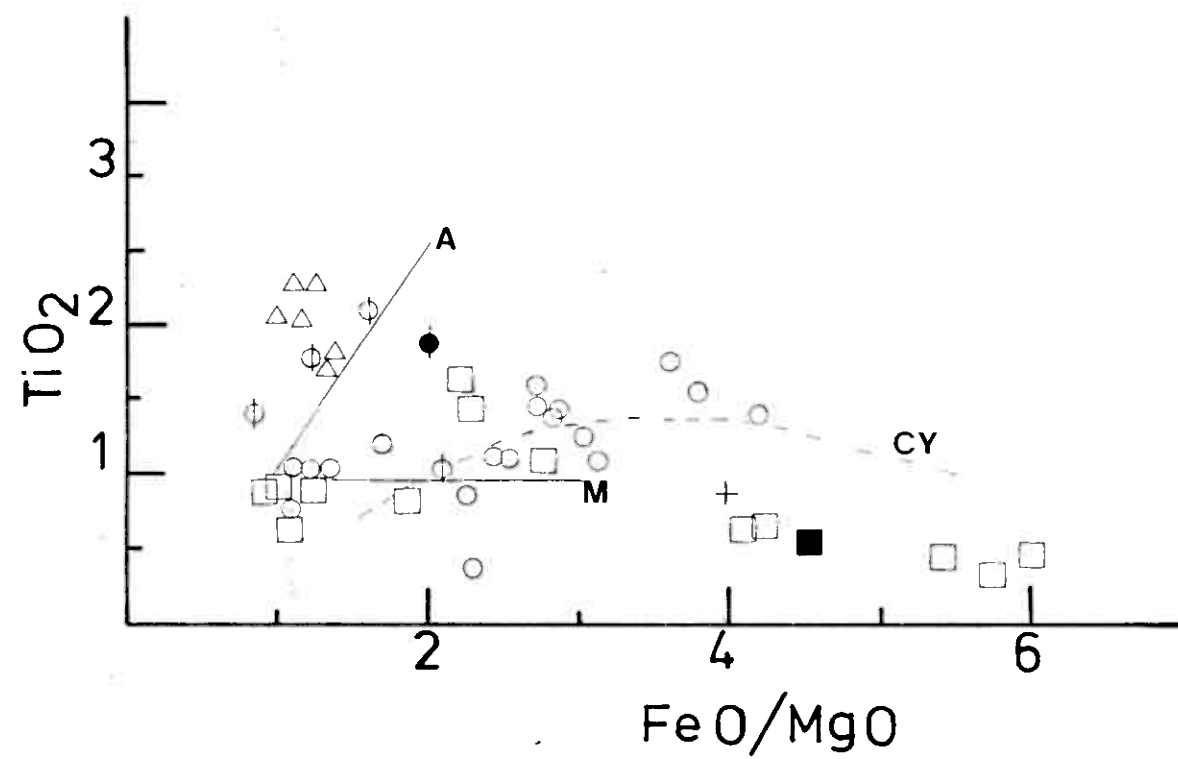
6

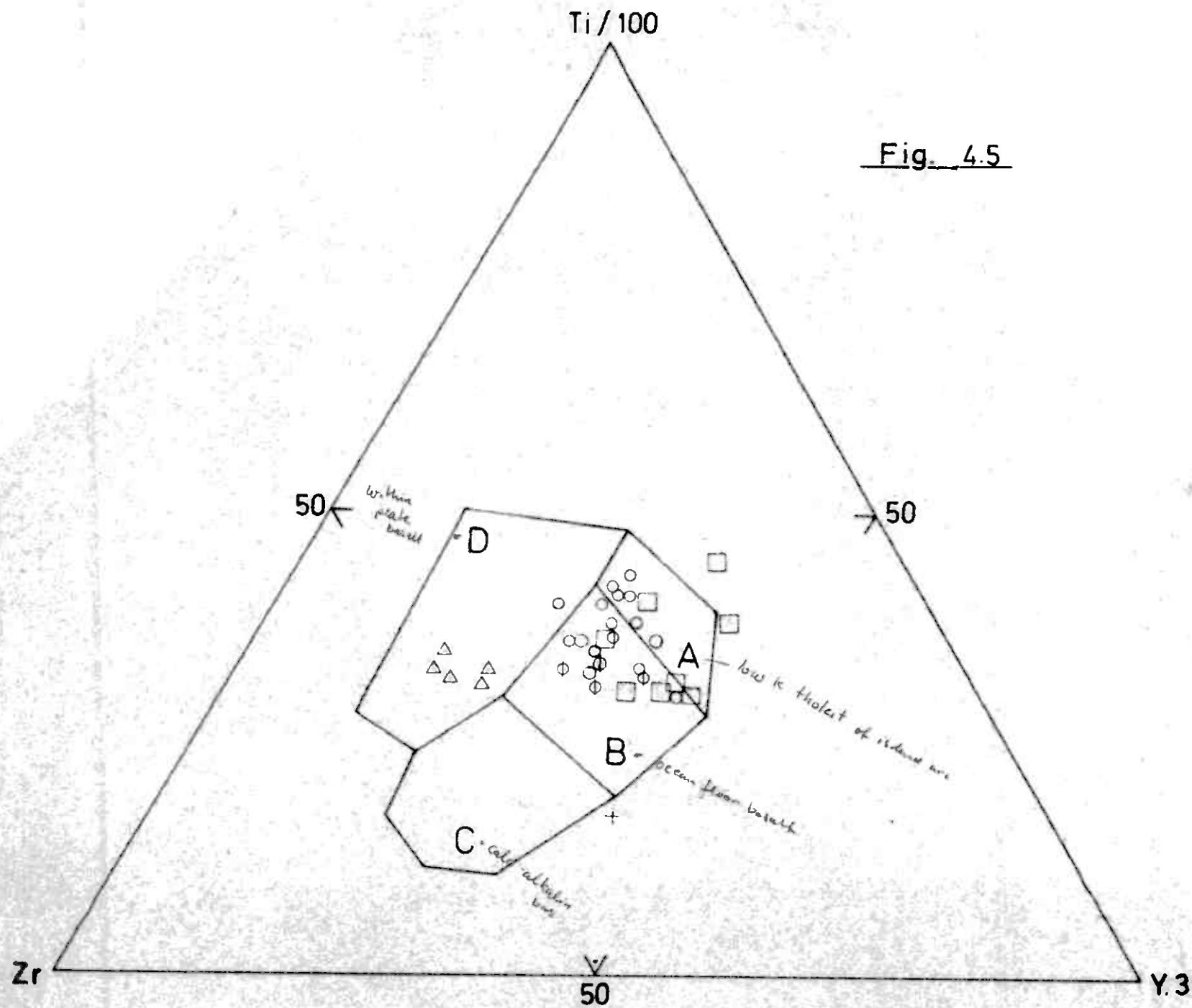
CA

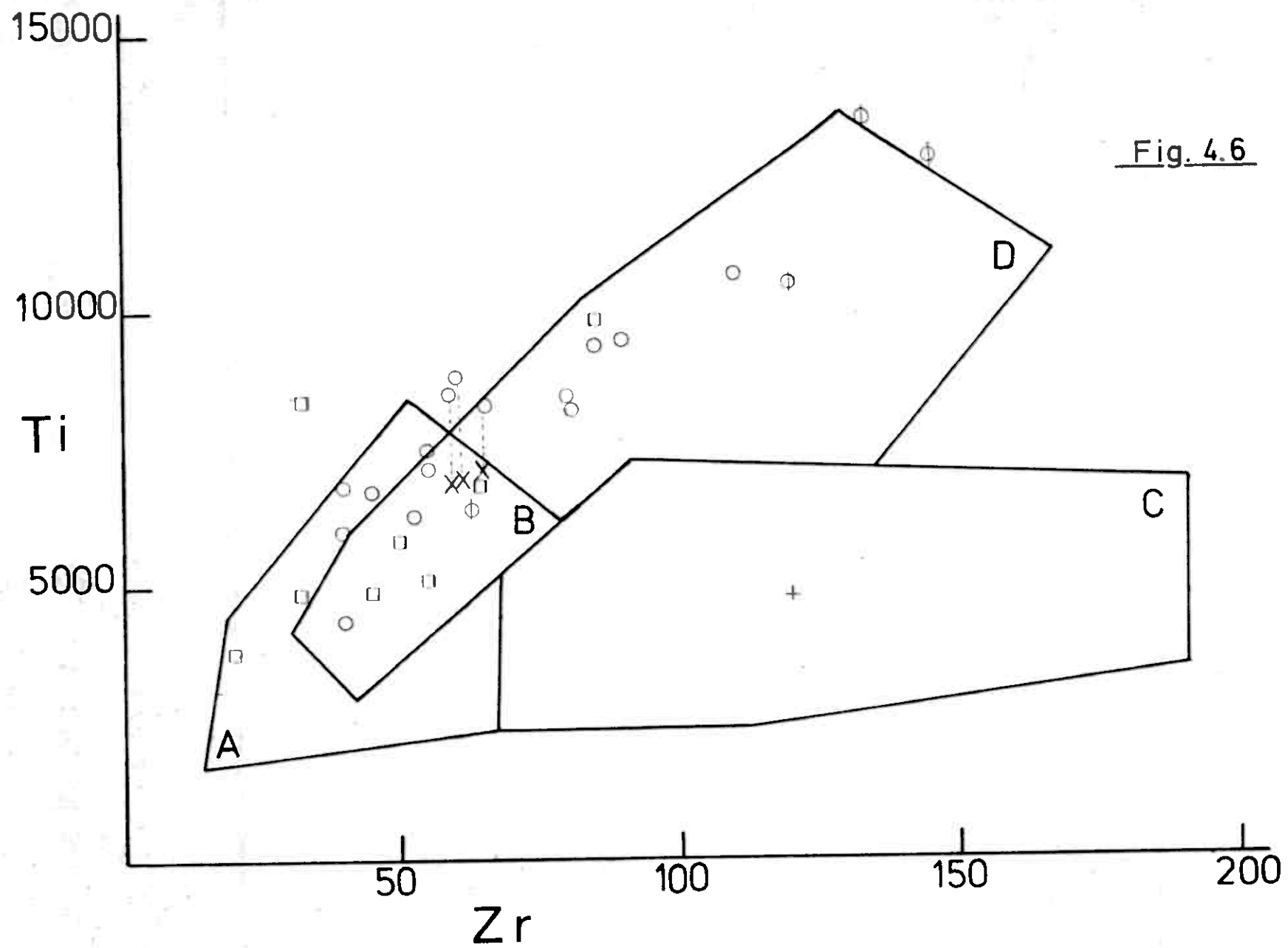
TH

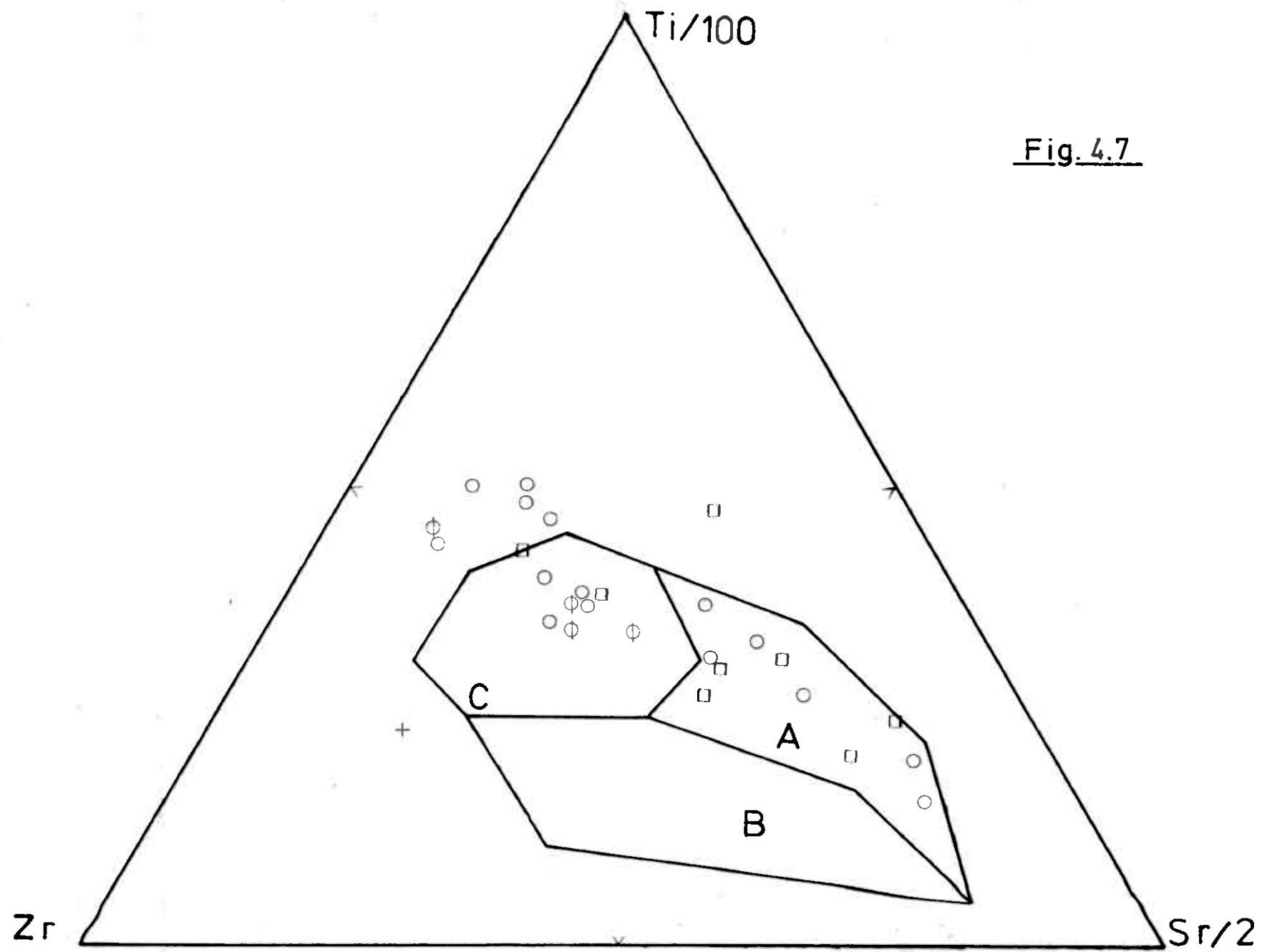
Fig. 4.3

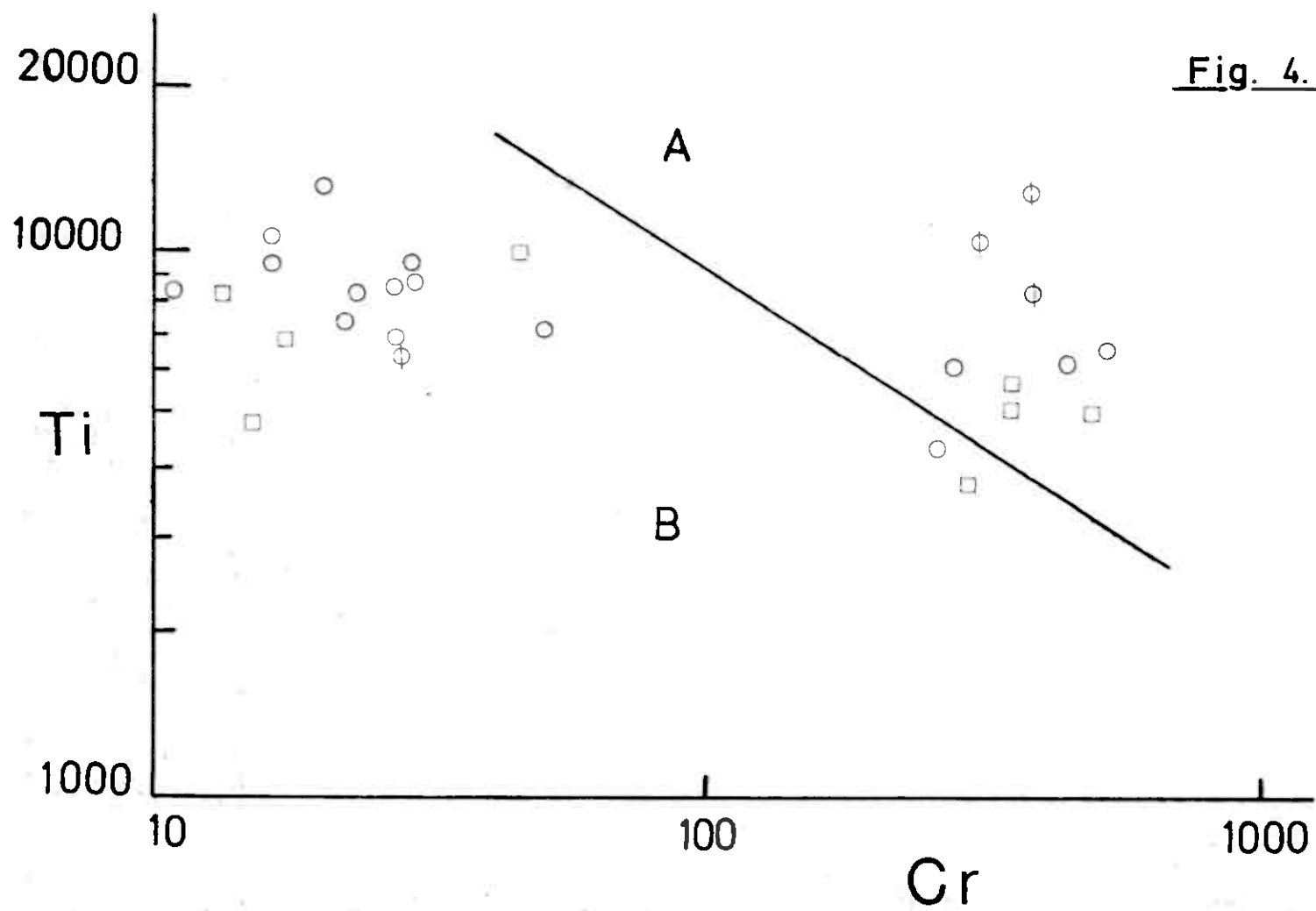














## 5. THE LØKKEN AREA

### 5.1 General geology.

The following brief account of the Løkken area geology is based largely on personal communications by G. Grammeltvedt and Dr. Ei Horikoshi, and short field excursions to the area. Detailed geological studies of the Løkken area are in progress and will be published in the near future (Horikoshi, pers. comm., 1974).

The greenstones of Løkken area form part of the Støren Group. These are bounded by schists and gneisses of the Gula Group in the north and by sedimentary rocks of the Hovin Group to the south. The Støren Group volcanics are in many places inverted (pillow attitudes) and the sediments of the Hovin group are also inverted (graded bedding). The overall major structure of the area is thus probably that of an inverted synform as a result of post- $S_1$  folding. In general, the Støren Group can be divided into at least two formations: a lower greenstone formation (LGF) and an upper greenstone formation (UGF). The lower greenstone occupies the core of the major synform, is at least several kms thick, and consists mainly of basaltic lavas and pillow lavas and gabbroic bodies which can be more than 1 km thick.

The lower greenstone is underlain on the north and south by the upper greenstone formation which attains a thickness of up to several kms in several places. This unit contains, in addition to basaltic lava and pillow lava, abundant basaltic pyroclastics and tuffs; jasper horizons can often be followed for several kms and minor sediments are occasionally present between successive lava units. A characteristic feature of this unit is the cyclical nature of the volcanism which in a complete cycle consist of (from bottom to top) basaltic lava - basaltic pillow lava - basaltic pyroclastics - jasper. Horikoshi (pers. comm. 1974) has been able to further subdivide the upper greenstone formation referred to here into two units, middle and upper. The upper greenstone is structurally underlain by metasediments of the lower Hovin Group which are stratigraphically younger than the Støren Group.

### 5.2 Analytical data.

The analyses of 49 samples collected in 1973 are presented in Part II of this report (NGU rapport 1228 B). The majority of these samples were

collected from the lower greenstone formation. One complete analysis and 12 partial analyses of drill core samples from holes drilled into the upper greenstone formation underlying the Løkken ore body are presented in Table 5.1.

### 5.3 Geochemistry.

The 49 analyses contained in Rapport 1228 B can be grouped as follows:

	No of Samples
Gabbro and dolerite	8
Basaltic lava and pillow lava	35
Agglomerate	4
Keratophyric intrusives	2

The 12 drill-core samples were taken from basaltic lava and pillow lava.

Mean, minimum and maximum values, and standard deviations for the basaltic lavas and agglomerates are given in Table 5.2 and the corresponding values for the basic intrusives are presented in Table 5.3. These values have not been recalculated on a volatile-free basis. Volatile free major element values have, however, been used in the preparation of the diagrams.

The alkali-silica diagram, Fig. 5.1, shows an absence of andesite lavas in the Løkken area. On a volatile-free basis the basic volcanics and intrusives have from 47 to 56 percent  $\text{SiO}_2$ , i.e. they are mainly basalts (less than 52%  $\text{SiO}_2$ ) with a few analyses falling within the  $\text{SiO}_2$  range of basaltic andesite (Jakeš and White, 1972).

It can be seen from Fig. 5.2 that the Løkken rocks (the 2 Keratophyres are not included in the following description) plot about the dividing line for alkaline and subalkaline basalts (Irvine and Barager, 1971). This is considered to be a result of Sodium addition during spilitization since it can be seen from Table 5.2 that the mean  $\text{K}_2\text{O}$  value is 0.31% with a standard deviation of 0.29%, well below the values found in alkaline basalts.

In Fig. 5.2, AFM diagram, the Løkken rocks show a tholeiitic trend but plot about the dividing line separating tholeiitic and calc-alkaline compositions (Irvine and Barager, 1971). Samples plotting in the calc-alkaline field of this diagram are considered to have undergone Sodium metasomatism. The iron enrichment trend for the intrusive rocks is apparent from this diagram. In Fig. 5.3 the tholeiitic nature of the volcanism is readily apparent from both the  $\text{FeO} - \text{FeO}/\text{MgO}$  and the  $\text{SiO}_2 - \text{FeO}/\text{MgO}$

Table 5.1 Additional data for the upper greenstone member, LØKKEN.

No.	DDH	Section	TiO <sub>2</sub>	Zr	Y	Sr	Rb	Zn	Cu	Ni	Cr	BA
1.	1089:	215 - 16.	1.23	78	25	195	0	77	0	39	154	41
2.	1091:	265 - 66.	1.10	68	20	203	0	50	0	38	143	19
3.	1240:	282 - 83.	1.07	60	19	165	0	69	45	51	162	82
4.	1240:	290 - 91.	1.30	75	23	172	0	61	25	65	191	35
5.	1240:	303 - 04.	1.09	71	19	153	0	72	67	12	186	112
6.	1240:	318 - 19.	1.04	53	19	103	2	34	37	63	262	62
7.	1240:	344 - 45.	1.13	71	28	201	4	85	35	168	387	0
8.	1240:	356 - 57.	1.00	59	18	144	0	67	32	132	309	5
9.	1240:	378 - 79.	1.32	54	21	128	0	78	41	119	310	77
10.	1240:	385 - 86.	1.09	63	20	173	4	74	26	110	280	59
11.	1241:	291 - 92.	1.18	68	24	242	0	71	35	15	215	31
12.	1240:	336 - 37.	1.10	54	20	121	0	72	32	123	312	59

12. 1240: 336-37

SiO <sub>2</sub>	45.39	Na <sub>2</sub> O	4.35
TiO <sub>2</sub>	1.10	K <sub>2</sub> O	0.59
Al <sub>2</sub> O <sub>3</sub>	15.33	H <sub>2</sub> O <sup>-</sup>	0.05
Fe <sub>2</sub> O <sub>3</sub>	2.37	H <sub>2</sub> O <sup>+</sup>	3.94
FeO	7.28	CO <sub>2</sub>	3.28
MnO	0.18	P <sub>2</sub> O <sub>5</sub>	0.08
MgO	6.87		
CaO	10.09	Total:	1000.90

Diamond drill hole 1089, section 215-216 meters

Samples supplied by G. Grammeltvedt.

Table 5.2

Summary data for 39 Løkken basalts

ELEMENT	MINIMUM	MAXIMUM	MEAN	STD. DEV
SI02	42.00	54.30	48.42	2.70
AL203	12.90	16.40	14.75	0.87
FE203	9.00	15.00	11.48	1.46
TI02	0.92	1.98	1.45	0.24
MGO	4.30	10.80	7.27	1.32
CAO	4.20	13.20	8.43	2.26
NA20	1.90	6.00	4.05	1.03
K20	0.00	1.12	0.31	0.29
MND	0.14	0.43	0.20	0.05
P205	0.05	0.14	0.09	0.02
L.O.I.	1.52	9.60	3.90	1.89
ZR	52.	137.	97.	23.
Y	14.	39.	26.	5.
SR	47.	347.	155.	78.
RB	0.	18.	3.	5.
ZN	59.	194.	90.	24.
CU	0.	93.	39.	21.
NI	5.	196.	75.	48.
CR	19.	501.	218.	129.
BA	0.	162.	29.	34.

Table 5.3

Summary data for 8 Løkken intrusives

ELEMENT	MINIMUM	MAXIMUM	MEAN	STD. DEV
SI02	45.80	51.70	49.65	1.87
AL203	14.20	16.40	14.89	0.69
FE203	7.80	14.40	11.11	2.06
TI02	1.08	1.62	1.34	0.19
MGO	4.60	9.70	7.40	1.83
CAO	5.80	12.90	8.24	2.52
NA20	2.60	5.20	4.20	0.90
K20	0.00	0.88	0.24	0.29
MND	0.13	0.24	0.19	0.04
P205	0.04	0.12	0.08	0.02
L.O.I.	1.79	4.66	2.76	0.88
ZR	42.	125.	77.	23.
Y	15.	37.	23.	7.
SR	54.	280.	150.	68.
RB	0.	8.	2.	3.
ZN	27.	103.	73.	25.
CU	8.	85.	40.	25.
NI	12.	167.	72.	46.
CR	21.	325.	190.	109.
BA	0.	100.	41.	36.

diagrams even though a few samples plot within the mildly calc-alkaline field (Miyashiro, 1974). On the FeO/MgO diagram the Løkken rocks plot about the trend for abyssal tholeiites (trend A). The tholeiitic trend of the Løkken rocks is further substantiated by the  $\text{TiO}_2$  - FeO/MgO diagram, Fig. 5.4; however, it is significant that the Løkken lower greenstones plot above the general field of Miyashiro's tholeiitic series in island arc systems (Miyashiro, 1974) and also most of them plot outside the field of island arc rocks from the Grong area (cf. Fig. 4.4), but around the trend for abyssal tholeiites.

On the Pearce and Cann (1973) discriminant diagrams the Løkken upper greenstone formation lavas, the lower greenstone formation lavas and the basic intrusives plot consistently in the fields for ocean floor and island arc rocks, (cf. Figs. 5.5, 5.6 and 5.7). On Fig. 5.5 one intrusive and four lavas of the lower greenstone plot within the field for within plate basalts (field D), this is attributed to low Yttrium values<sup>22</sup> for these particular samples which has resulted in their shifting away from the Y-apex of the figure. This is further supported by the fact that the major and trace element concentrations (other than Y) for these samples are similar to those of the other samples which plot in the OFB and LKT fields.

In Fig. 5.6 the majority of the intrusives and the lower greenstone formation lavas plot firmly within the field for ocean floor basalts (field D) while the lavas of the upper greenstone plot mainly in the field of overlapping ocean-floor and island arc compositions (field B).

In Fig. 5.7 the lower greenstone lavas plot mainly within the field of ocean-floor basalts (OFB) while those of the upper greenstone plot near the island arc (LKT) and OFB field boundary. This indicates either that the upper greenstone lavas are of island arc origin and have been depleted in Sr during sea-floor weathering and metamorphism (Pearce and Cann, 1973) or that there is a continuum of compositions between the lower and upper greenstone formation. The samples plotting to the left of the OFB field (field C) in Fig. 5.7 are considered to be ocean-floor basalts that have lost some Sr.

On the Ti-Cr diagram, Fig. 5.8, the majority of the samples fall within the field for ocean floor basalts (field A); however, the lower greenstone samples plotting within the field of island arc rocks (field B) include only 3 of the samples plotting within or close to the field for island arc + ocean-floor rocks in Fig. 5.6. Although the upper greenstone lavas do plot below  
(<sup>x</sup> i.e. analytical error)

those of the lower greenstone lavas on Fig. 5.8, this reflects lower Titanium in the upper greenstone lavas rather than a difference in Cr content.

#### 5.4 Summary.

The basic lavas and intrusives of the Løkken area are splilitized tholeiitic basalts. The trace element contents of these rocks show that the lower greenstone lavas are similar to ocean-floor basalts. Although the upper greenstone lavas as a group have lower Titanium and Zirconium than the lower greenstone lavas and plot within or close to the fields for island arc and island arc + ocean-floor rocks on the Ti-Zr diagram, the upper greenstone cannot be readily separated from the lower greenstone lavas by means of either the Ti-Zr-Sr or Ti-Cr discriminants. This means that it may not be possible to distinguish the earliest island arc tholeiites from those of ocean floor tholeiites. Thus an island arc origin for the upper greenstone formation has not been substantiated, even though it is still a possibility on the basis of the cyclical nature of the volcanism and the abundance of pyroclastic material in the upper greenstone in contrast to the lower greenstones; they could be directly related to the lower greenstones and represent more differentiated material from the same magma chamber. Further studies now in progress are directed towards the question of the origin of the upper greenstone magma.

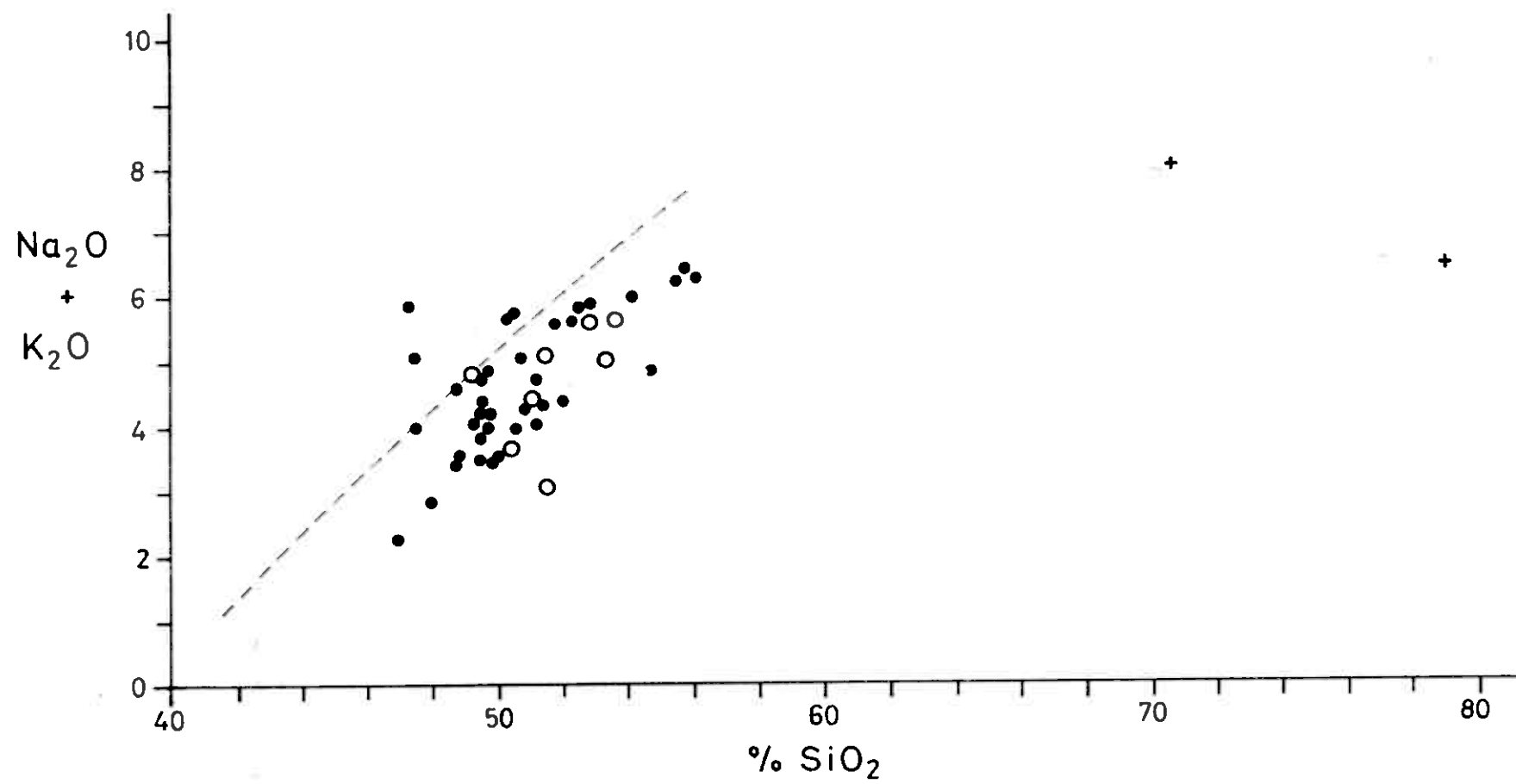
Captions for figures in section 5.

Figure 5.1 Alkali-Silica variation diagram for rocks of the Løkken area. Oxides as wt.% (volatile free). The boundary line separating alkaline compositions (above) from subalkaline compositions (below) is after Irvine and Barager (1971). The symbols identifying different rock types are: ● lower greenstone lavas; ■ upper greenstone lavas; + acidic rocks; ○ gabbro

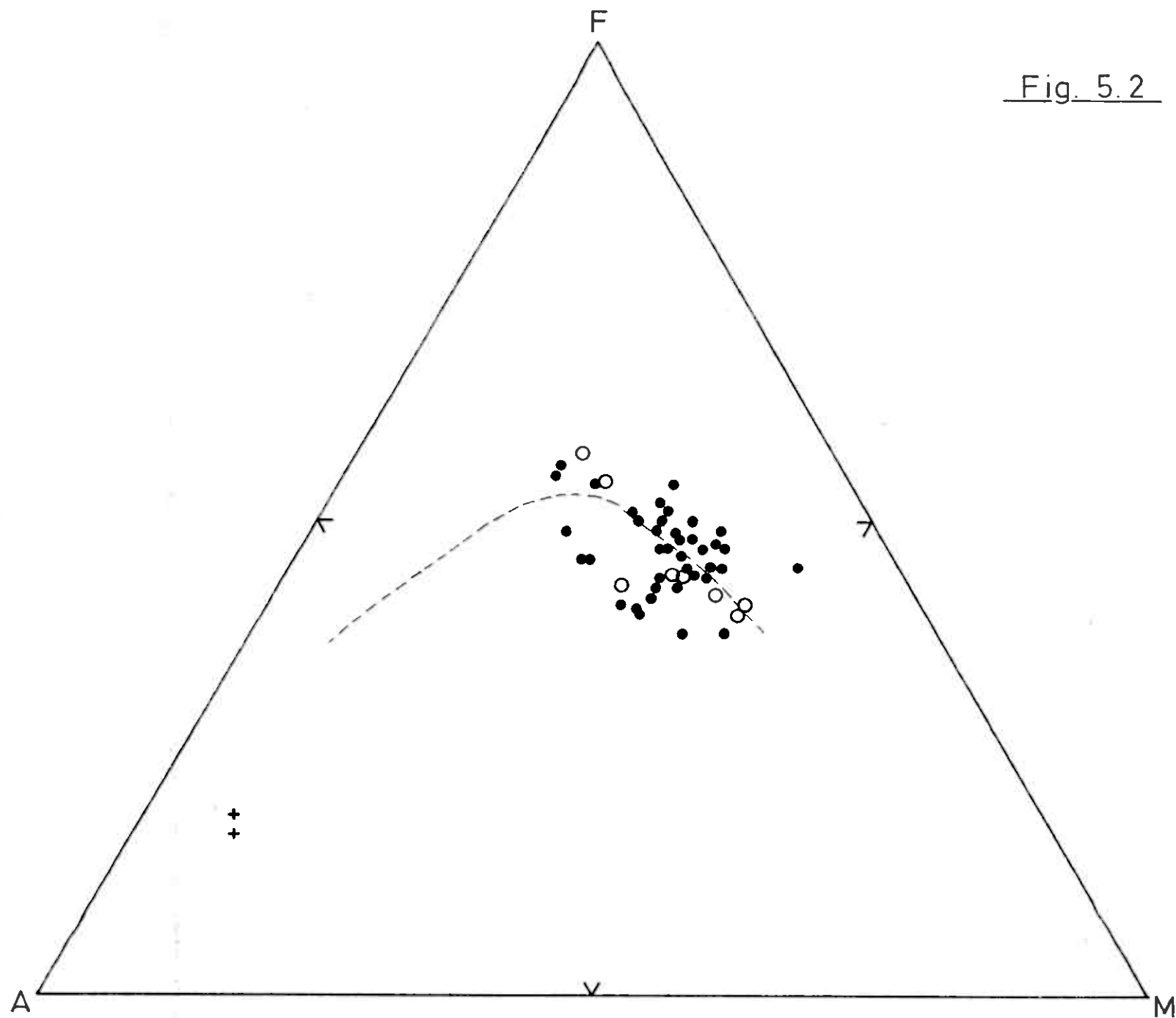
Figure 5.2  $A(\text{Na}_2\text{O} + \text{K}_2\text{O}) - F(\text{FeO, total Fe}) - M(\text{MgO})$  variation diagram. The boundary line separating tholeiitic compositions (above) from calc-alkaline compositions (below) is after Irvine and Barager (1971). Symbols as in Fig. 5.1.

- Figure 5.3 FeO - FeO/MgO and SiO<sub>2</sub> - FeO/MgO variation diagrams. Oxides as wt.% (volatile free); total iron as FeO. The field boundaries separating the tholeiitic (TH) and calc-alkaline (CA) series, and the trend lines for abyssal tholeiites (A) and the Macauley Island tholeiites (M) are after Miyashiro (1974). Symbols as in Fig. 5.1.
- Figure 5.4 TiO<sub>2</sub> - FeO/MgO variation diagram. The trend lines for abyssal tholeiites (A), the Macauley Island tholeiite series (M) and the Cyprus tholeiite series (CY) are after Miyashiro (1974). Symbols for Fig. 5.5 (a) as in Fig. 5.1; as in Fig. 6.1 for Fig. 5.5 (b) - the Støren rocks.
- Figure 5.5 Discriminant diagram using Ti, Zr, Y to distinguish "within-plate" basalts (field D) from ocean floor type basalts (field B), calc-alkaline basalts (field C) and low-potassium tholeiites of island arcs (fields A and B). Field boundaries after Pearce and Cann (1973). Symbols as in Fig. 5.1.
- Figure 5.6 Discriminant diagram using Ti and Zr for distinguishing ocean-floor type basalts (fields B and D), calc-alkaline basalts (field C) and low-potassium tholeiites of island arcs (fields A and B). Field boundaries after Pearce and Cann (1973). Symbols as in Fig. 5.1.
- Figure 5.7 Discriminant diagram using Ti, Zr and Sr for distinguishing ocean-floor type basalts (field C), low-potassium tholeiites (field A) and calc-alkaline basalts (field B). Field boundaries after Pearce and Cann (1973). Symbols as in Fig. 5.1.
- Figure 5.8 Discriminant diagram to distinguish ocean-floor basalts (field A) from low-potassium tholeiites of island areas (field B). Symbols as in Fig. 5.2. The field boundary is after Pearce (pers. comm., 1974).

Fig. 5.1







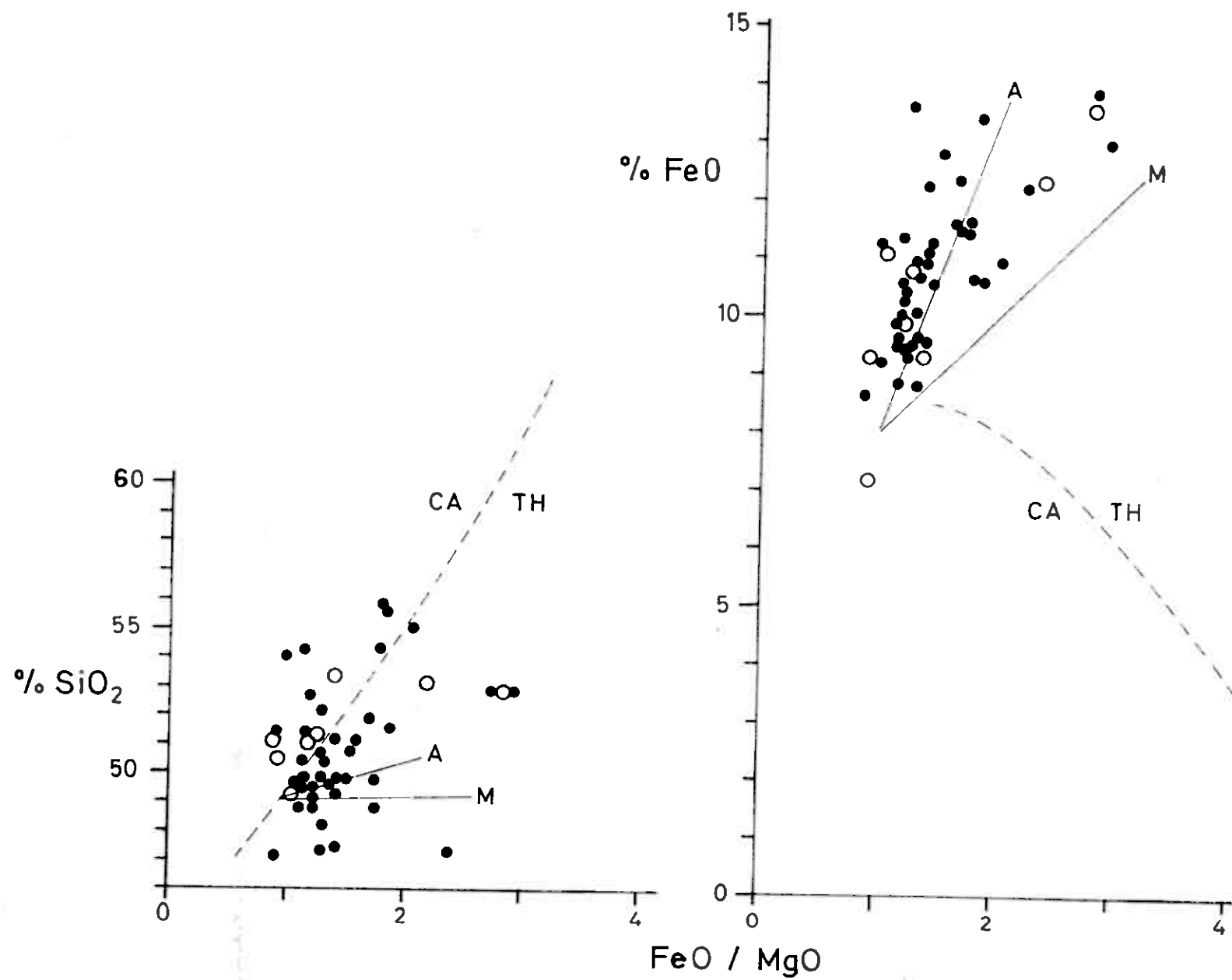


Fig. 5.3

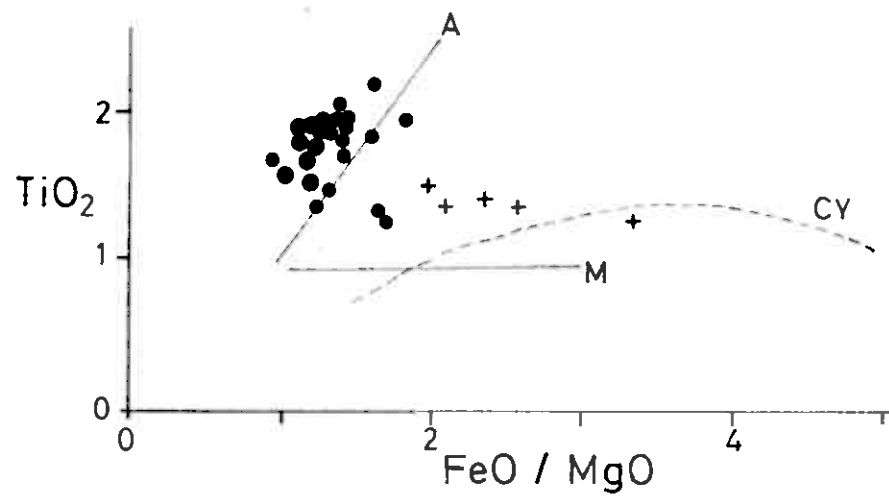


Fig. 5.4 (b)

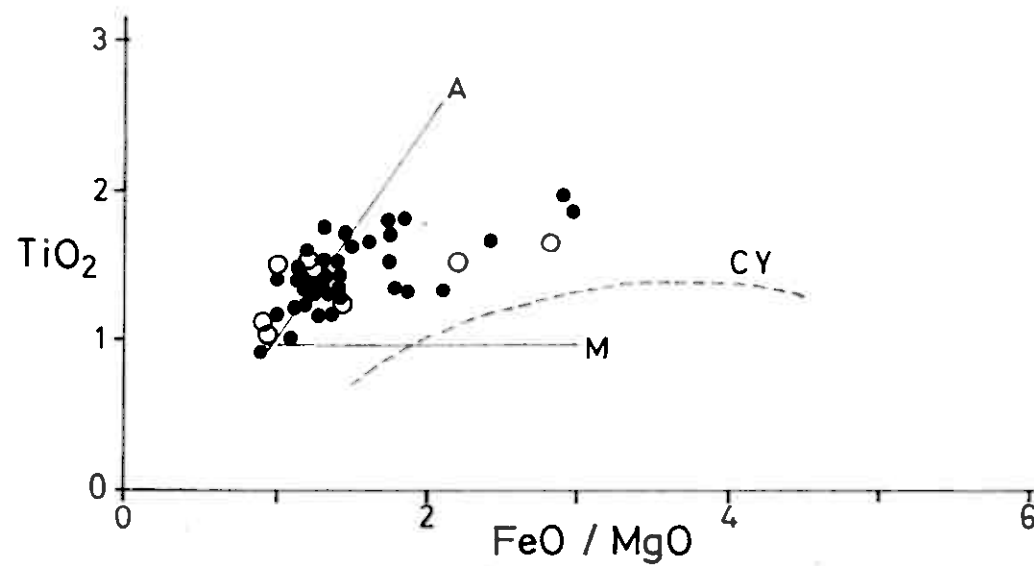
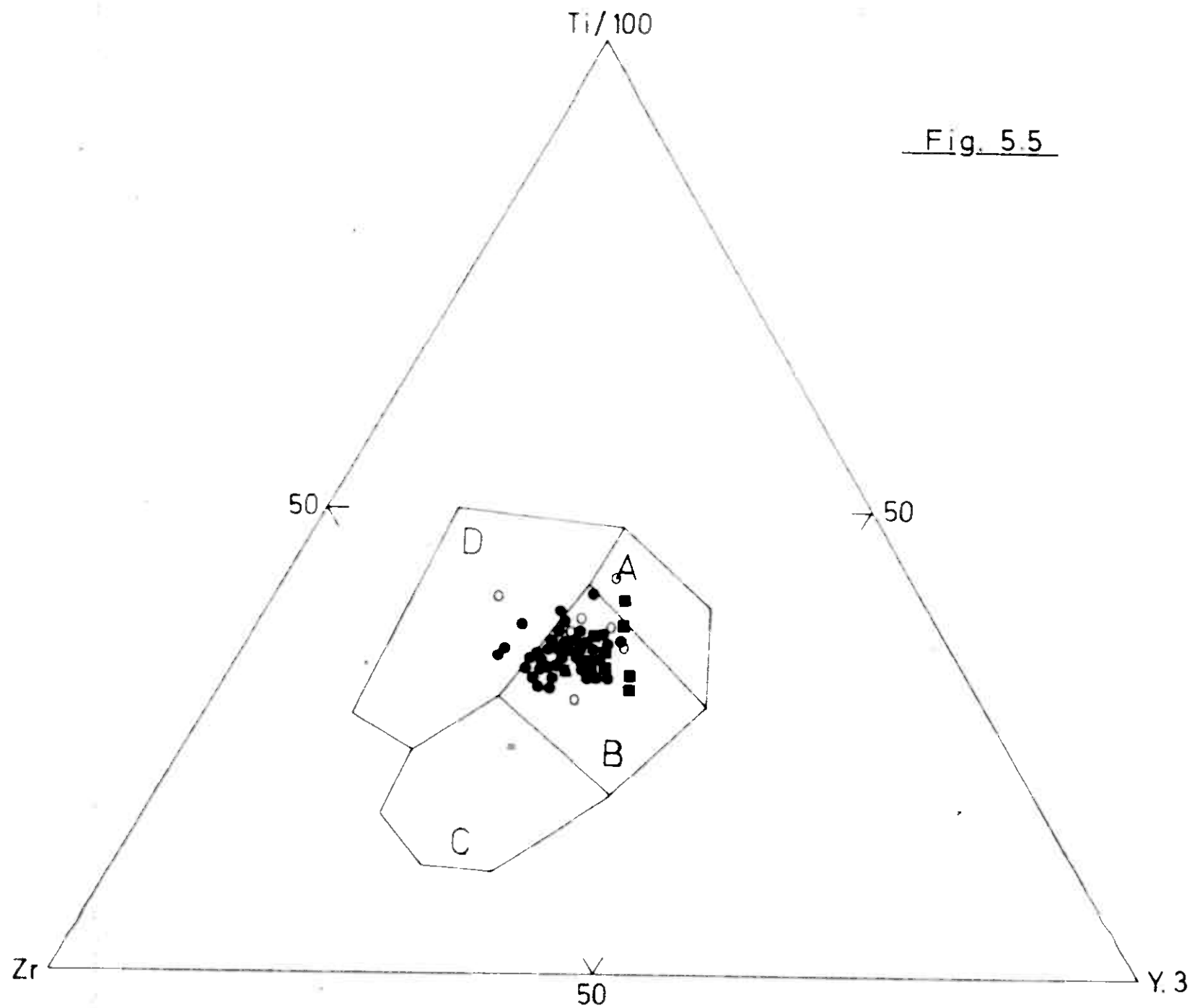
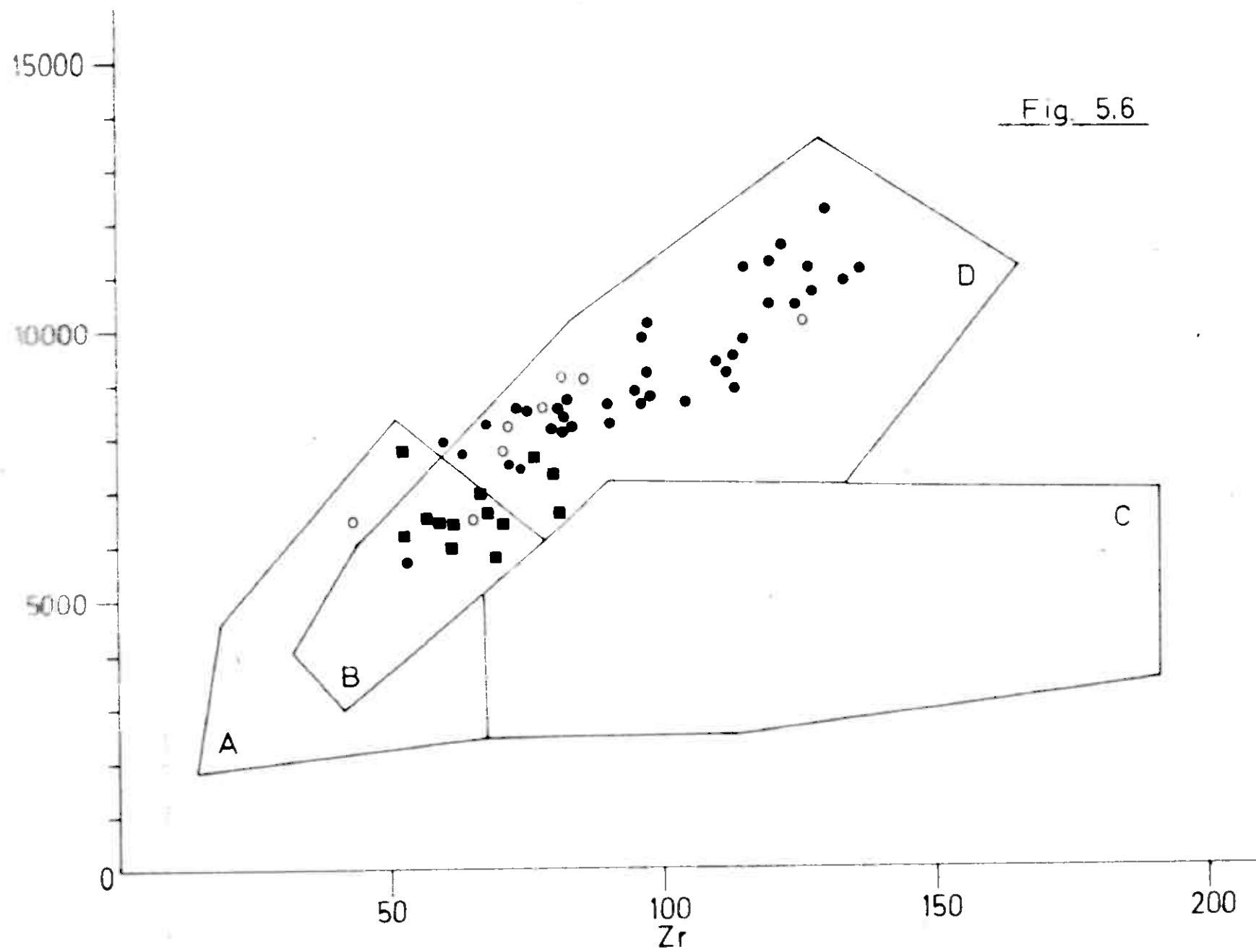
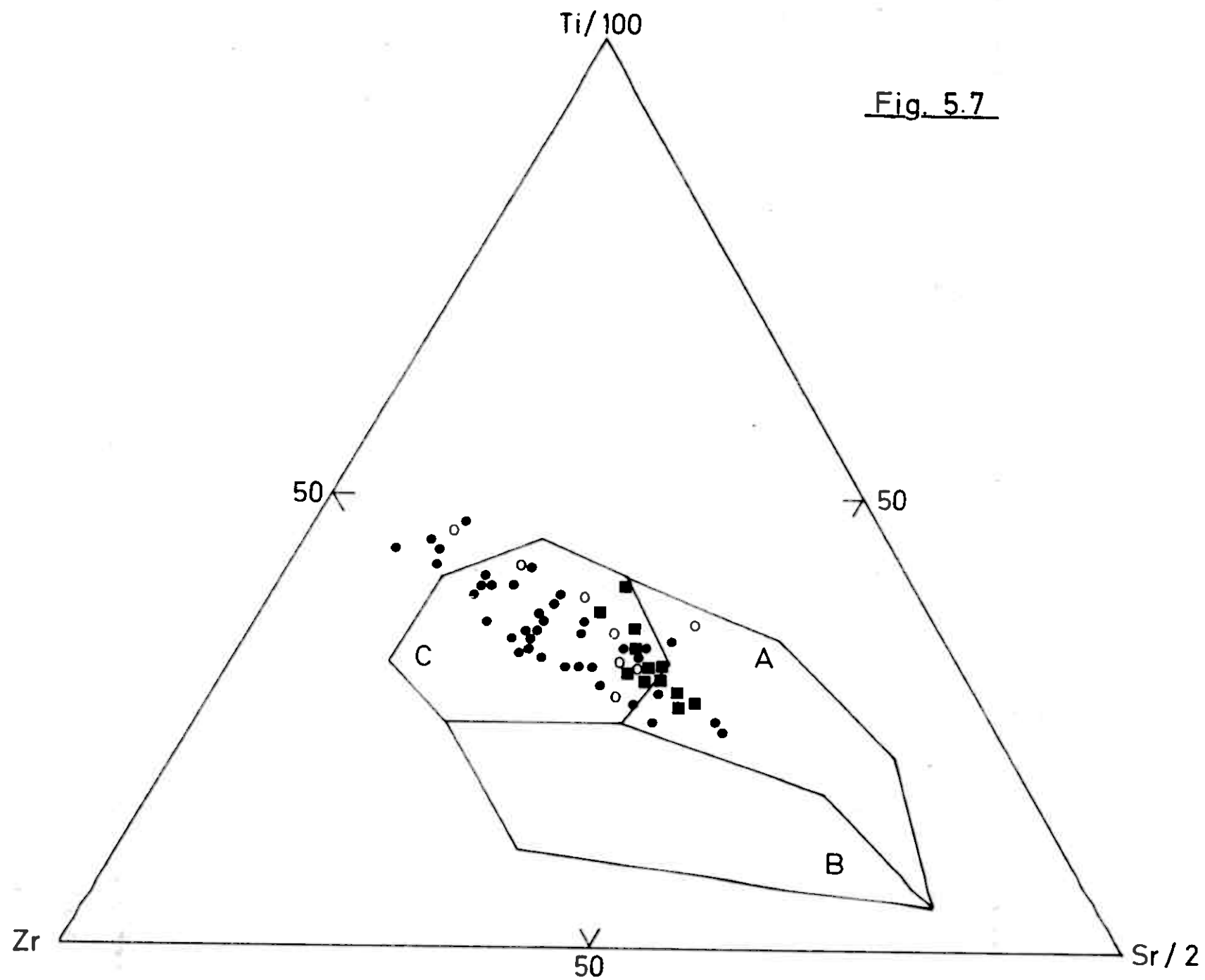
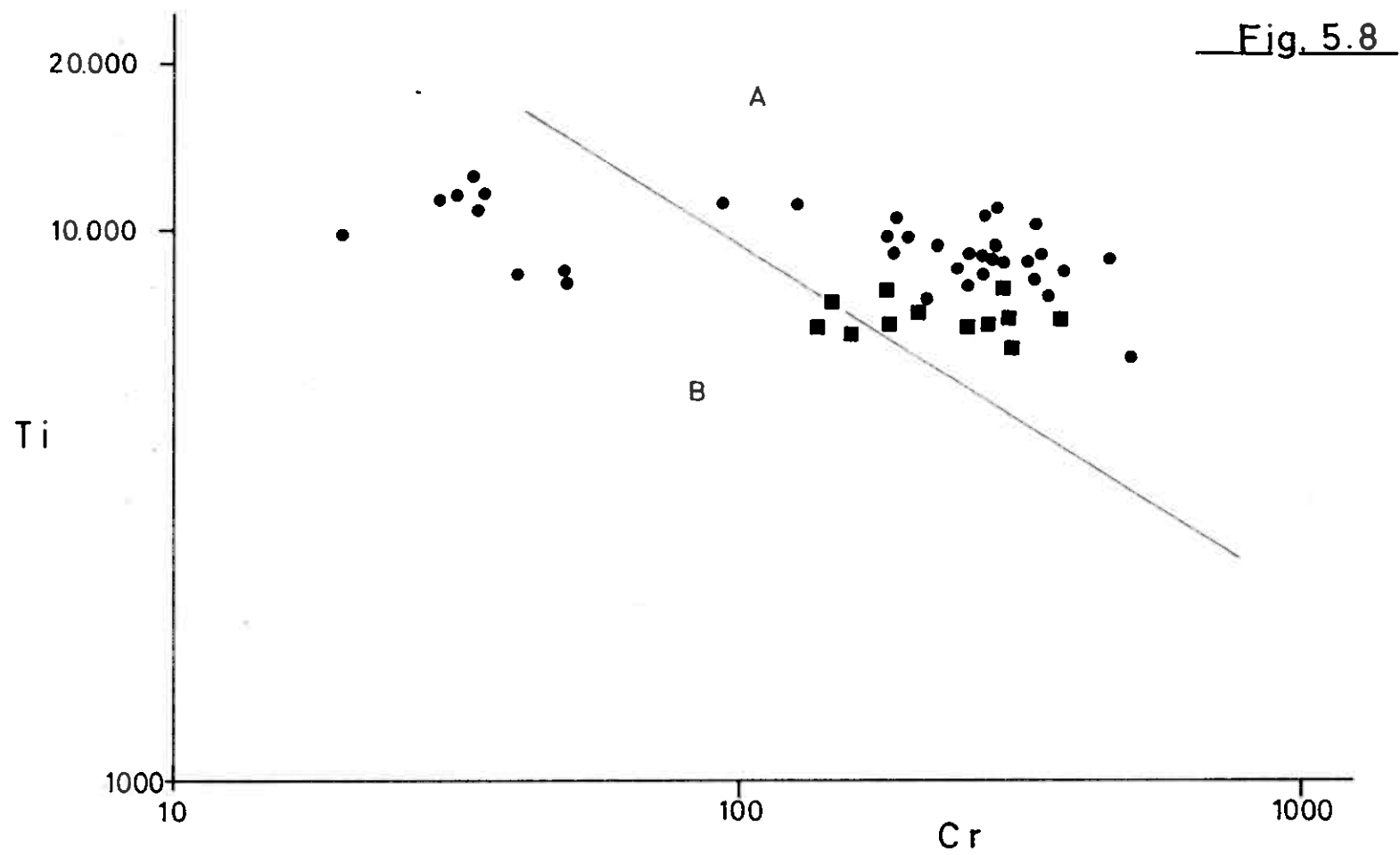


Fig. 5.4 (a)









## 6. STØREN AREA

### 6.1 Introduction.

A suite of samples was collected in the vicinity of the Haga bridge in order to obtain an idea of the geochemistry of the type area for the Støren Group. Greenstones collected along the north-west shores of Grøtvatnet and Bennasjøen are also considered here. The analytical data for the "Støren area" in report 1228 B also includes data for the Hølonda porphyry and one analysis of the type trondhjemite (Goldschmidt, 1916) from Folstad, near Støren.

The Støren Group consist mainly of pillow lavas and lavas. Basic pyroclastic rocks are also present near the top of the unit. The Støren Group overlies metasediments of the Gula Schist Group and is in turn overlain by metasediments of the Lower Hovin Group, (Vogt 1945, Chaloupsky 1970). The Grøtvatnet and Bennasjøen greenstones are considered the stratigraphic equivalents of the Støren greenstones at Haga bridge.

The Hølonda porphyry includes both intrusive and extrusive rocks. Dikes of the porphyry intrude the greenstones of the Løkken area, and small intrusive bodies as well as pyroclastics are found in the vicinity of Svorksjøen, NW of the village of Hølonda. The Holonda porphyry is described by Chalopsky (1970) as being "composed of plagioclase and pyroxene phenocrysts enclosed in a groundmass of fine albite laths, chlorite, epidote, ore minerals etc. Plagioclases are partly or completely saussuritized and of albite composition. Pyroxene, which is colourless up to green is almost fully replaced by chlorite and urallite".

### 6.2 Analytical data.

The analytical data for the rocks of the Støren area are presented in Table 4.2 of rapport 1228 B. These include:

- 15 samples of basic lava and pillow lava (analyses 170 to 182, 185 and 186) from the Haga bridge section.
- 9 samples of greenstones (analyses 163-169, 183 and 184) from Grøtvatnet and Bennasjøen.
- 5 samples of the Hølonda porphyry (analyses 250-406)
- 1 sample of the Folstad trondhjemite (analysis 249)



### 6.3 Geochemistry of the Støren area basalts.

The mean values and standard deviations for the Støren area basalts are presented in Table 6.1. All the samples are considered together here since inspection of the data did not reveal any difference between analyses from the Haga bridge profile and those from Grøtvatnet and Bennasjøen. On the Alkali-Silica diagram, Fig. 6.1, the basalts plot about the dividing line for subalkaline and alkaline basalts. This is probably due to the addition of Na during spilitization since the mean  $K_2O$  value is 0.26 % and only one analysis, No. 175, has more than 0.70%  $K_2O$ . The AFM diagram shows the analyses to scatter about the Irvine and Barager (1971) dividing line for separating tholeiitic and calc-alkaline magmas. The analyses do not show a tholeiitic fractionation trend and if any trend can be deduced from Fig. 6.2 it is a calc-alkaline one. The analyses do, however, plot within the tholeiitic fields in Fig. 6.3 (% FeO - FeO/MgO, and %  $SiO_2$  - FeO/MgO) and in Fig. 5.5 (b) ( $TiO_2$  - FeO/MgO) they plot well above the trend for island arc tholeiitic (and calc-alkaline rocks) due to their higher  $TiO_2$  contents and close to the trend for abyssal tholeiites.

On the basis of the elements Ti, Zr, Sr, Y and Cr the Støren basalts can be classified as ocean-floor type basalts (OFB) since they plot firmly within the fields for ocean-floor basalts in Figures 6.4, 6.5, 6.6 and 6.7. Four of the samples (Nos. 175, 177, 178 and 185) plot in the field for within plate basalts (WPB) on Fig. 6.4 (field D).

In contrast to the ocean-floor basalts of the Løkken area those of the Støren area all plot in the OFB field (field A) on the Ti-Cr diagram (Fig. 6.7). The  $TiO_2$  contents of the Støren OFB are higher than those of the Løkken OFB which suggests that the Støren basalts formed at a mid-ocean ridge while those of the Løkken area were generated in a marginal basin behind a developing island arc system (J. Pearce pers. comm., 1974). It is therefore possible that Cr contents of marginal basin ocean-floor type basalts exhibit a greater variation in Cr than mid-ocean ridge basalts. This could then explain why the Ti-Cr discriminant appears to be applicable in some areas and not in others.

Table 6.1 Summary data for 24 Støren basalts and 5 Hølonda porphyry with comparison.

ELEMENT	STØREN				HØLONDA		
	MINIMUM	MAXIMUM	MEAN	STD. DEV.	MEAN	STD. DEV.	S8 <sup>x</sup>
SI02	45.40	50.30	47.46	1.40	54.42	2.74	55.0
Al2O3	13.20	16.70	14.82	0.80	18.06	0.82	17.0
FE2O3	7.40	13.10	10.57	1.39	7.50	1.66	8.0
TI02	1.24	2.04	1.70	0.18	1.38	0.10	1.1
MGO	4.20	10.10	7.30	1.43	2.88	1.13	4.9
CAO	6.70	13.80	10.12	2.33	5.48	2.61	7.3
NA2O	2.40	5.35	3.63	0.82	5.06	1.34	4.0
K2O	0.00	1.39	0.26	0.30	1.79	0.85	1.6
MNO	0.12	0.21	0.17	0.02	0.10	0.04	0.11
P2O5	0.05	0.17	0.10	0.03	0.26	0.04	0.30
L.O.I.	2.13	8.49	4.20	1.71	2.86	0.41	0.7
ZR	77.	159.	135.	21.	283.	46.	190
Y	22.	39.	30.	5.	21.	12.	8
Sr	106.	528.	224.	101.	745.	243.	770
RB	0.	18.	2.	4.	52.	24.	35
ZN	24.	113.	74.	20.	72.	8.	
CU	19.	138.	55.	26.	89.	42.	70
NI	60.	203.	125.	36.	11.	5.	40
CR	205.	644.	353.	94.	31.	21.	130
BA	0.	214.	27.	51.	646.	352.	350

<sup>x</sup> an "Andean Andesite" taken from Sigers et al (1969, Table 1, No. 8, p. 883). See also Table 8.6 for further comparisons.

#### 6.4 Geochemistry of the Hølanda porphyry.

Mean and standard deviations for 5 samples of the Hølanda porphyry are presented in Table 6.1.

Although the Hølanda porphyry exhibits a range of compositions, four of the samples can be classified as andesites, i.e. they have  $\text{SiO}_2$  values in the range 52-63%. The Hølanda porphyry plots in the calc-alkaline field on the AFM diagram, Fig. 6.2, but there is no clear separation of this unit on the other major element variation diagrams. The major and trace element contents of the Hølanda porphyry are quite dissimilar from those of calc-alkaline rocks of island arcs (cf. Jakeš and White, 1972, Tables 2A and 2B) in that they have higher  $\text{TiO}_2$ , Sr, Zr, Rb and Ba as well as lower K/Rb (280) than island arc calc-alkaline rocks with the same  $\text{SiO}_2$  content. Jakeš and White (1972) report that the "trace elements of the potassium type (Ba, Sr, Rb) and Zr, Th and U are higher in the Andean type (Siegers et al, 1969), whereas K/Rb ratios are lower (i.e. than in island arc calc-alkaline associations). Thus it would seem that the Hølanda porphyry represents a continental margin magmatism of the "Andean type". A typical analysis of an Andean andesite at the same  $\text{SiO}_2$  content as the mean value for the Hølanda porphyry is presented in Table 6.2.

This probably explains why the trace element discriminants cannot be applied to these rocks since they tend to plot outside the fields established by Pearce and Cann (1973).

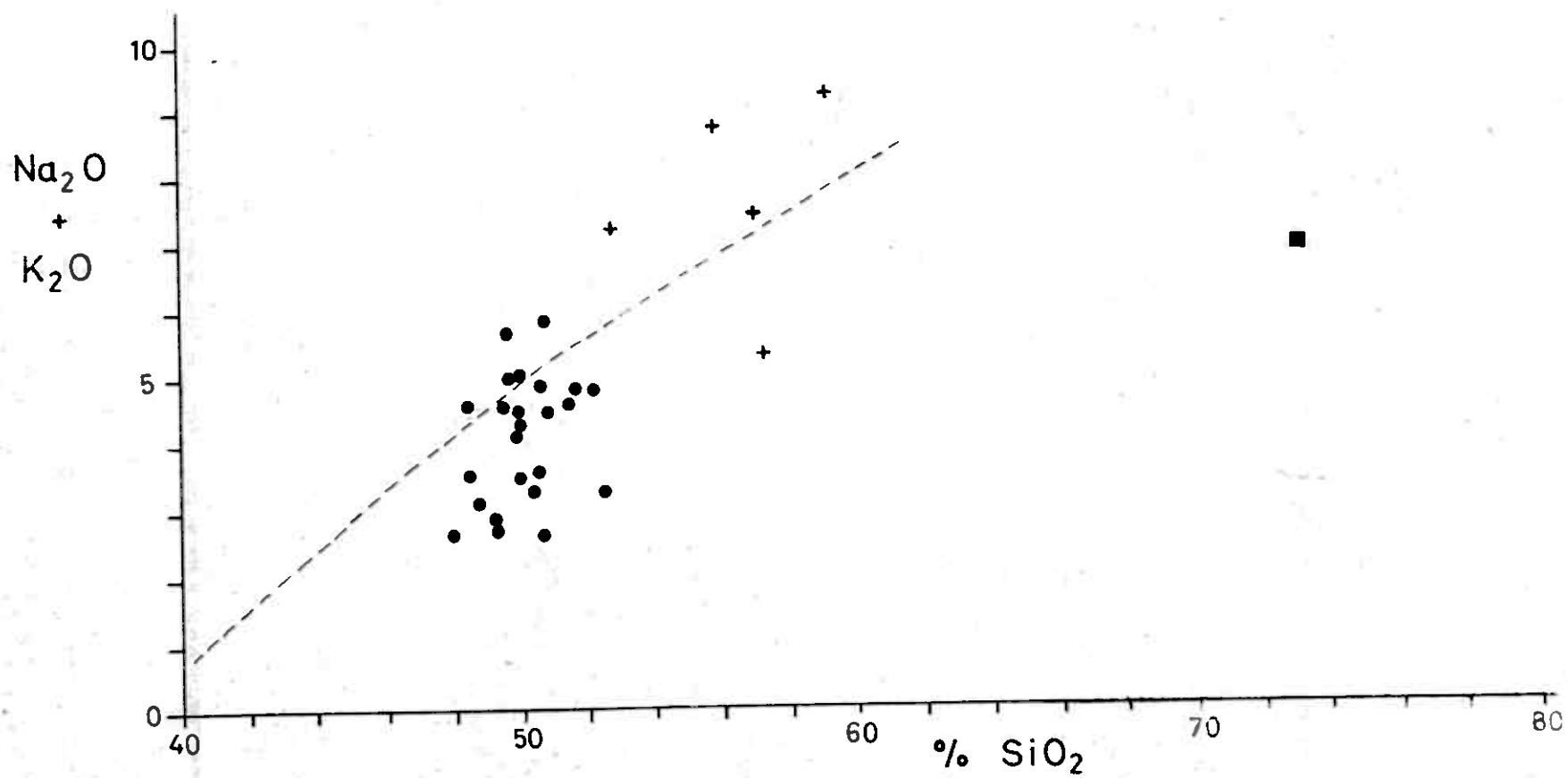
#### 6.5 Summary.

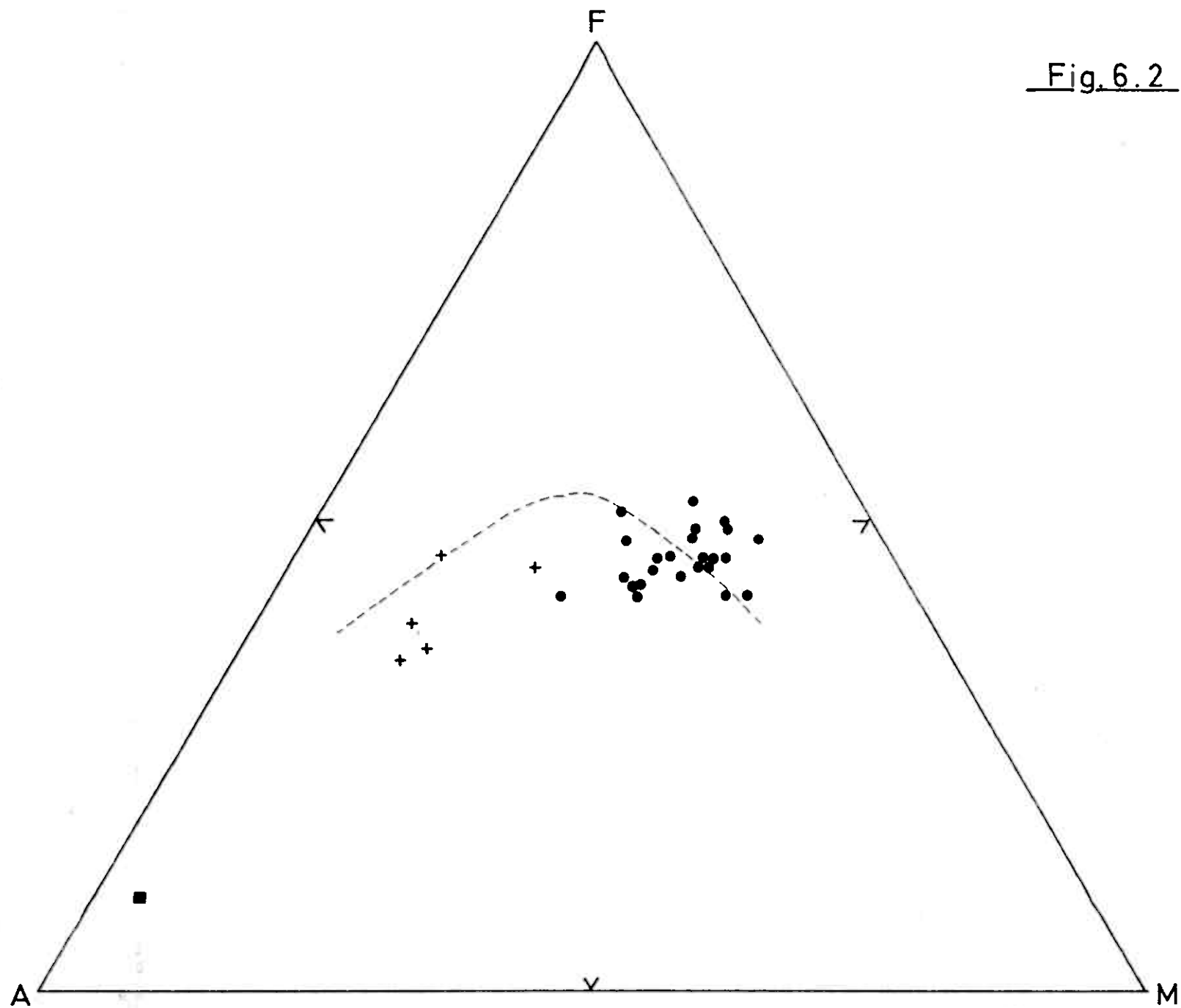
The greenstones of the Støren area are submarine tholeiitic basalts. These rocks have trace element characteristics of ocean floor basalts. The  $\text{TiO}_2$  contents are significantly higher than those of the Løkken area ocean-floor basalts and probably reflect a mid ocean ridge environment for generation of the Støren magmas as opposed to a marginal basin spreading environment for the Løkken ocean-floor magma. The section of the Støren Group volcanics sampled in this study does not contain any volcanics with geochemical characteristics of island arc magmas.

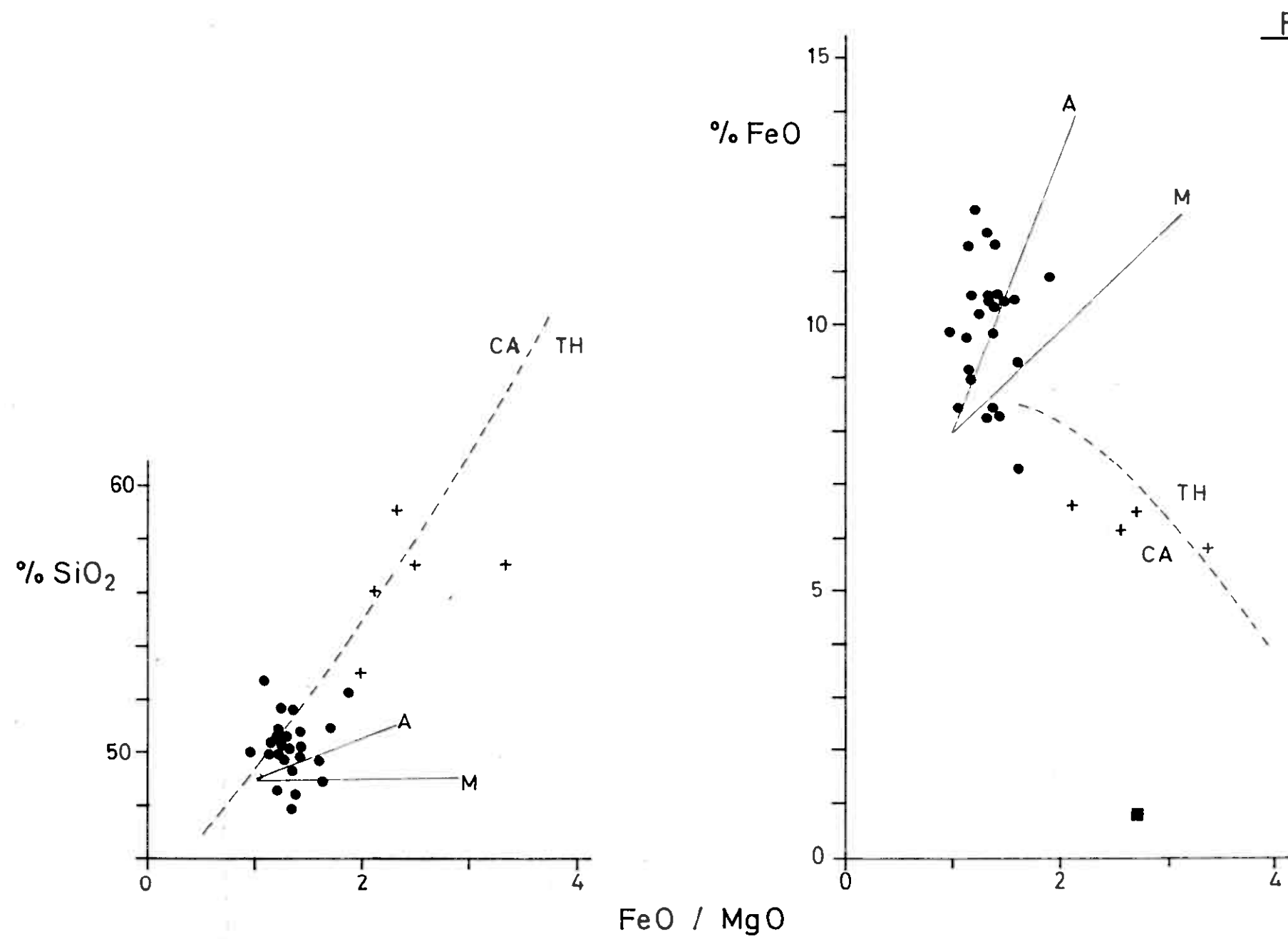
On the basis of a small sample population the hypabyssal and extrusive rocks of the Hølanda porphyry exhibit geochemical characteristics of calc-alkaline "Andean type" magmas and are quite different from calc-alkaline magmas of island arc terrains.

Captions for figures in section 6.

- Figure 6.1 Alkali-Silica variation diagram for rocks of the Støren area. Oxides as wt.% (volatile free). The boundary line separating alkaline compositions (above) from subalkaline compositions (below) is after Irvine and Barager (1971). The symbols are: ● Støren lavas; + Hølanda porphyry; ■ Trondhemite.
- Figure 6.2  $A(\text{Na}_2\text{O} + \text{K}_2\text{O}) - F(\text{FeO, total Fe}) - M(\text{MgO})$  variation diagram. The boundary line separating tholeiitic composition (above) from calc-alkaline composition (below) is after Irvine and Barager (1971). Symbols as in Fig. 6.1.
- Figure 6.3  $\text{FeO} - \text{FeO}/\text{MgO}$  and  $\text{SiO}_2 - \text{FeO}/\text{MgO}$  variation diagrams. Oxides as wt.% (volatile free). Total iron as FeO. The field boundaries separating the tholeiitic (TH) and calc-alkaline (CA) series and the trend lines for abyssal tholeiites (A) and the Macauley Island tholeiites (M) are after Miyashiro (1974). Symbols as in Fig. 6.1.
- Figure 6.4 Discriminant diagram using Ti, Zr, Y to distinguish "within plate" basalts (field D) from ocean-floor type basalts (field B), calc-alkaline basalts (field C) and low-potassium tholeiites of island arcs (fields A and B). Field boundaries after Pearce and Cann (1973). Symbols as in Fig. 6.1.
- Figure 6.5 Discriminant diagram using Ti and Zr for distinguishing ocean-floor type basalts (fields B and D), calc-alkaline basalts (field C) and low-potassium tholeiites of island arcs (fields A and B). Field boundaries after Pearce and Cann (1973). Symbols as in Fig. 6.1.
- Figure 6.6 Discriminant diagram using Ti, Zr and Sr for distinguishing ocean-floor type basalts (field C), low-potassium tholeiites (field A) and calc-alkaline basalts (field B). Field boundaries after Pearce and Cann (1973). Symbols as in Fig. 6.1.
- Figure 6.7 Discriminant diagram to distinguish ocean-floor basalts (field A) from low-potassium tholeiites of island arcs (field B). The field boundary is after Pearce (pers. comm. 1974). Symbols as in Fig. 6.1.







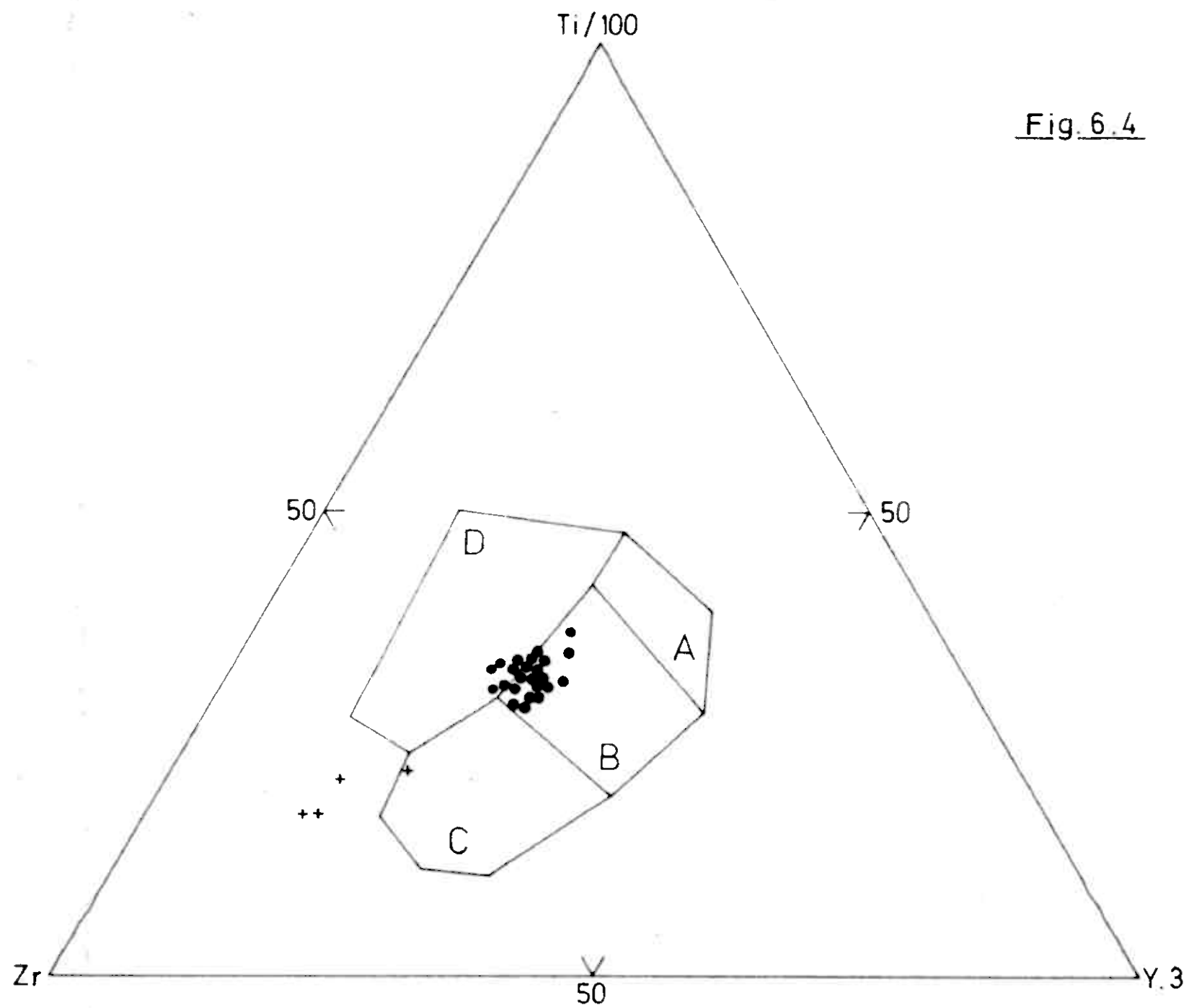
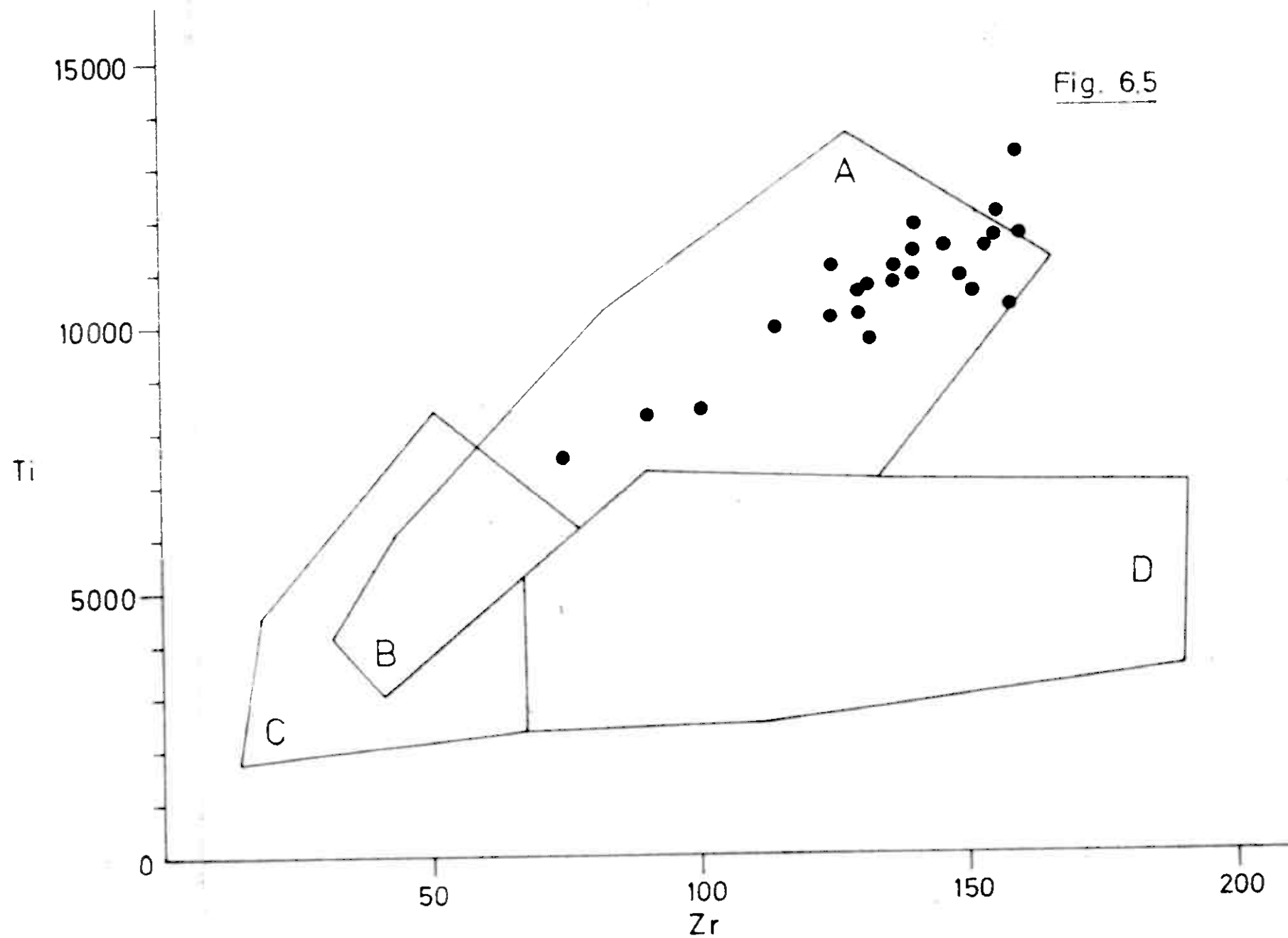
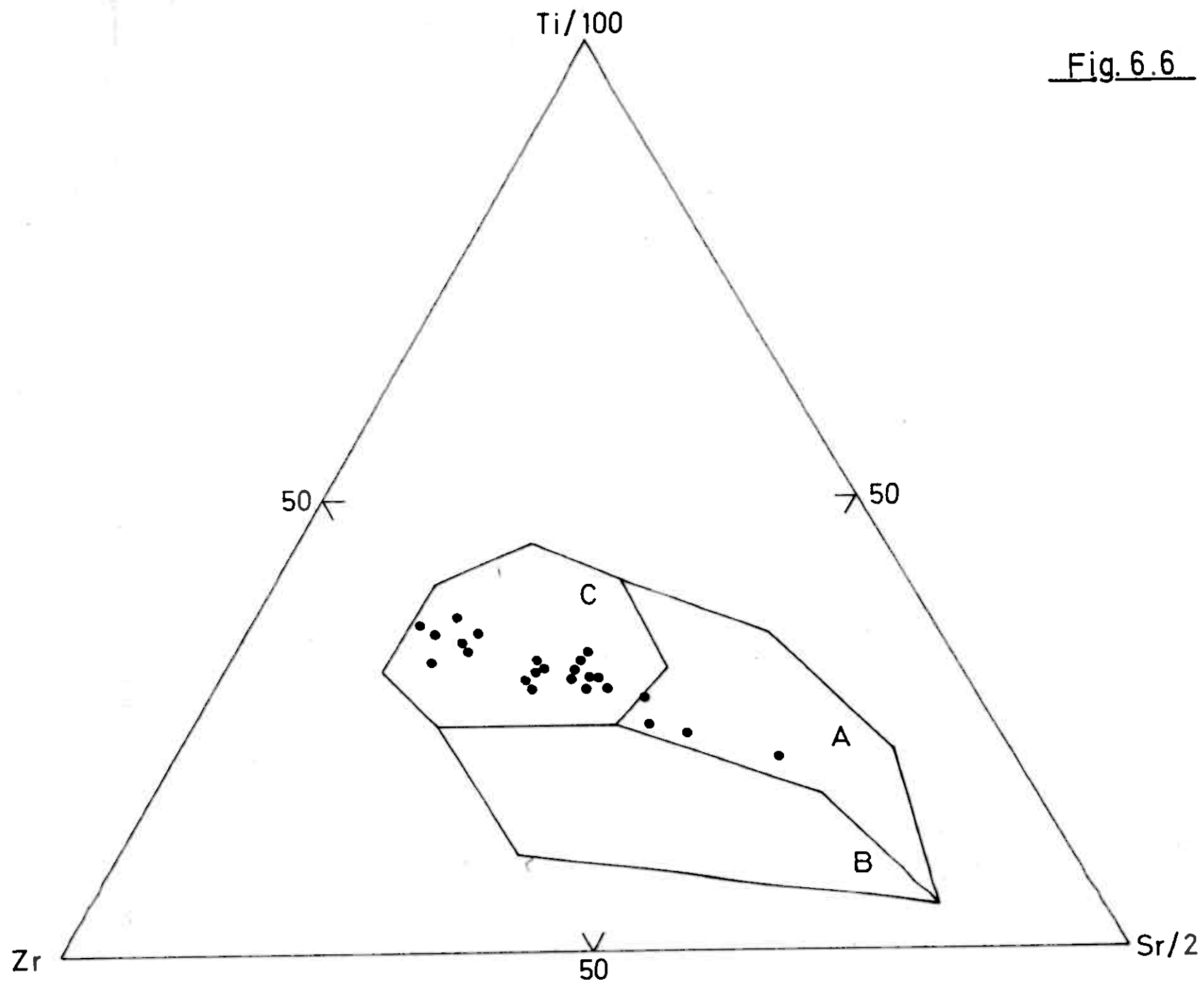
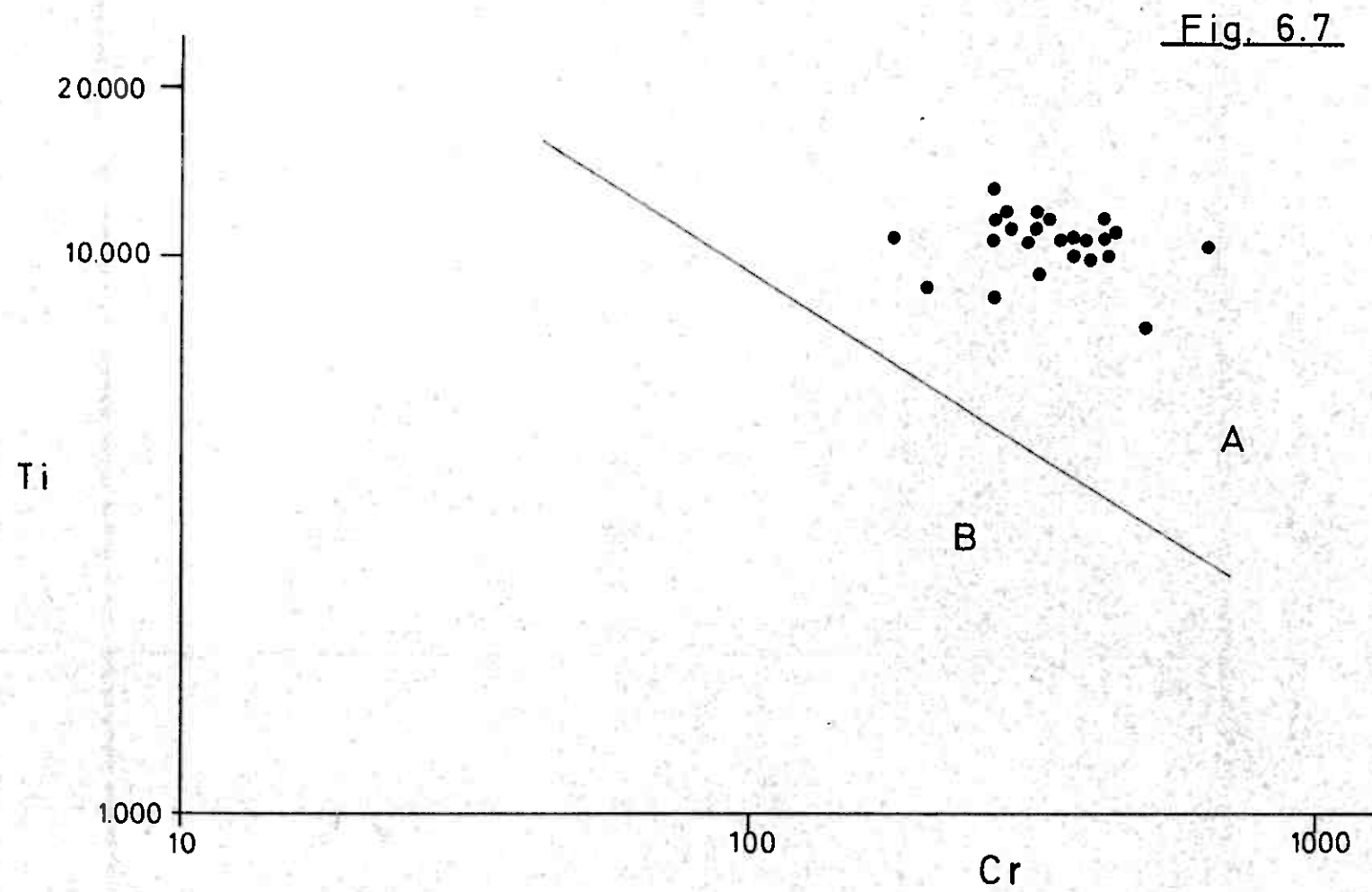




Fig. 6.5







## 7. THE STAVENES AREA

### 7.1 Introduction.

The peninsula between Stongfjord and Stavfjorden in West-Norway is comprised mainly of lower Palaeozoic basic volcanic rocks, the Grimeli Formation of the Stavenes Group (Skjerlie, 1974). The Grimeli Formation, from which all of the samples considered here were collected, is described by Skjerlie as follows:

"The Grimeli Formation, which is comprised mainly of metabasaltic rocks, occurs in the south-eastern part of the Stavfjord district. The oldest exposed rocks within this formation are a sequence of pillow lavas (Pl. 1, Fig. 2) containing meta-hyaloclastite breccias and calcareous metagreywacks. This succession is followed by a thick sequence of meta-basalts (massive greenstones) in which pillow structures are sporadically developed. The meta-basalts may occasionally be porphyritic and contain plagioclase phenocrysts. Within the meta-basalts zones of meta-hyaloclastite breccias occur and these contain both individual pillows and epidotic lenses of variable size. Pyroclastic rocks (meta-tuffs) are only found at two localities in the upper half of the unit. The layers are not mappable, being less than 1 m in thickness and of relative limited extent. The thickness of the Grimeli Formation must be about 2000 m.

Within the Moldvær Formation, which occurs in the north-western part of the Stavfjord district, meta-tuffs and meta-tuffites are predominant, meta-basaltic rocks are only found in small occurrences in the eastern part of Svanøy (Lunøe 1972)."

Skjerlie (1974, p.4).

The detailed unpublished geological maps of Skjerlie upon which Fig. 1 is based were made available to the writer at the time of sampling in 1972. It was thus possible to obtain a suite of samples that were representative of the Grimeli Formation.

The rocks of the Grimeli Formation form part of the Stavfjord Anticline, a major fold structure which has been thrust towards the south-east (Furness and Skjerlie, 1972, Skjerlie 1969). The development of the main schistosity, which is related to the formation and thrusting of the Stavfjord anticline, was the second deformational event to affect the rocks of this

region; it was preceded by the thrusting of mangerite rocks of the Dalsfjord Nappe (Skjerlie, 1969, 1974). The general geology of the Stavenes area is shown in Figure 7.1 (after Skjerlie, 1974, Plate 1). For further detailed descriptions of the geology of this area the reader is referred to the papers by Skjerlie (1969, 1974) and Furnes and Skjerlie (1972). Furnes (1974) describes metavolcanic sequences in the Solund area to the south which can be correlated with the Stavenes Group on a litho-stratigraphical basis.

## 7.2 Analytical data.

Twelve complete major and trace element analyses (Nos. 320-331) and 7 major element analyses (nos. 9-15) are contained in Rapport 1228 B. Trace element data for 5 of the analyses in Rapport 1228 B with only major element data are now available and are presented along with the major element data in Table 7.1.

## 7.3 Geochemistry.

Summary data for the 12 complete analyses contained in rapport 1228 B are given in Table 7.2. Only one of the analyses in Table 7.1, No. 13, is significantly different from these analyses. Analysis No. 13 has higher  $\text{Al}_2\text{O}_3$ ,  $\text{K}_2\text{O}$ , Sr, Rb and Ba and lower  $\text{TiO}_2$ ,  $\text{Na}_2\text{O}$ , Zr, Y, Ni and Cr than the other analyses from the Stavenes area, i.e. it represents a completely different rock-type. The presence of this rock, probably a dike, within an otherwise uniform sequence is difficult to interpret, other than as a separate magma type.

On the AFM diagram, Fig. 7.2 (a) the Stavenes basalts, exhibit a definite iron enrichment and plot within the field for tholeiitic compositions as defined by Irvine and Barager (1971). They also plot within the field of subalkaline magmas on the Alkali Silica diagram, Fig. 7.2 (b) and in the fields for tholeiitic basalts on Fig. 7.3. Furthermore they exhibit a trend similar to that of abyssal tholeiites and Macauley Island (Kermadecs) tholeiites on the  $\text{SiO}_2$  -  $\text{FeO}/\text{MgO}$  diagram and a trend identical to that of abyssal tholeiites on the  $\text{FeO}$  -  $\text{FeO}/\text{MgO}$  diagram. The trend exhibited on the  $\text{TiO}_2$  -  $\text{FeO}/\text{MgO}$  diagram is quite similar to the trend of abyssal tholeiites figured by Miyashiro (1974).

The trace elements, Ti, Zr, Sr, Y and Cr are used in the construction of discriminant diagrams (Fig. 7.4, 7.5, 7.6 and 7.7) for determining

Table 7.1 Additional trace element data for rocks of the Stavenes Area.

	<sup>9</sup> 1228 / 99A	<sup>10</sup> 1228 / 98A	<sup>11</sup> 1226 / 98D	<sup>12</sup> 1228 / 105A	<sup>13</sup> 1228 / 108	<sup>14</sup> 1228 / 112	<sup>15</sup> 1228 / 117
SI02	46,50	46,72	48,13	47,29	48,05	47,85	47,70
AL203	14,48	14,43	14,90	14,17	18,49	15,43	15,79
FE203	13,13	12,65	10,87	13,42	9,90	10,46	10,95
TI02	2,40	2,30	1,75	2,41	0,54	1,99	2,03
MG0	7,17	6,56	7,60	6,92	6,15	7,93	6,50
CA0	11,57	12,30	11,73	11,27	10,48	11,03	12,06
NA20	2,56	2,64	3,09	2,69	1,76	3,78	3,26
K2O	0,12	0,13	0,12	0,14	1,30	0,30	0,12
MNO	0,23	0,21	0,21	0,30	0,15	0,19	0,17
P2O5	0,14	0,12	0,12	0,12	0,11	0,13	0,17
L.O.I.	3,15	3,32	2,74	3,11	3,86	2,75	2,28
TOTAL	101,45	101,58	101,26	101,84	100,79	101,84	101,03
PPM							
ZR	157	152	117	-	63	185	-
Y	43	43	35	-	17	33	-
SR	106	110	149	-	614	256	-
RB	0	0	0	-	35	0	-
ZN	107	90	81	-	78	67	-
CU	39	48	3	-	54	49	-
NI	44	48	49	-	27	35	-
CR	156	166	276	-	92	215	-
BA	13	71	24	-	777	42	-

Table 7.2 Summary data for 12 volcanic rocks from the Stavenes area.

ELEMENT	MINIMUM	MAXIMUM	MEAN	STD. DEV
SI02	47.10	49.70	48.46	.94
AL2O3	13.10	16.20	14.08	1.02
FE2O3	9.70	14.70	12.97	1.86
TI02	1.38	2.54	2.10	.38
MG0	3.30	9.00	6.54	1.37
CAD	9.50	12.60	11.44	.83
NA2O	2.40	3.65	2.85	.33
K2O	.09	.41	.16	.11
MNO	.17	.28	.23	.04
P2O5	.07	.14	.12	.02
L. O. 1.	1.18	2.59	1.75	.46
ZR	99.	216.	167.	36.
Y	28.	52.	43.	9.
SR	128.	224.	168.	29.
RB	0.	2.	0.	1.
ZN	60.	120.	95.	20.
CU	19.	79.	43.	16.
NI	46.	113.	68.	17.
CR	142.	361.	226.	69.
BA	0.	65.	21.	23.

the tectonic environment of magma generation after the method of Pearce and Cann (1973). On these diagrams the analyses plot consistently in the fields for ocean floor basalts with the exception of a dolerite dike, analysis 329, which plots in the within plate basalt field on the Ti-Zr-Y diagram, and analysis 13 of table 7.1 which plots well away from the other analyses. On the Ti-Zr diagram Fig. 7.5, the analyses plot mainly at the end of the field for ocean-floor basalts. According to Julian Pearce (pers. comm. 1974) and Nesbitt and Pearce (1974), ocean-floor basalts formed at mid-ocean ridges, with fast spreading rates have higher Titanium and Zirconium than those used in constructing the boundaries for ocean-floor basalts in Fig. 7.5 (field D).

The intrusive rocks of the Stavenes area have been interpreted as synvolcanic intrusives (Skjerlie, 1974). Both the major and the trace element data of the intrusives with the exception of low Ytterium in the dolerite, are similar to that of the basaltic rocks (excluding of course the anomalous analysis, No. 13) and therefore provide supporting evidence for Skjerlie's interpretation that they have a common magmatic origin.

#### 7.4 Summary.

Both major and trace element data indicate that the basalts of the Grimeli Formation are ocean-floor type basalts and that the doleritic dikes were probably derived from the same magma as that producing the basalts.

#### Captions for figures in section 7.

Figure 7.1 Geology of the Stavenes area (after Skjerlie, 1974) with location of analyses.

Figure 7.2(a)  $A(\text{Na}_2 + \text{K}_2\text{O}) - F(\text{FeO, total Fe}) - M(\text{MgO})$  variation diagram. The field boundary separating tholeiitic (above) from calc-alkaline (below) compositions is after Irvine and Barager (1971). The symbol (x) identifies analysis 13, - (0) identifies the two intrusives, analyses 329 and 15, and (●) identifies lavas and pillow lavas.

Figure 7.2(b) Alkali-Silica variation diagram. Oxides as Wt.% (volatile free). The field boundary separating alkaline (above) from sub-alkaline (below) compositions is after Irvine and Barager



(1971). Symbols as in Fig. 7.2 (a).

- Figure 7.3  $\text{TiO}_2$  -  $\text{FeO}/\text{MgO}$ ,  $\text{FeO}$  -  $\text{FeO}/\text{MgO}$  and  $\text{SiO}_2$  -  $\text{FeO}/\text{MgO}$  variation diagrams. Oxides as wt. % (volatile free), total iron as  $\text{FeO}$ . The field boundaries separating the tholeiitic (TH) and calc-alkaline (CA) series, and the trend lines for the abyssal tholeiites (A), Macauley islands arc tholeiite series (M) and the Amagi calc-alkaline series (Am) are after Miyashiro (1974). Symbols as in Fig. 7.2 (a).
- Figure 7.4 Ti-Zr-Y discriminant diagram to distinguish "within plate" basalts (field D) from low-potassium tholeiites of island arcs (Fields A and B) ocean-floor type basalts (field B) and calc-alkaline basalts (field C). Field boundaries are after Pearce and Cann (1973). Symbols as in Fig. 7.2 (a).
- Figure 7.5 Ti-Zr discriminant diagram for distinguishing ocean-floor type basalts (fields B and D), calc-alkaline basalts (field C) and low-potassium tholeiites of island arcs (fields A and B). Field boundaries after Pearce and Cann (1973). Symbols as in Fig. 7.2(a).
- Figure 7.6 Ti-Zr-Sr discriminant diagram for distinguishing ocean-floor type basalts (field C), low-potassium tholeiites (field A) and calc-alkaline basalts (field B). Field boundaries after Pearce and Cann 1973). Symbols as in Fig. 7.2 (a).
- Figure 7.7 Ti-Cr discriminant to distinguish ocean-floor basalts (field A) from low-potassium tholeiites of island arcs (field B). Symbols as in Fig. 7.2 (a). The field boundary is after Pearce (pers. comm., 1974).

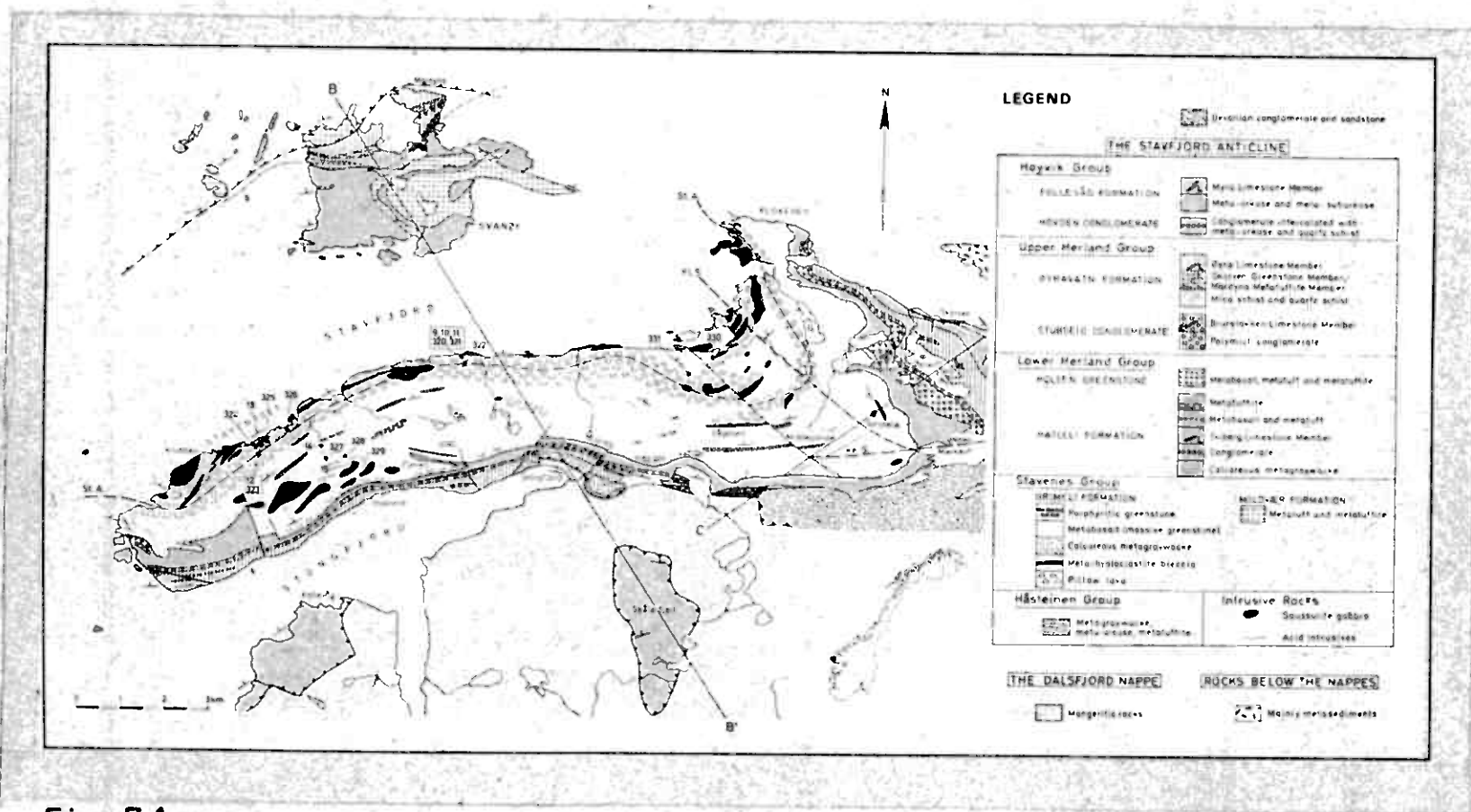


Fig. 7.1

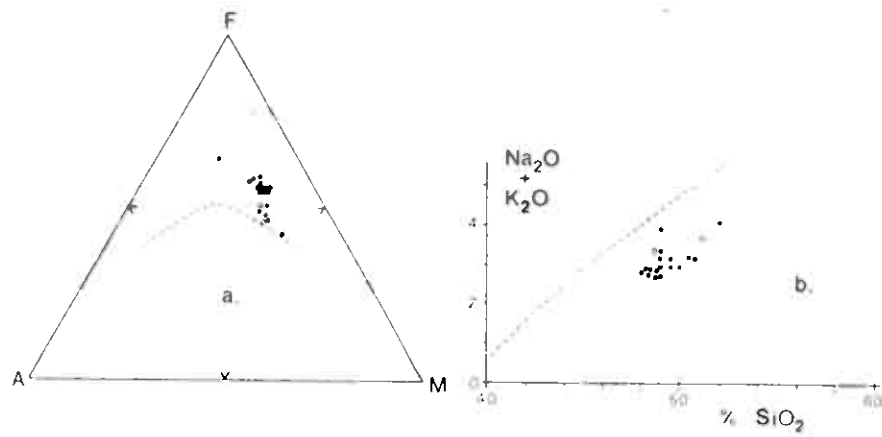


Fig. 7.2

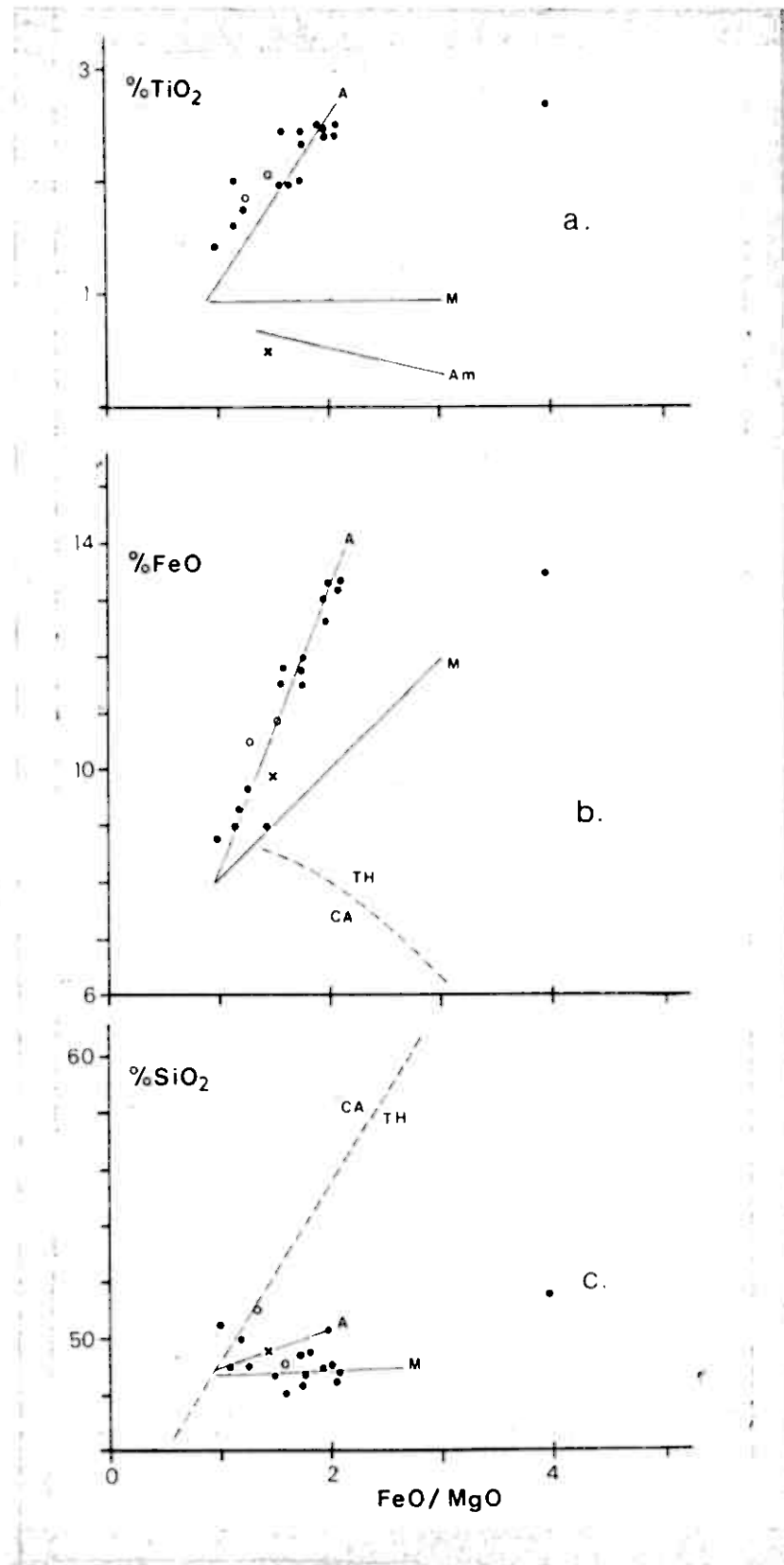


Fig. 73

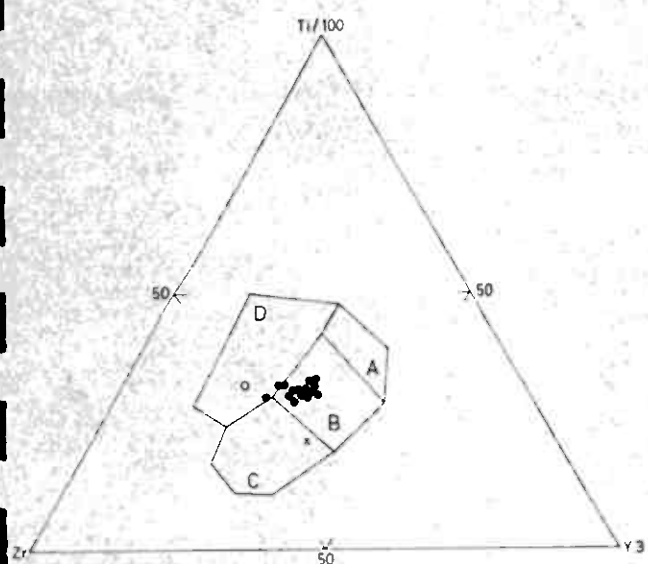


Fig. 7.4

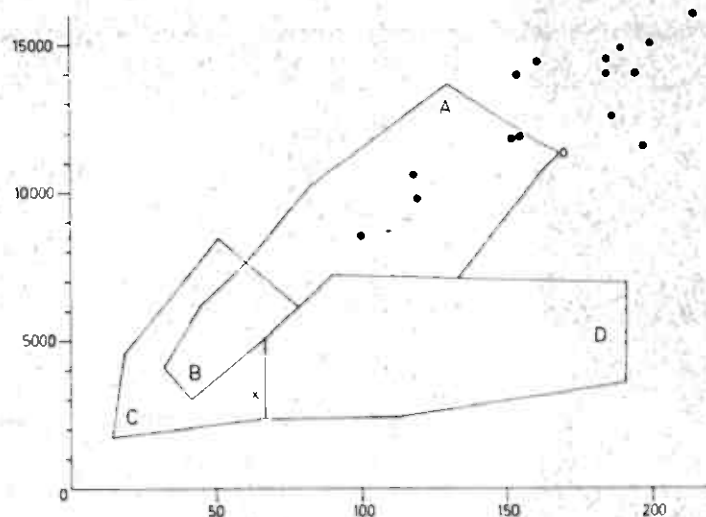


Fig. 7.5

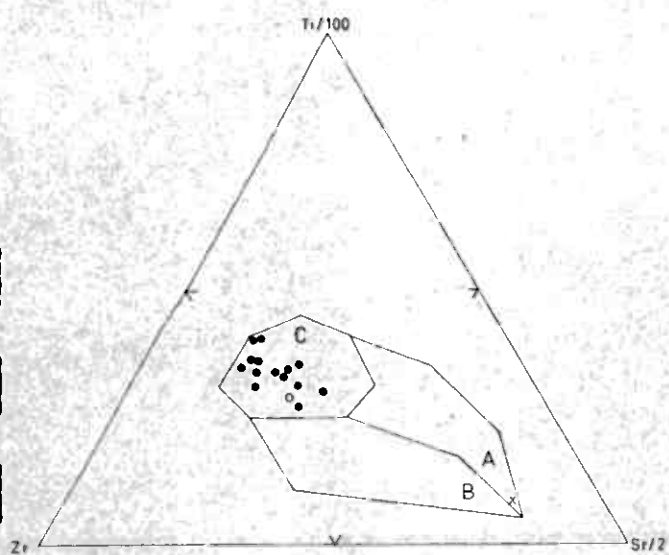


Fig. 7.6

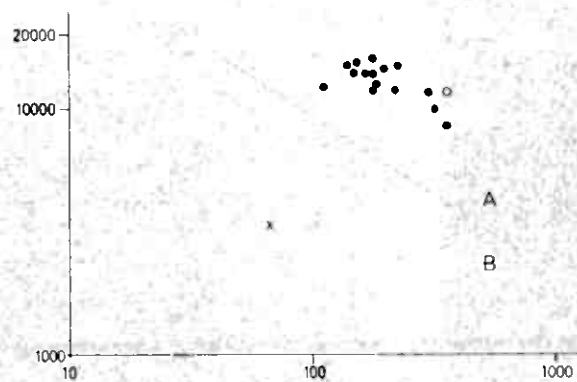


Fig. 7.7

## 8. BØMLO AND STORD

### 8.1 Introduction.

The most recently published account of the geology of Bømlo is that of Reusch (1888). The geology of the south-eastern part of the island of Stord has been described by Skordal (1948). The central part of the island of Bømlo has been described by Songstad (1971) in an unpublished thesis at the University of Bergen. A general outline of the geology of the Bømlo area after Reusch and Songstad is presented in Fig. 8.1.

### 8.2 Analytical data.

Major and trace element analyses of 69 extrusive rocks from Bømlo and Stord are presented in NGU report 1228 B. The location of analyses from Bømlo are indicated on Fig. 1.

### 8.3 Geochemistry of the basic rocks.

It became apparent during an initial inspection of the data that the analyses from different parts of Bømlo could be divided into fairly distinctive and homogeneous sets. Thus for the purpose of this presentation the island of Bømlo is divided into the following subareas:

- a. East Block (east of Vikafjord)
- b. Central Block (Vikafjord to Løkling)
- c. West Block
- d. Finaasviki Block

#### The East Block

This area is underlain mainly by clastic and volcanoclastic sediments derived principally from a basic volcanic terrain. Basic lavas and tuffs are present in at least the western part of this area. Small bodies of basic and acidic rocks intrude the sediments. Acidic fragmental rocks were noted at several localities in the eastern part of the area. Songstad (1971) was the first to report pillowed lavas from this area.

Rocks analysed from this area include:

- |                                   |                                     |
|-----------------------------------|-------------------------------------|
| 1 dolerite dike                   | Analysis 286                        |
| 9 basaltic lavas and pillow lavas | Analyses 151-154, 275-277, 287, 288 |
| 3 acidic intrusives               | Analyses 255-257.                   |

Summary data for the basaltic lavas are presented in Table 8.1.

On the alkali-silica variation diagram (Fig. 8.2) the East Block lavas plot mainly in the field for calc-alkaline compositions defined by Irvine and Barager (1971), and if these lavas exhibit any trend it is more like that of a calc-alkaline suite rather than a tholeiitic suite. In Fig. 8.4 these lavas appear to have a calc-alkaline rather than a tholeiitic trend in both the  $\text{SiO}_2$ -FeO/MgO and FeO-FeO/MgO plots. In the  $\text{TiO}_2$ -FeO/MgO variation diagram, Fig. 8.5, they plot in the field which characterises the island arc tholeiite series but do not show any definite trend.

In Fig. 8.6 the analyses plot mainly in the field for ocean-floor and island arc basalts although one analysis falls well within the field for "within plate basalts". (This analysis probably represents a low Yttrium determination rather than a "hot spot" magma representative since the Yttrium value recorded (8 ppm) is near the analytical detection limit, also the Titanium content of this analysis is similar to that of the other rocks in the same area and considerably lower than the Titanium values found in hot-spot lavas). On the Ti-Zr diagram, Fig. 8.7, these analyses all plot in the field common to ocean-floor and island arc tholeiites but in Fig. 8.8, the Ti-Cr diagram, three of the data sets plot in the field for ocean-floor basalts. The three samples (analyses 276, 152, 153) plotting in the field for ocean-floor basalts are separated from the other samples in this area by a fault zone (of unknown dimensions), thus it is quite possible that volcanic rocks from two different tectonic regimes, i.e. island arc and ocean-floor, are juxtaposed in this area.

In view of the small sample population and the limited areal distribution of the lavas sampled in this investigation, as well as the very sparse geological information on this area, it is not possible to establish with any certainty the tectonic environment of magma generation in this area. An island arc environment appears to be more consistent with both the geochemical (i.e.  $\text{TiO}_2$ , AFM, Ti/Cr, Ti/Zr) and the little that is known about the geology (i.e. volcan-clastic sediments, basic tuffs, acidic fragmentals and conglomerates) than an ocean-floor environment, although it is plausible that slices of ocean-floor material, upon which island arc material developed have been thrust into the island arc sequence.

#### The Central Block.

The rocks between Vikafjord and Løklingfjord consist predominantly of basic to intermediate subaerial lavas and pyroclastics. Acidic lavas

Table 8.1 Summary data for 10 East Block basic lavas.

ELEMENT	MINIMUM	MAXIMUM	MEAN	STD. DEV
SIO <sub>2</sub>	48,40	53,70	50,40	1,67
AL <sub>2</sub> O <sub>3</sub>	14,00	16,40	15,16	0,91
FE <sub>2</sub> O <sub>3</sub>	8,20	10,70	9,41	0,79
TIO <sub>2</sub>	0,69	1,84	0,94	0,34
MGO	5,10	11,00	7,57	1,59
CAO	7,00	11,20	8,95	1,35
NA <sub>2</sub> O	1,55	5,25	3,78	1,00
K <sub>2</sub> O	0,06	1,45	0,37	0,43
MNO	0,11	0,20	0,15	0,03
P <sub>2</sub> O <sub>5</sub>	0,02	0,12	0,06	0,03
L.O.I.	2,13	4,68	3,04	0,78
ZR	33	167	57	40
Y	8	23	15	5
SR	50	617	200	174
RB	0	43	7	13
ZN	59	92	73	11
CU	31	131	70	27
NI	33	265	104	75
CR	79	841	295	270
BA	3	783	107	239



Table 8.2 Summary data for 17 basaltic to andesitic rocks from the Central Block, 6 rhyolitic rocks from the Central Block and 1 rhyolitic rock from the Finaasviki Block.

<u>Basaltic to andesitic</u>					<u>Rhyolitic</u>				
ELEMENT	MINIMUM	MAXIMUM	MEAN	STD.DEV	ELEMENT	MINIMUM	MAXIMUM	MEAN	STD.DEV
SIO2	46,20	55,50	50,51	2,93	SIO2	70,40	75,80	73,06	2,07
AL2O3	14,40	17,80	15,99	0,85	AL2O3	12,40	13,30	12,81	0,34
FE2O3	9,30	12,20	10,75	0,89	FE2O3	1,40	5,40	2,74	1,47
TIO2	1,62	2,36	1,99	0,18	TIO2	0,43	0,76	0,59	0,13
MGO	2,90	5,80	4,42	0,74	MGO	0,00	0,50	0,31	0,20
CAO	5,20	11,00	8,59	1,68	CAO	0,00	2,10	0,77	0,66
NA2O	1,80	4,65	3,32	0,76	NA2O	1,30	3,65	2,73	0,80
K2O	0,10	2,15	0,92	0,53	K2O	4,67	7,90	5,91	1,07
MNO	0,14	0,19	0,16	0,02	MNO	0,00	0,07	0,02	0,03
P2O5	0,09	0,20	0,14	0,02	P2O5	0,03	0,09	0,05	0,02
L.O.I.	2.20	5.78	3,61	1,09	L.O.I.	0,87	1,18	1,02	0,11
ZR	168	262	206	27	ZR	242	744	375	194
Y	20	33	26	4	Y	18	67	33	18
SR	210	523	369	92	SR	61	135	82	27
RB	0	83	31	21	RB	171	354	245	56
ZN	79	118	96	11	ZN	28	98	53	26
CU	17	78	44	15	CU	0	0	0	0
NI	11	91	6	24	NI	0	4	1	2
CR	25	46	95	35	CR	0	4	1	2
BA	17	423	210	100	BA	451	1715	870	432

Table 8.3 Summary data for 10 Finaasviki Block basaltic to andesitic lavas.

ELEMENT	MINIMUM	MAXIMUM	MEAN	STD. DEV
SIO <sub>2</sub>	49,40	66,50	54,61	5,21
AL <sub>2</sub> O <sub>3</sub>	13,00	17,80	14,77	1,81
FE <sub>2</sub> O <sub>3</sub>	7,00	15,00	11,00	3,01
TIO <sub>2</sub>	0,88	3,12	2,05	0,68
MGO	0,40	5,30	3,26	1,47
CAO	2,80	8,80	6,46	2,03
NA <sub>2</sub> O	1,90	5,75	2,97	1,13
K <sub>2</sub> O	0,85	3,16	1,80	0,72
MNO	0,11	0,25	0,19	0,04
P <sub>2</sub> O <sub>5</sub>	0,09	0,30	0,16	0,06
L. O. I.	0,63	4,28	2,27	1,27
ZR	175	560	285	112
Y	26	58	36	10
SR	188	624	303	122
RB	26	123	72	34
ZN	77	149	108	26
CU	0	40	11	13
NI	2	26	9	7
CR	0	228	88	91
BA	130	707	394	162

(rhyolitic) and pyroclastics are the dominate rocks locally. Volcanic-derived sediment and thin limestone horizons are also present but are of limited areal extent. A small body of strongly tectonized serpentinite occurs in the village of Løkling at the extreme western margin of this area. For details of the geology of this area the reader is referred to the unpublished thesis of Songstad (1971).

Analysed specimens from this area include:

- 17 basaltic to andesitic lavas (Analyses 155-162, 278-283, 290, 292)
- 6 silicic lavas and pyroclastics (Analyses 258-263).

Summary data for the Central Block rocks are given in Table 8.2.

On a volatile free basis the  $\text{SiO}_2$  contents of the basic rocks range from 49-57% i.e. they are basalts, basaltic andesites and andesites. The analyses plot mainly in the subalkaline field on the alkali silica variation diagram, Fig. 8.2, and mainly within field for calc-alkaline compositions as defined by Kuno (1966) - - This does not however mean that they are calc-alkaline rocks of island arc affinity (see below). On the AFM diagram they plot about the Irvine and Barager (1971) dividing line for separating tholeiitic and calc-alkaline compositions and do not exhibit any clear enrichment trend.

When plotted on Miyoshiro's discriminant diagrams (which were designed to separate tholeiitic and calc-alkaline suites of island arc affinity and thus are not strictly applicable here), the data fall in the field for tholeiitic basalts on both the  $\text{SiO}_2$ -FeO/MgO and the FeO-FeO/MgO plots (Fig. 8.4). The  $\text{TiO}_2$ -FeO/MgO plots shows a trend similar to that of Skaergaard'.

On the trace element discriminant diagram, Ti-Zr-Y, the Central Block lavas plot in the field for "within plate" basalts. The Titanium and Zirconium values of these lavas are both considerably higher than island arc rocks and if plotted on Fig. 8.7 they will plot well outside the fields for the island arc tholeiitic and calc-alkaline basalts.

#### The Finaasviki Block.

The lavas in this area are dominantly subaerial, and are both texturally and compositionally comparable to those of the Central Block. Two of the analyses from this area with 63 % and 68 %  $\text{SiO}_2$  (volatile free) represent andesitic to dacitic flows and indicate that there may be a continuous sequence from basalt to rhyolite in the Central and Finaasviki subaerial lavas.

Rocks analysed from this area are:

9 basic lavas	Analyses 267, 289, 313-316, 304-306
1 acidic lava	Analysis 268

The Finaasviki lavas plot within or very close to Kuno's (1966) field for calc-alkaline rocks (Fig. 8.2) but plot within the field for tholeiitic compositions on the AFM diagram (Fig. 8.3). On the Ti-Zr-Y diagram (Fig. 8.6) only the two analyses with high  $\text{SiO}_2$  (analyses 306 & 313) plot outside the field for "within plate" basalts which is not surprising since these diagrams are based on basaltic compositions (Pearce and Cann, 1973).

It can easily be seen from the variation diagrams that the Finaasviki Block lavas represent a lateral continuation of the same volcanic pile as that of the Central Block and thus were derived from the same tectonic environment.

When the Central and Finaasviki lavas are considered together they represent a continuum from basaltic to rhyolitic compositions (cf. Fig. 8.2). Since the lavas plot in the field for "within plate basalts" (Fig. 8.6) this indicates that these are either "hot-spot" oceanic island lavas or continental margin type volcanoes. The subalkaline character of the magma and the lack of abundant submarine volcanism in the two areas tends to rule out a correlation with the ocean island type of magma (e.g. Hawaiian) and suggests that a continental margin is the most probable tectonic environment in which these magmas were formed. Furthermore, these lavas exhibit a distinctive calc-alkaline trend on the alkali-silica variation diagram which is typical for calc-alkaline rocks of both island arcs and "Andean type" continental margins, the trace element data disputes an island arc affinity (cf. Jakeš and White, 1972). The  $\text{FeO}/\text{MgO}$  of these lavas are generally greater than 2 whereas in island arc, calc-alkaline rocks the  $\text{FeO}/\text{MgO}$  is less than 2. Rocks with  $\text{K}_2\text{O}/\text{Na}_2\text{O}$  greater than 1 are common in continental margin areas but decidedly atypical of island arcs, the Bømlø calc-alkaline rocks with more than 60 %  $\text{SiO}_2$  have  $\text{K}_2\text{O}/\text{Na}_2\text{O}$  ratios of 1 or more. In calc-alkaline island arc sequences rocks with more than 63 %  $\text{SiO}_2$  are rare while rocks with less than 56 %  $\text{SiO}_2$  are rare in continental areas. A definite overlapping of major element compositions in calc-alkaline island arc and continental margin magmas has been noted by a number of authors (see Jakeš and White, 1972).

Figs. 8.4 and 8.5 conclusively show that these are not typical calc-alkaline rocks of island arc terrains.

The Bømlø calc-alkaline lavas have higher Rb, Ba, Sr, Zr and Ti than the island arc calc-alkaline lavas and have values which closely resemble those

of the continental margin volcanics.

Although a clear discrimination cannot be made at this time, the bulk of the geochemical data favours a continental margin rather than an island arc tectonic setting as the origin of the Central and Finaasviki lavas. It can be seen from Table 8.6 that the analyses are not totally comparable with Andean-type magmas. Furthermore the presence of minor pillow lavas and limestones within the subaerial lavas do not necessarily rule out an Andean-type continental margin. We could however be dealing with a continental margin environment that split to form a back arc marginal basin. In this environment one can find subaerial within plate basalts, submarine sedimentation and volcanism and magmas that have compositions transitional between the ocean-floor and continental margin environments (e.g. the East Block island arc and ocean-floor type lavas). In the initial stages of formation the magmatism should be largely subaerial but will tend to become more submarine and have characteristics of ocean-floor type magmas as the marginal basin increases in size with spreading.

#### The West Block.

In the West Block the extent of the basic lavas is not known. The area has not been remapped since the work of Reusch (1888) who shows the area to be underlain by diorite, quartz porphyry, quartz porphyry tuff, greenstone, basic tuff and "other layered rocks". From my own brief observations of new roadside exposures it seems that the acidic rocks are more abundant than indicated on Reusch's map. The large body of "dioritic rocks" north-west of Hiskosen shown on Reusch's map is a mixture of fine- and medium-grained gabbro with some basic lava.

The analysed samples from this area are widely scattered and give only a rough idea of the compositional range of the West Block basic lavas.

Analyses from this area include:

- |                    |   |
|--------------------|---|
| 6 basic lavas      | (Analyses 293, 297, 298, 301, 310, 312)     |
| 1 basic tuff       | (Analysis 295)                              |
| 9 basic intrusives | (Analyses 294, 296, 299, 302, 307-309, 311) |

The West Block basic lavas are mainly subalkaline (Fig. 8.2) and plot within the tholeiitic field on the AFM diagram (Fig. 8.3).

In contrast to the East Block lavas those of the West Block plot consistently in the field for tholeiitic compositions on the  $\text{SiO}_2$  -  $\text{FeO}/\text{MgO}$  and  $\text{FeO}$  -  $\text{FeO}/\text{MgO}$  diagrams and exhibit the same trends as the basic intrusives

from this area (Fig. 8.4). On the  $\text{TiO}_2$  -  $\text{FeO}/\text{MgO}$  diagram these lavas do not exhibit any trend comparable to modern island arc tholeiites or ocean floor basalts (Fig. 8.5).

The trace element data from this area are difficult to interpret. The Ti-Zr-Y diagram shows ocean-floor "within plate", and calc-alkaline compositions. On the Ti-Zr diagram the data plot mainly in the field for ocean-floor basalts (analyses 310 and 312 which plot in the calc-alkaline and "within plate" fields, respectively, have high Zr and plot to the right on Fig. 8.7) while the analyses which plot in the ocean-floor field on Fig. 8.7 plot in the low-potassium island arc field on the Ti-Cr diagram (Fig. 8.8). An elucidation of the tectonic environment of this area must necessarily await further geological and geochemical investigations.

The basic intrusive rocks (gabbros) are mainly subalkaline. One of the West Block intrusives (analysis 308) as well as the gabbro and granodiorite from Stord (analyses 319, 269 resp.) are decidedly alkaline (Fig. 8.2) and plot in the central parts of the AFM diagram - a trend typical for alkaline magmas.

#### 8.4 Geochemistry of the acidic volcanics.

Acidic lavas and intrusives of the East and West Blocks are chemically different from those of the Central and Finaasviki Blocks. Analytical data are given in Tables 8.4 and 8.5.

In the absence of detailed data on the structural relationships of the East and West Block acidic rocks it is difficult to give a proper evaluation of the geochemical data. In particular, two of the analyses, Nos. 255 and 256, from the East Block are distinctive from the third, No. 257, which is an analysis of a Sodium-rich intrusive Keratophyre from the base of the Bergefjell nappe. Analyses 255 and 256 are from an acidic rock which intrudes metasediments. These two analyses are quite distinctive from other acidic rocks on Bømlo in that they have high Zirconium values which are more characteristic of plutonic rocks (cf. with analysis 269 of the Stord granodiorite). The erratic behaviour of alkalies between analyses 255 and 256 is attributed to the loss of potassium (and Rb) with an addition of Sodium at the margin of the intrusive (analysis 256) in comparison to the central parts of the mass (analysis 255).

Table 8.4 Bømlø east and west block acidic rocks.

	255 x	256 x	257 x	264	265	300	266
	1228 / 6	1228 / 7	1228 / 12	1228 / 43	1228 / 54	1220 / 58B	1228 / 62
SIO <sub>2</sub>	73,90	77,10	75,30	81,50	79,40	75,80	82,00
AL <sub>2</sub> O <sub>3</sub>	12,10	10,80	13,20	10,30	10,60	11,50	10,50
FE <sub>2</sub> O <sub>3</sub>	3,80	3,40	2,40	1,50	1,50	3,20	1,50
TIO <sub>2</sub>	0,60	0,53	0,55	0,20	0,38	0,36	0,27
MGO	0,20	0,10	0,61	0,10	0,60	0,80	1,00
CAO	0,00	0,80	0,70	0,40	0,10	0,50	1,60
NA <sub>2</sub> O	4,30	5,45	6,95	5,75	3,90	4,75	3,95
K <sub>2</sub> O	5,02	1,69	0,08	0,08	1,13	1,12	0,44
MNO	0,00	0,01	0,04	0,00	0,00	0,03	0,00
P <sub>2</sub> O <sub>5</sub>	0,05	0,03	0,02	0,00	0,02	0,02	0,02
L.O.I.	0,26	0,50	0,75	0,52	1,15	1,31	0,75
TOTAL	100,23	100,41	100,59	100,35	98,78	99,39	102,03
PPM							
ZR	1522	1362	195	340	182	239	238
Y	135	116	24	120	25	49	50
SR	54	66	157	34	40	70	75
RB	60	19	0	3	25	16	7
ZN	241	166	31	2	9	77	54
CU	0	0	0	0	0	0	0
NI	0	0	1	0	0	0	4
CR	0	0	3	0	0	3	3
BA	679	254	88	37	53	169	62

x East Block

Table 8.5 Bømlø Central and Finaasviki acidic rocks.

	258	259	260	261	262	263	268 <sup>x</sup>	0	0
	1228 / 35	1228 / 36	1228 / 37	1228 / 39	1228 / 40	1228 / 41	1228 / 83A	KN7113	KN7114
SiO <sub>2</sub>	74,90	75,80	73,40	74,20	71,80	70,40	70,90	72,00	69,50
Al <sub>2</sub> O <sub>3</sub>	12,40	12,50	12,60	12,80	13,20	12,90	13,30	14,76	14,93
Fe <sub>2</sub> O <sub>3</sub>	1,70	1,40	2,00	1,70	3,20	5,40	3,80	2,37	3,85
TiO <sub>2</sub>	0,55	0,45	0,58	0,43	0,60	0,75	0,76	0,25	0,33
MgO	0,40	0,10	0,50	0,00	0,30	0,40	0,50	0,23	0,19
CaO	0,00	0,80	0,90	0,50	0,70	0,40	2,10	0,52	0,80
Na <sub>2</sub> O	2,60	2,15	1,30	3,65	3,00	2,95	3,45	4,44	3,82
K <sub>2</sub> O	5,90	6,34	7,90	4,86	6,00	5,72	4,67	5,20	6,00
MnO	0,00	0,00	0,02	0,00	0,03	0,07	0,05	0,60	0,05
P <sub>2</sub> O <sub>5</sub>	0,05	0,04	0,05	0,03	0,03	0,05	0,09	0,00	0,02
L.O.I	1,08	1,07	1,18	0,87	0,97	1,06	0,91	0,44	0,42
TOTAL	99,58	100,65	100,43	99,04	99,83	100,10	100,53	100,81	99,91
PPM									
ZR	242	273	284	242	547	744	293	0	0
Y	21	25	22	18	44	67	36	0	0
SR	61	69	68	62	101	75	135	0	0
RB	260	228	354	213	247	242	171	0	0
ZN	39	29	43	28	78	98	55	0	0
CU	0	0	0	0	0	0	0	0	0
NI	3	0	0	4	1	2	0	0	0
CR	3	0	0	4	0	0	2	0	0
BA	627	693	1715	563	999	1039	451	0	0

<sup>x</sup> Finaasviki profile

KN7113 and KN7114 are from Kattnakken (T. Torske, unpublished data, P.R. Graff, analyst).



Table 8.6 Comparison of Bømlø calc-alkaline rocks with calc-alkaline rocks from island arcs and the Andes.

	278	JW4	OIB	S 11	291	S 15	JW 6	306	JW 8	S 4
SiO <sub>2</sub>	49.87	50.59	48.07	52.7	57.2	57.2	59.05	62.91	58.52	62.7
Al <sub>2</sub> O <sub>3</sub>	17.26	16.29	16.87	16.3	15.72	16.6	17.07	17.88	16.20	16.0
Fe <sub>2</sub> O <sub>3</sub>	10.45	9.1	12.3	8.8	9.16	7.2 <sup>x</sup>	6.6 <sup>x</sup>	6.63	6.5	5.4
TiO <sub>2</sub>	2.17	1.05 <sup>x</sup>	3.12 <sup>x</sup>	1.4 <sup>x</sup>	1.91	1.2 <sup>x</sup>	.69 <sup>x</sup>	1.64	.76 <sup>x</sup>	.7 <sup>x</sup>
MgO	4.79	8.96 <sup>x</sup>	5.69	6.2 <sup>x</sup>	3.39	4.3	3.25	1.79	4.14 <sup>x</sup>	1.5
CaO	11.08	9.50	10.22	8.5 <sup>x</sup>	8.42	6.8	7.09	2.95	5.59 <sup>x</sup>	3.6
Na <sub>2</sub> O	3.38	2.89	3.46	3.4	3.05	3.8	3.80	2.63	3.64	3.5
K <sub>2</sub> O	.67	1.07	1.39	1.7 <sup>x</sup>	1.03	1.8 <sup>x</sup>	1.27	3.32	2.67	3.0
MnO	.17	.17	-	.14	.14	.10	.15	.12	.09	.04
P <sub>2</sub> O <sub>5</sub>	.15	.21	-	.4 <sup>x</sup>	.15	.35 <sup>x</sup>	.20	.14	.25 <sup>x</sup>	.24 <sup>x</sup>
		52 %				58 %			63 %	
Zr	195	100 <sup>x</sup>	215	180	212	230	110 <sup>x</sup>	334	100 <sup>x</sup>	190
Y	33	20	29	8 <sup>x</sup>	28	7 <sup>x</sup>	24	28	20	6 <sup>x</sup>
Sr	523	330	433	600	322	890 <sup>x</sup>	385	188	460	750 <sup>x</sup>
Rb	22	10	15	45 <sup>x</sup>	47	35	30	123	45 <sup>x</sup>	115
Zn	87	-	-	-	91	-	-	79	-	-
Cu	49	-	-	50	35	75	-	0	-	80
Ni	67	25	-	30	53	50	18	26	5	6
Cr	121	40	280	250 <sup>x</sup>	98	60	25	191	13	20
Ba	140	115	-	560 <sup>x</sup>	258	680 <sup>x</sup>	270	707	520	870

x = different than Bømlø. JW4, JW6, JW8 from Jakes and White (1972); S 11, S 15, S 4 from Siegers *et al* (1969); OIB (ocean island Basalt) from Pearce (pers. comm. 1974)

The four analyses from the West Block acidic rocks are considered to represent intrusives - analysis 300 is from a small acidic body that can be either a dike or a lava, since the contacts are not exposed. Analysis 300 is rather similar to that of analysis 265 and is also comparable to analysis 266 even though the  $K_2O$  and Rb contents of 266 are lower. Analysis 264 differs from the other three in its lower  $K_2O$  and higher  $Na_2O$ , Zr and Y. All four analyses, however, probably represent one episode of acidic magmatism. The analysis are comparable to those of keratophyres and fine-grained acidic intrusives in island arc terrains elsewhere in the Caledonides, e.g. those of the Grong area.

The Central and Finaasviki silicic lavas and pyroclastics, analyses 258-263 and analysis 268, respectively, are distinctly different from the acidic rocks in the other areas investigated in this project. For example the  $K_2O$  contents of these rocks are significantly greater than the  $Na_2O$  contents. The only other rocks with  $K_2O/Na_2O > 1$  are the intrusive from the East Block (analysis 255) the Stord granodiorite (analysis 269) and several of the andesitic lavas from the Central and Finaasviki Blocks.

The Zr and Ba contents of these lavas are significantly higher than those of silicic lavas from the Grong island arc silicic rocks. In addition, these lavas are distinctive in having  $Sr/Rb < 1$  when compared with the other acidic rocks analysed in this study.

Rhyolites from Kattnakken, Stord, (collected by T. Torske and analysed by P.R. Graff, see Table 8.5 analyses 7114 and 7113) have major element compositions and Sr and Rb values (Priem and Torske, 1973) comparable with those of the Central and Finaasviki rhyolites. Thus, it can readily be argued on the basis of similarities in chemistry that the rhyolitic rocks on Bømlo have the same parentage and age (455±5my) as the rhyolites on Stord (Priem and Torske, 1973).

#### 8.5 The Stord analyses.

Four specimens were analysed from the island of Stord. These include a gabbro (analysis 319), a dolerite (317), a basalt (318) and a granodiorite (269). The basalt is a tholeiite and plots in the fields for ocean-floor basalts on the trace element diagrams (see Fig. 8.2 to 8.7).

The granodiorite which has  $Na_2O/K_2O < 1$  is probably related to the magmatism producing the subaerial volcanics on Stord and Bømlo.

## 8.6 Summary.

Subaerial basaltic, andesitic and rhyolitic lavas from the central part of the island of Bømlo and the Finaasviki area are geochemically distinctive from those of the southeastern and northwestern parts of Bømlo. The basic lavas in the southeastern part of Bømlo resemble island arc tholeiites and the area may contain slices of ocean-floor type material. The basic lavas in the western and northwestern area appear to be a mixture of ocean-floor, island arc and "within plate" volcanics on the basis of a small sample population over a large area. The subaerial lavas are "within plate" volcanics and were most likely generated in a continental margin tectonic environment. The submarine tholeiitic lavas were probably generated by rifting and spreading to form a marginal basin within the continent.

Captions for figures in section 8.

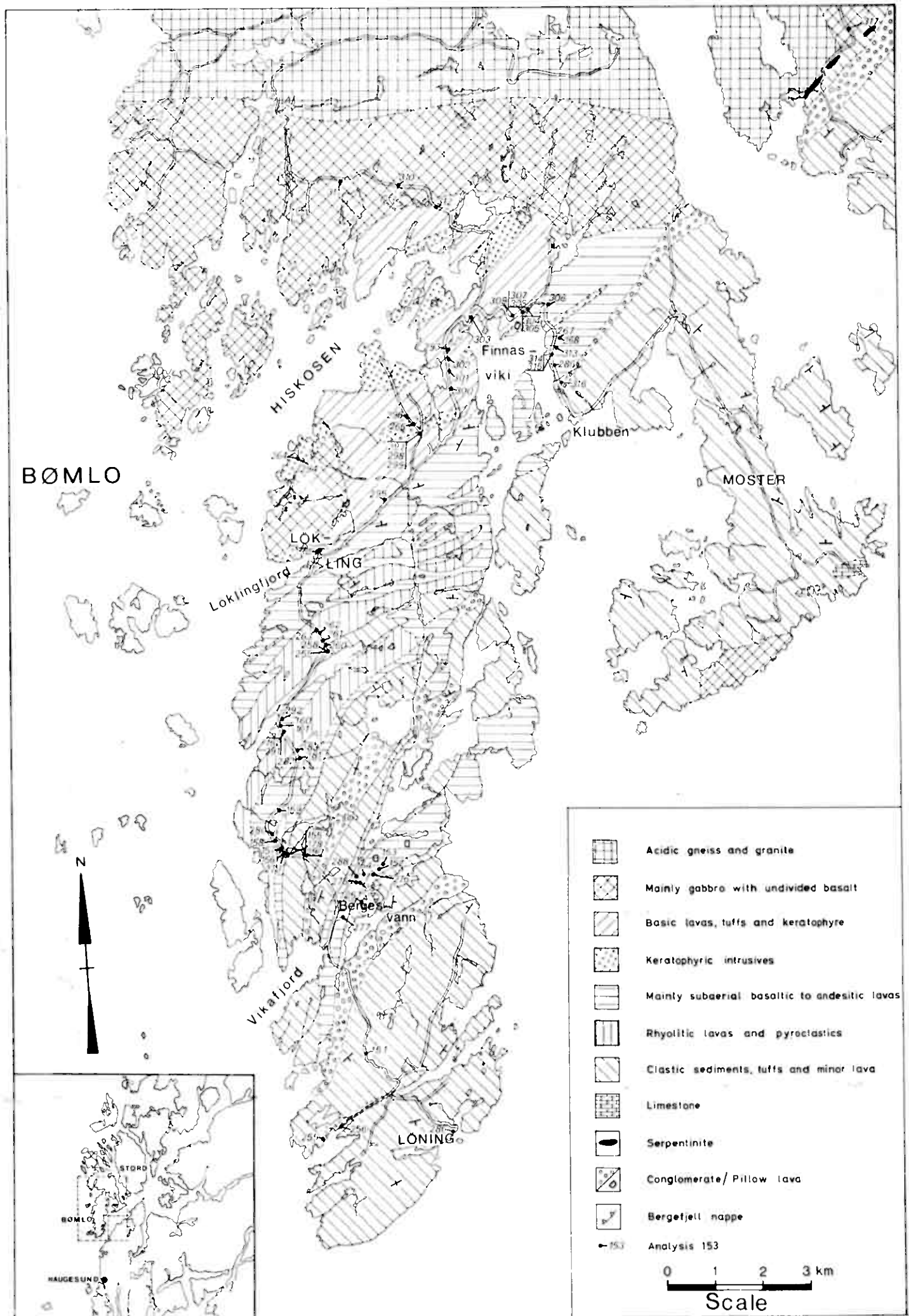
Figure 8.1 Generalized geology of Bømlo after Reusch (1888) and Songstad (1971).

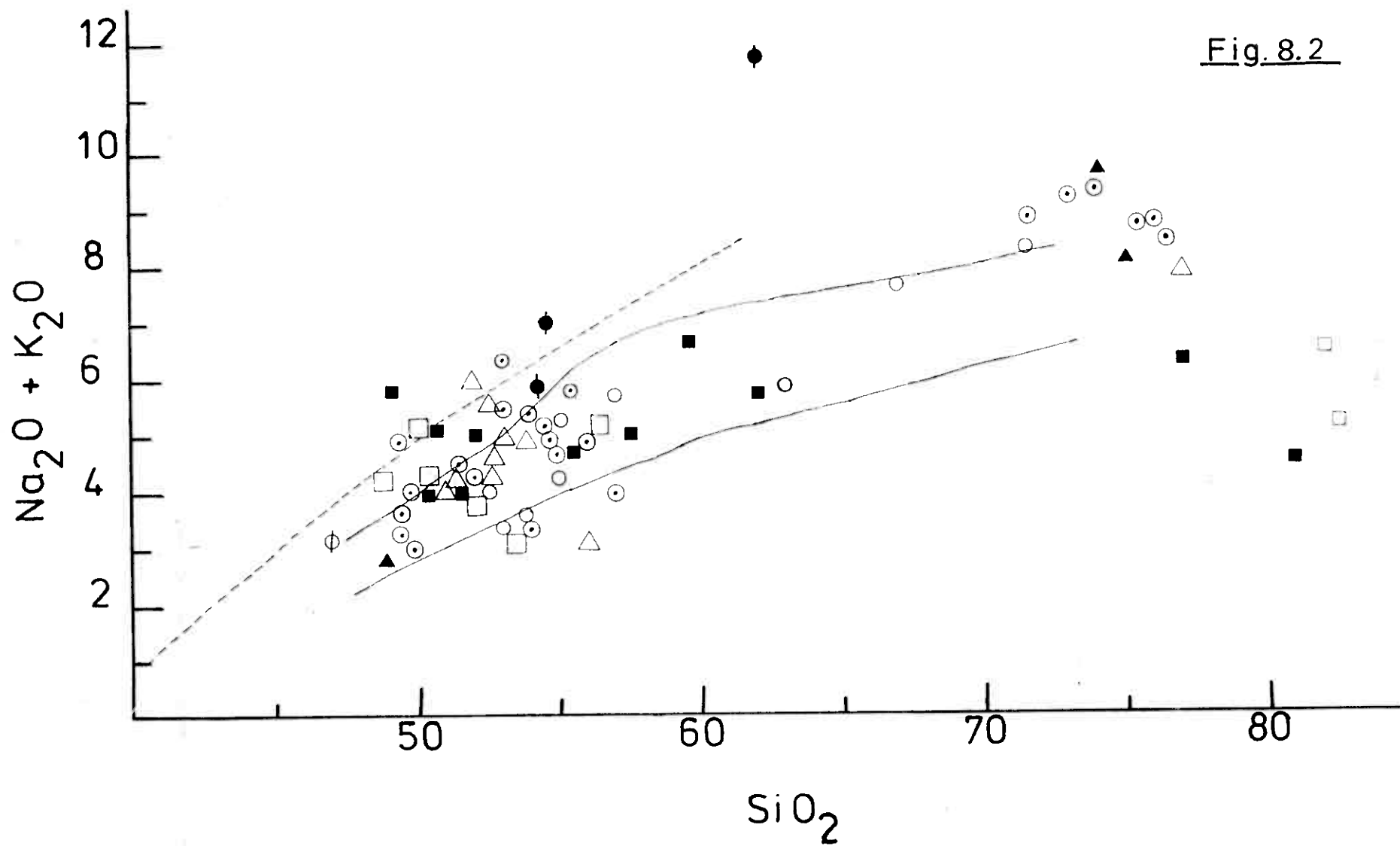
Figure 8.2 Alkali-Silica variation diagram for rocks of the Bømlo-Stord area. Oxides as wt.% (volatile free). The dashed boundary line separating alkaline compositions (above) from subalkaline compositions (below) is after Irvine and Barager (1971). The solid boundary lines are those of Kuno (1966) alkaline (above), calc-alkaline (between) and Tholeiitic (below) compositions. The symbols identifying rocks from the subareas are:  $\emptyset$  Stord,  $\Delta$  East Block,  $\bigcirc$  Central Block,  $\bigcirc$  Finaasviki Block,  $\square$  West Block. Solid symbols represent intrusive rocks.

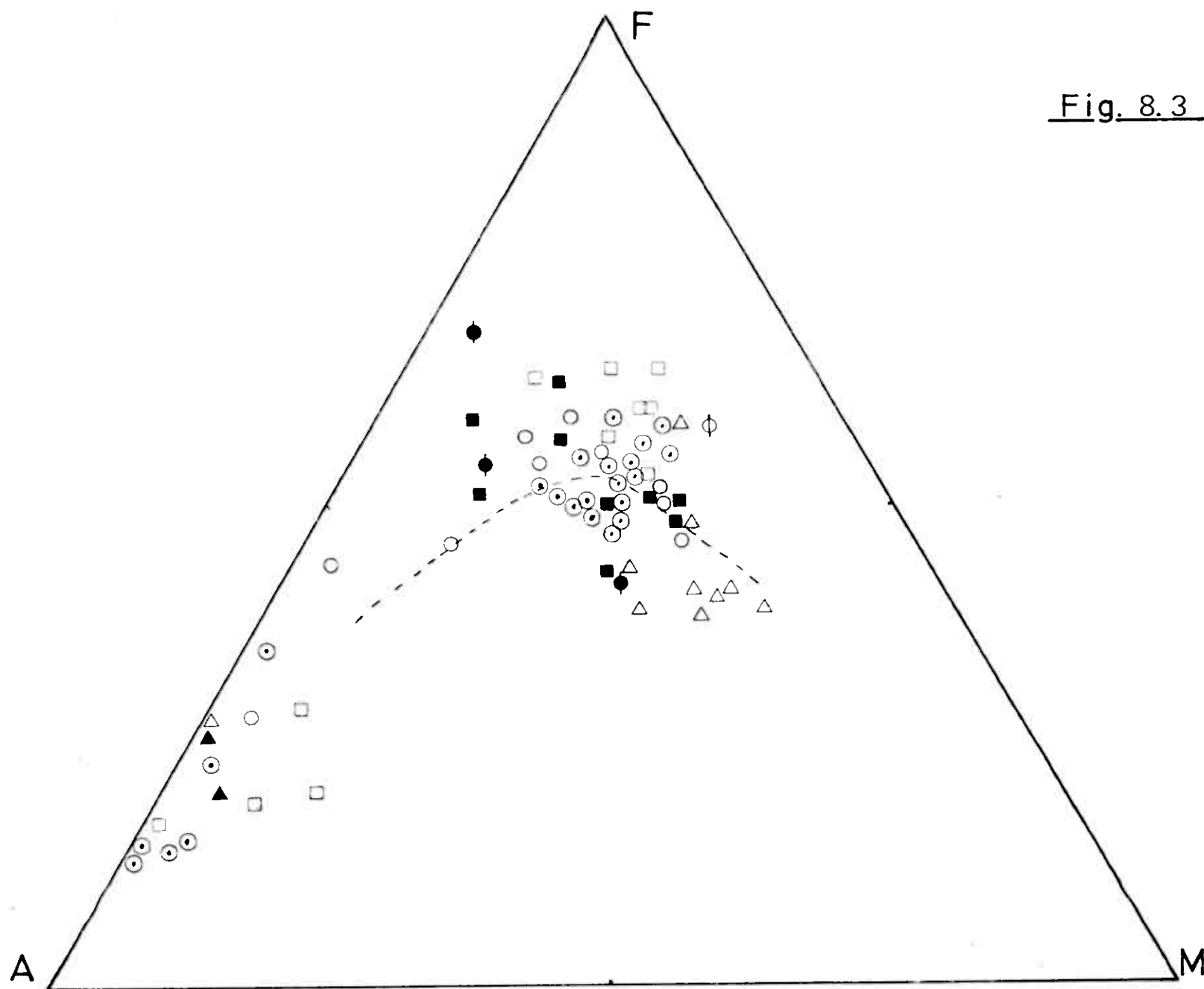
Figure 8.3  $A(\text{Na}_2\text{O}+\text{K}_2\text{O}) - F(\text{FeO, total Fe}) - M(\text{MgO})$  variation diagram. The boundary line separating tholeiitic compositions (above) from calc-alkaline compositions (below) is after Irvine and Barager (1971). Symbols as in Fig. 8.2.

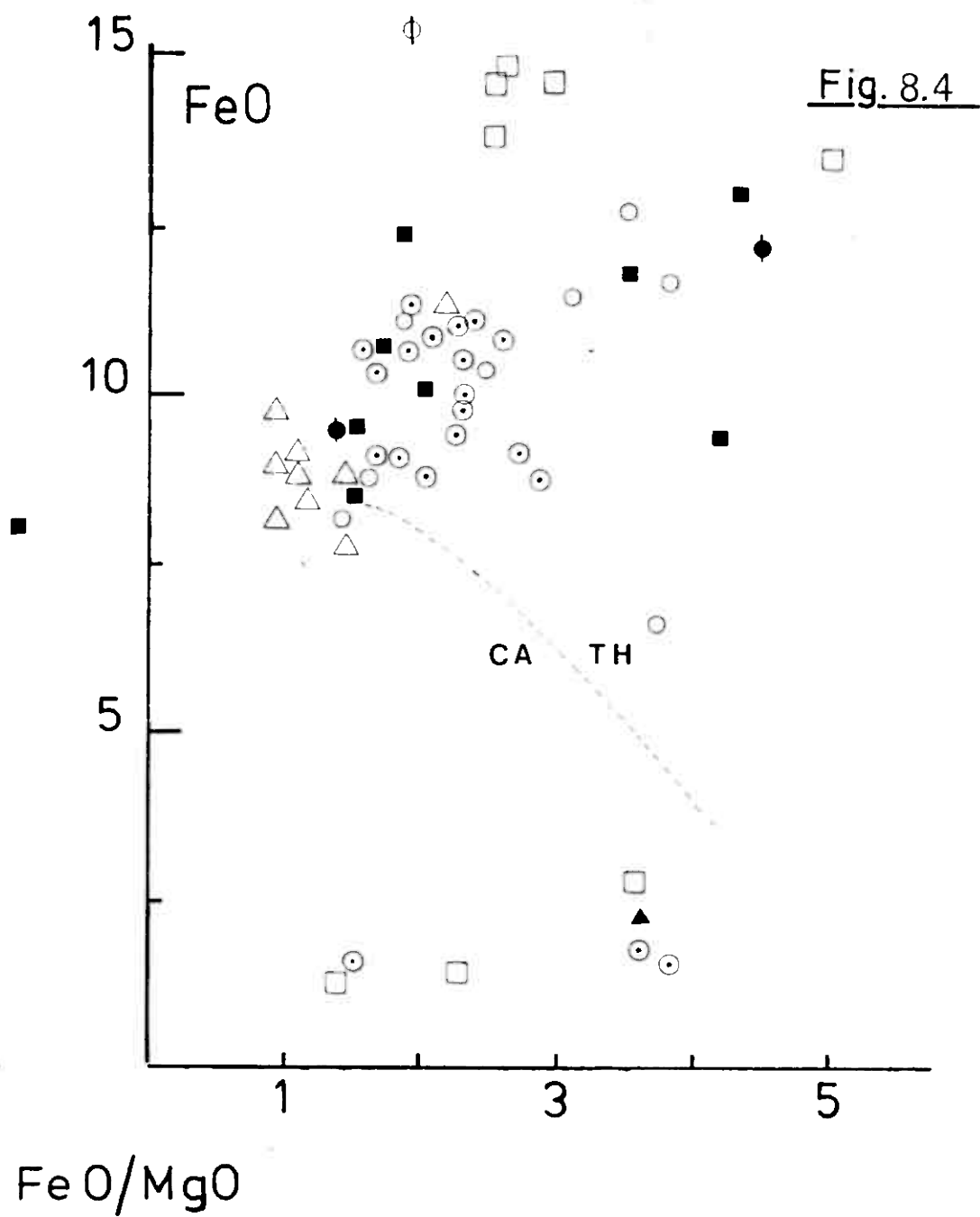
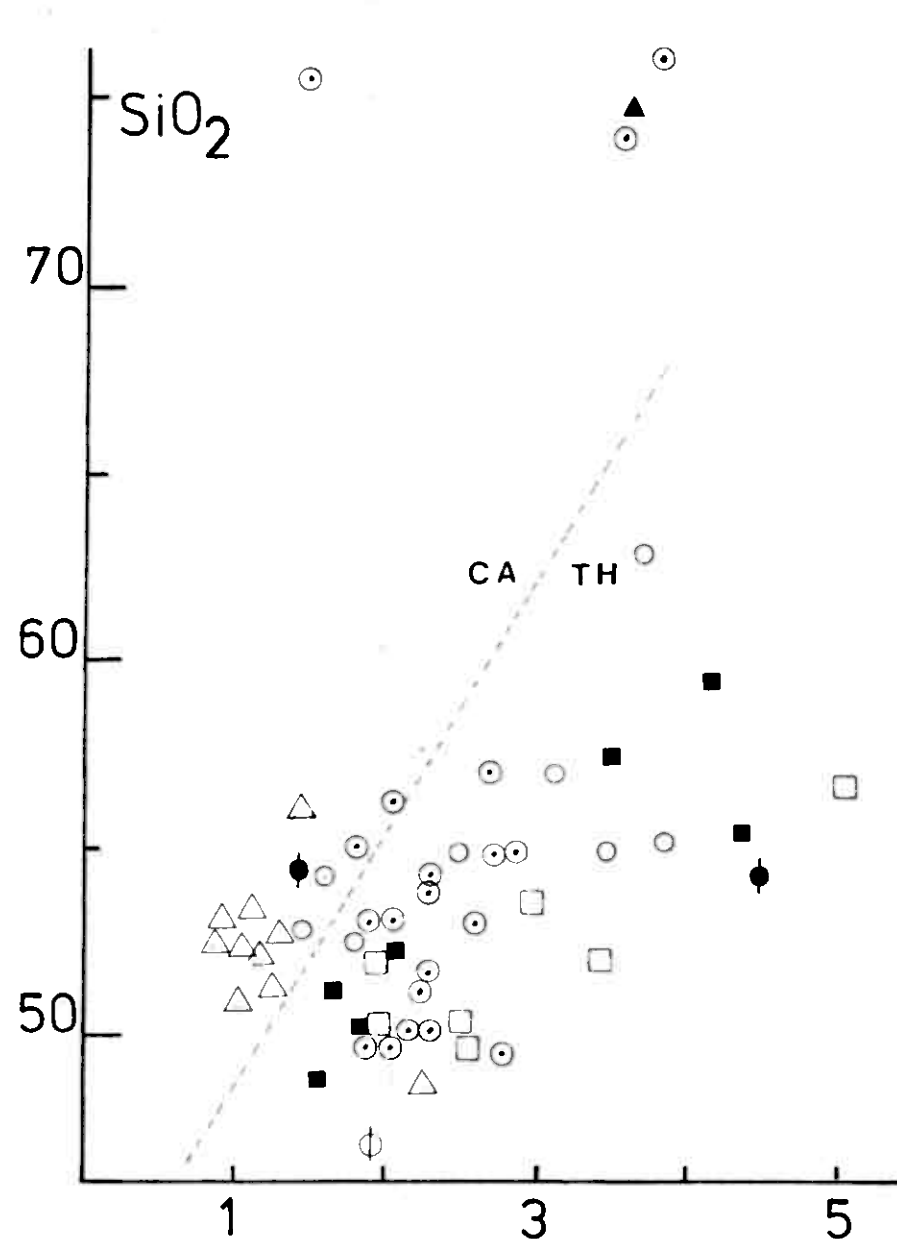
Figure 8.4  $\text{FeO} - \text{FeO}/\text{MgO}$  and  $\text{SiO}_2 - \text{FeO}/\text{MgO}$  variation diagrams. Oxides as wt.% (volatile free). Total iron as FeO. The field boundaries separating the tholeiitic (TH) and calc-alkaline (CA) series and the trend lines for abyssal tholeiites (A) and the Macauley island tholeiites (M), are after Miyashiro (1974). Symbols as in Figure 4.1.

- Figure 8.5  $\text{TiO}_2$  -  $\text{FeO/MgO}$  variation diagram. The trend lines for abyssal tholeiites (A), the Macauley Island tholeiite series (M) and the Cyprus tholeiite series (CY) are after Miyashiro (1974). Symbols as in Fig. 8.2.
- Figure 8.6 Discriminant diagram using Ti, Zr, Y to distinguish "within plate" basalts (field D) from ocean-floor type basalts (field B), calc-alkaline basalts (field C) and low-potassium tholeiites of island arcs (fields A and B). Field boundaries after Pearce and Cann (1973). Symbols as in Fig. 8.2.
- Figure 8.7 Discriminant diagram using Ti and Zr for distinguishing ocean-floor type basalts (fields B and D), calc-alkaline basalts (field C) and low-potassium tholeiites of island arcs (fields A and B). Field boundaries after Pearce and Cann (1973). Symbols as in Fig. 8.2.
- Figure 8.8 Discriminant diagram to distinguish ocean-floor basalts (field A) from low-potassium tholeiites of island arcs (field B). The field boundary is after Pearce (pers. comm. 1974). Symbols as in Fig. 8.2.

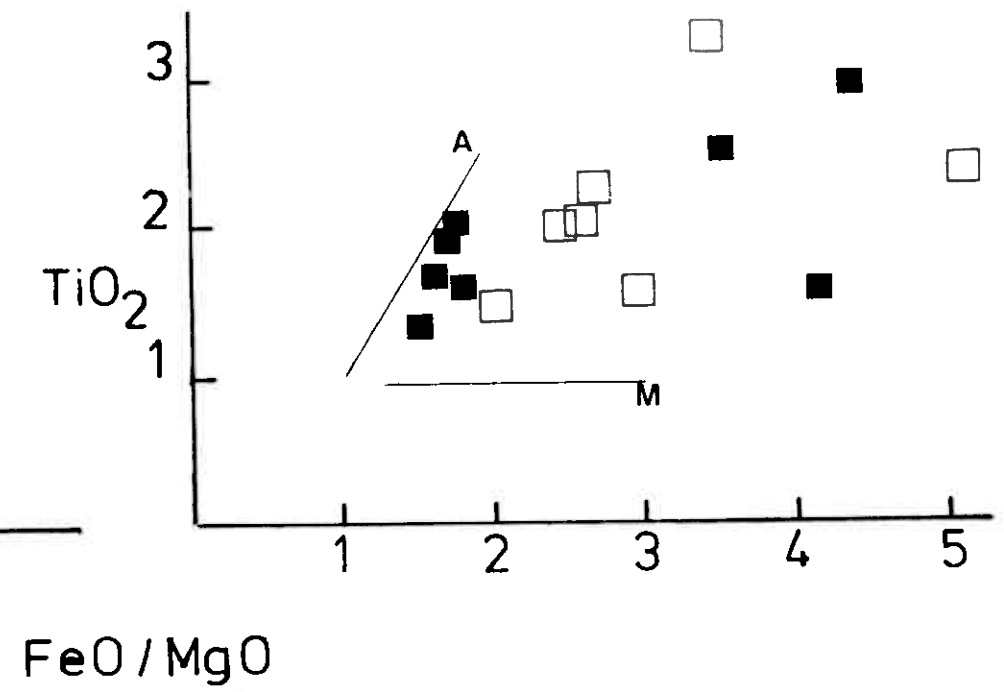
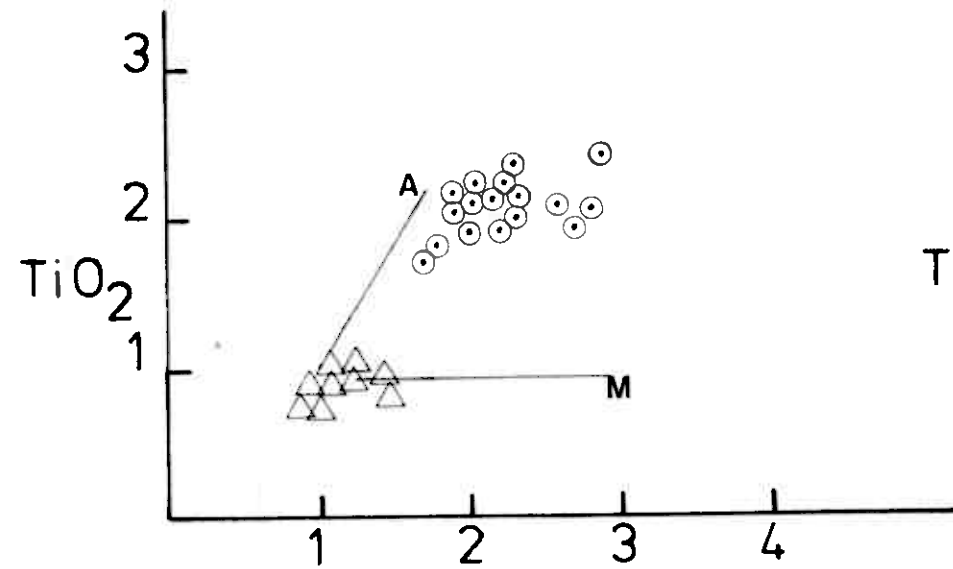
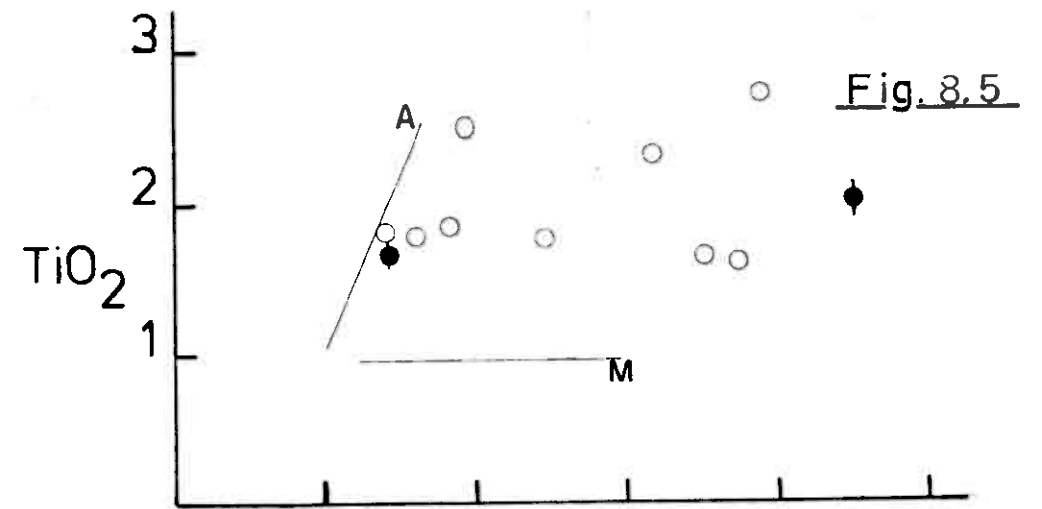


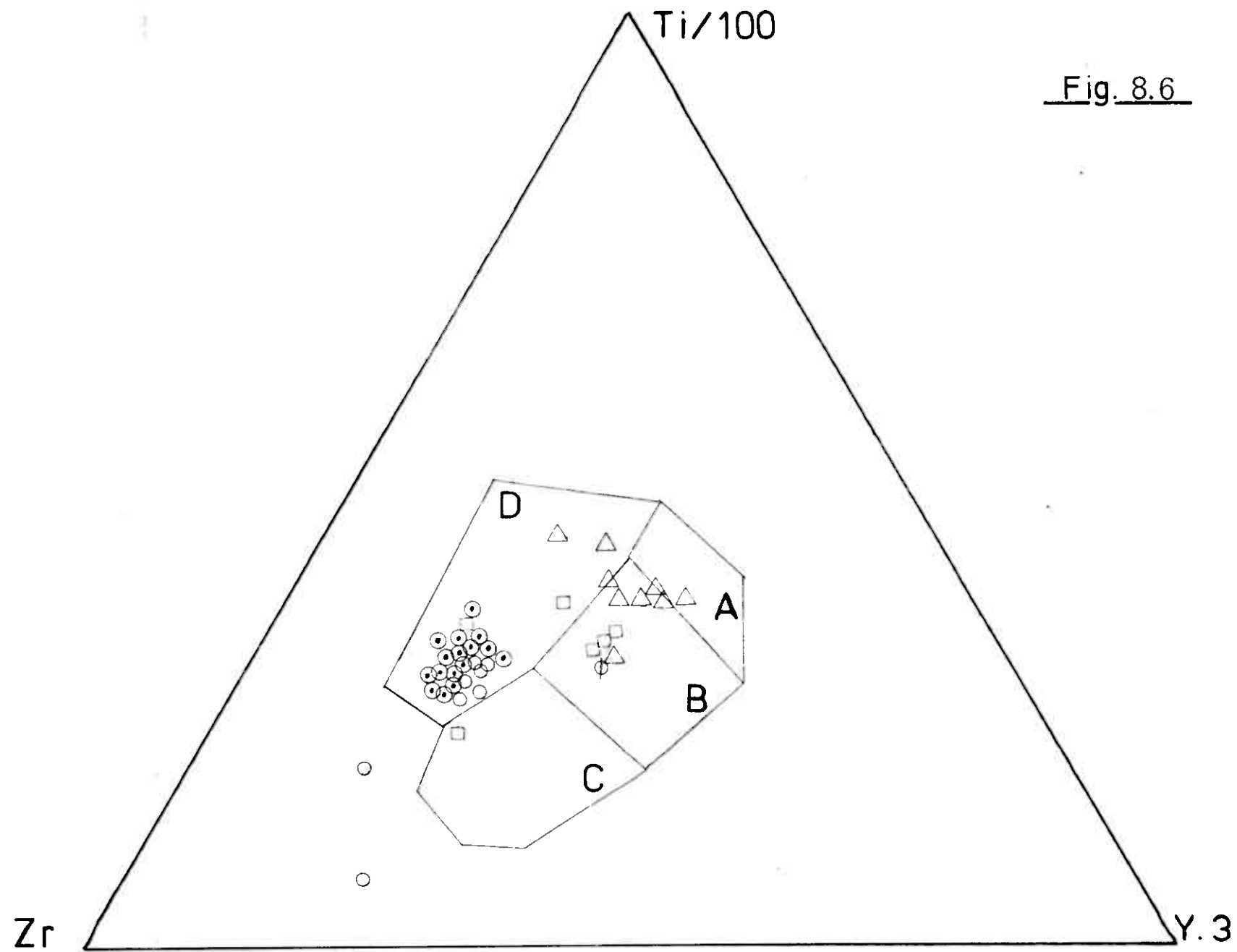












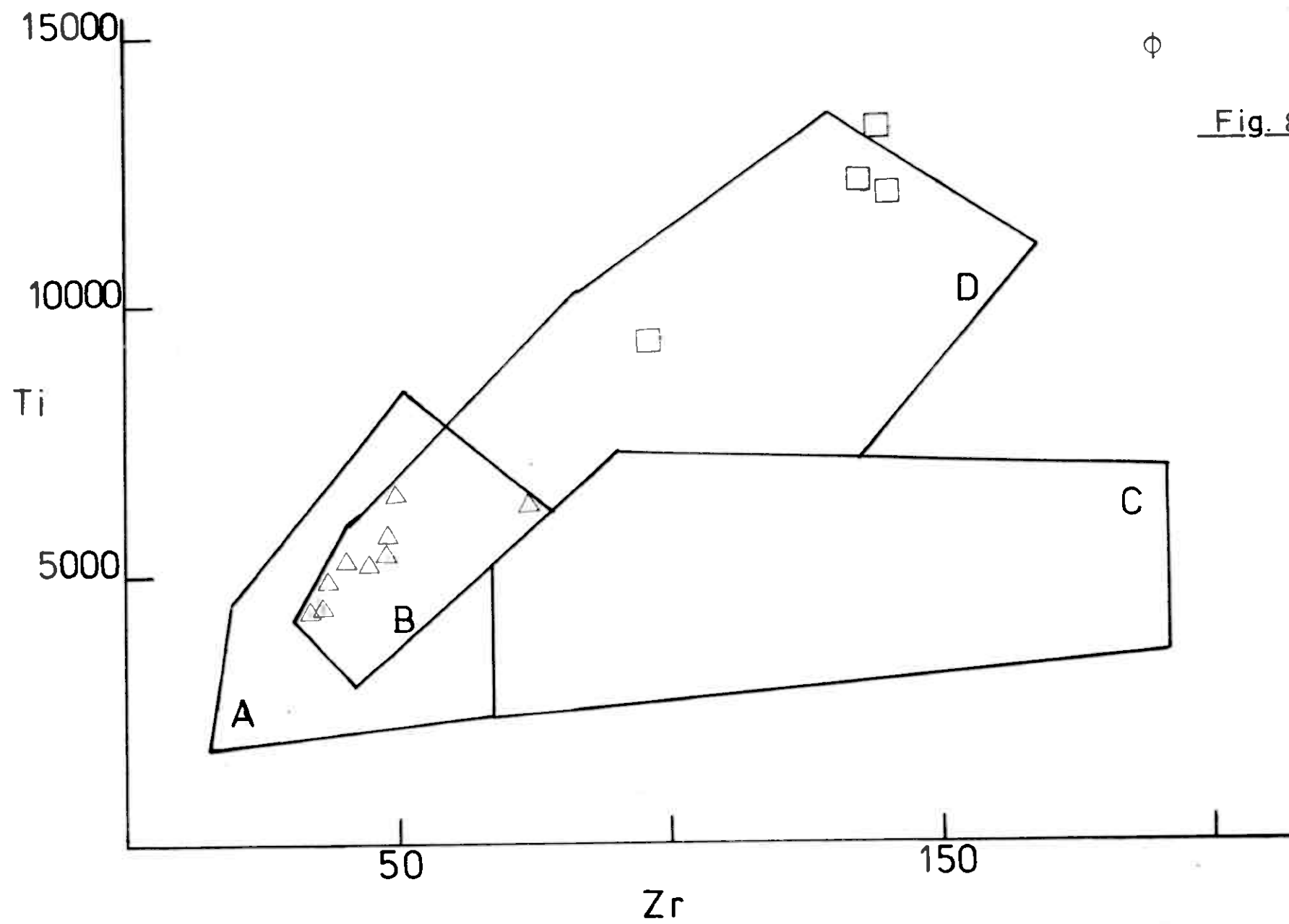
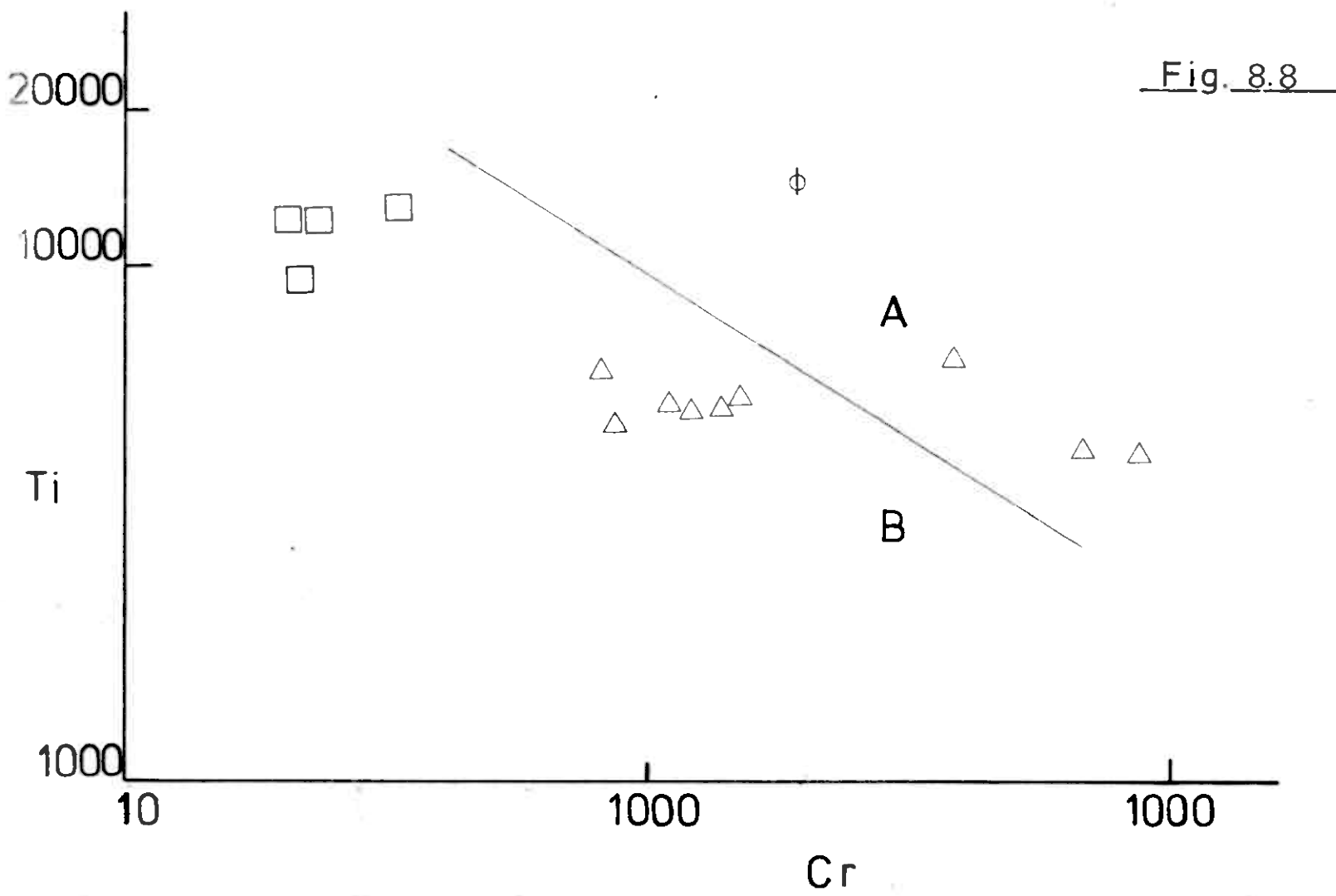


Fig. 8.7



## CONCLUSIONS

It has been possible with the aid of whole rock geochemistry to make a start at understanding the Caledonian volcanic belts in Norway, so that we can now progress beyond the stage of considering them under all-inclusive terms such as "greenstone", "basic volcanics" and other generalizations and begin to think in terms of specific magmatic types, e.g. island arc tholeiites, island arc calc-alkaline suites, ocean-floor type lavas, etc.. It has recently been shown that a knowledge of the environment of magma formation can have considerable bearing on understanding local stratigraphy and in correlating non-fossiliferous units containing volcanic rocks as well as being absolutely necessary in establishing a plate tectonic model for the Caledonides (Gale and Roberts, 1974).

One of the aims of this investigation was to establish if there existed correlations between greenstone geochemistry and the occurrence of massive sulfide deposits. There is a broad correlation between the occurrence of massive sulfide deposits and the geochemical affinities of their host volcanics. Vokes and Gale (1975) show that the volcanogenic massive sulfide deposits of the southern part of the Caledonides can be fitted into the plate tectonic model established by Gale and Roberts (1974) and that there is an overall increase in mineralogical complexes. In particular, galena and sphalerite are more abundant in copper-bearing massive sulfide deposits with increasing maturity of the island arc development in comparison with deposits associated with the initial stages of island arc magmatism which contain insignificant amounts of lead, and zinc is less abundant than copper.

As a result of geochemical studies in the Løkken area it appears that the ore deposits there are located at or near the contact between ocean floor type basalts and early island arc tholeiitic basalts. A similar relationship has been noted in Cyprus (Julian Pearce, pers. comm., 1974) and appears to exist in the York Harbour area of western Newfoundland.

If the interpretation of the Joma lavas as part of a "hot-spot" or oceanic island is correct, then this is the first known reported instance of a massive sulfide deposit associated with that magma type (Vokes and Gale, 1975).

On a regional basis there appears to be a strong correlation between the tectonic environment of magma generation and the presence of major

massive sulfide deposits. The island arc terrain of the Grong area has a number of volcanogenic massive sulfide deposits while the continental margin lavas of the Bømlo area do not have any known massive sulfide deposits. The massive sulfide deposits on Stord are probably associated with an island arc volcano-clastic sequence. Although there are ocean floor basalts in the Løkken, Støren and Stavenes areas, major massive sulfide deposits are associated only with the ocean-floor basalts of the Løkken area. The Løkken ocean-floor basalts are considered to have formed in a back arc marginal basin in response to subduction of oceanic crust beneath oceanic crust while the ocean-floor basalts of the Støren and Stavenes areas were formed at a spreading mid-ocean ridge. Massive sulfide deposits found to date in the Støren and Stavenes area have been small, copper-bearing pyrite deposits of little or no economic interest.

Although more work is necessary to establish if other examples exist it would appear from the present study that there is a greater probability of finding massive sulfide deposits of economic interest in association with ocean floor basalts formed in a marginal basin than in association with ocean-floor basalts formed at a mid-ocean ridge. This conclusion is substantiated to some extent by the absence of massive sulfides in ophiolite suites generated in a major ocean, and the presence of massive sulfide deposits, in some ophiolite suites generated in a marginal basin environment (e.g. Cyprus, York Harbour).

This investigation of volcanic rocks in central and south Norway has shown that the previous plate tectonic model proposed by Gale and Roberts (1972) was overly simplified and that the island arc sequences were complicated by extensive obduction of island arc, ocean-floor and "hot-spot" volcanics (and associated sediment) onto the Palaeozoic continental shelf during continental collision (see Gale and Roberts, 1974). With the recognition of continental margin type volcanics in the Støren area (the Hølanda porphyry) and the Bømlo-Stord area it is now possible to make further modifications to the proposed model in order to accomodate local variations, although the general model as established recently (Gale and Roberts, 1974) is still considered valid for the regional development of the Caledonides in central and south Norway.

As outlined above, the broad aims of the reconnaissance geochemistry survey of volcanic rocks in central and south Norway have been fully realized.

In conclusion, I recommend that this investigation be continued and extended to:

- 1) provide a reconnaissance study of all greenstone terrains in the Caledonides of Norway,
- 2) carry out detailed investigations of volcanic terrains with which massive sulfide deposits are associated in order to establish if any further correlations between massive sulfide occurrences and the chemistry of volcanic rocks exist,
- 3) provide a basis for stratigraphical correlations between different volcanic units,
- 4) establish by detailed investigations around massive sulfide deposits if the volcanics directly associated with the ore-forming processes have a chemical "signature" indicating the presence of the sulfide deposit, and,
- 5) test further and modify, if necessary, ideas about the tectonic evolution of the Caledonides.

Trondheim 16.12.1974

*George H. Gale*  
George H. Gale

## 10. REFERENCES

- Cann, J.R. (1969) Spilites from the Carsberg Ridge Indian Ocean, *Jour. Petrol.*, 10, 1.
- Cann, J.R. (1970) Rb, Sr, Y, Zr and Nb in some ocean floor basaltic rocks. *Earth and Planet. Sci. Letters*, 10, 7-11.
- Cann, J.R. (1971) Major element variation in ocean-floor basalts. *Phil. Trans. Roy. Soc. Lond.*, A 268, 663.
- Chaloupsky, J. (1970) Geology of the Hølanda - Hulsjøen Area, Trondheim Region. *Norges Geologiske Unders.*, 266, 277-304.
- Fiala, F. (1974) Some notes on the problem of spilites. *in*, G.C. Amstutz (Ed) *Spilites and Spilitic Rocks*. Springer-Verlag, Berlin.
- Gale, G.H. (1974) Geokjemiske undersøkelser av kaledonske vulkanitter og intrusiver i midt- og syd-Norge: Del II - Analytiske data. Rapport nr. 1228 B, *Norges Geol. Unders.*
- Gale, G.H. and Roberts, D. (1972) Palaeogeographical implications of greenstone petrochemistry in the southern Norwegian Caledonides, *Nature Phys. Sci.*, 238, 60-61.
- Gale, G.H. and Roberts, D. (1974) Trace element geochemistry of Norwegian lower Palaeozoic basic volcanics and its tectonic implications. *Earth and Planet. Sci., Letters*, 22, 380-390.
- Goldschmidt, V.M. (1916) Übersicht der Eruptivgesteine im kaledonischen Gebirge zwischen Stavanger und Trondheim. *Kristiania Vidensk.-selsk. Skr.*, Math.Naturv. 140 p.
- Irvine, J.N. and Barager, W.R.A. (1971) A Guide to the classification of the common volcanic rocks. *Can. Jour. Earth Sci.*, 8, 523-548.
- Jakeš, P. and White, A.J.R. (1972) Major and Trace element abundances in volcanic rocks of orogenic areas. *Geol. Soc. Amer. Bull.*, 83, 29-40.
- Kuno, H. (1966) Lateral variation of basalt magma across continental margins and island arcs. *in*, W.H. Poole (Ed) *Continental Margins and Island Arcs*. *Geol. Surv. Can.* paper 66-15, 317-334.
- Miyashiro, A. (1974) Classification, characteristics, and origin of ophiolites. *Jour. Geol.* (in press).



- Nesbitt, E. and Pearce, J.A. (1973)  $\text{TiO}_2$  as a possible guide to past oceanic spreading rates. *Nature*, 246, 468-470.
- Pearce, J.A. and Cann, J.R. (1973) Tectonic setting of basic volcanic rocks determined using trace element analyses. *Earth and Planet. Sci. Letters*, 19, 290-300.
- Reusch, H. (1888) Bømmeløen og Karmøen. Kristiania 422 p.
- Siegers, A., Pickhler, H. and Zeil, W., (1969) Trace element abundances in the "Andesite" Formation of Northern Chile. *Geochim. et Cosmochimica Acta*, 33, 882-887.
- Songstad, P. (1971) Geologiske undersøkelser av den ordoviciske lagrekken mellom Løkling og Vikafjord, Bømlo, Sunnhordland. Univ. of Bergen, cand.real. hovedoppgave (unpublished).
- Vogt, T. (1945) The geology of part of the Høllonda - Horg district. *Norsk geol. Tidsskr.*, 25, 449-527.
- Vokes, F.M. and Gale, G.H. (1975) Metallogeny relateable to continental drift in southern Scandinavia. *Geol. Assoc. of Canada Special Paper on Metallogeny and Plate Tectonics*. (in press).